STUDY AND OPTIMIZATION OF ABRASIVE EDM PROCESS PARAMETERS WITH TOOL ROTATION

Thesis submitted in fulfilment of requirements for the degree

Doctor of Philosophy

in

Mechanical Engineering

Submitted by

AJAY LAMBA

2K14/PHD/ME/09

Under the Supervision of

Dr. VIPIN

Professor

Department of Mechanical Engineering

Delhi Technological University

DEPARTMENT OF MECHANICAL ENGINEERING

DELHI TECHNOLOGICAL UNIVERSITY

BAWANA ROAD, DELHI-110042, INDIA

FEBRUARY, 2023

Dedicated to

My

Guru's

and

Beloved Parents

DELHI TECHNOLOGICAL UNIVERSITY

BAWANA ROAD

DELHI-110042 (INDIA)

DECLARATION OF ORIGINALITY

I hereby declare that the research work presented in this thesis titled "***Study and optimization of abrasive EDM process parameters with tool rotation***", is an original and authentic work carried out by me under the supervision of **Dr. Vipin**, Professor, Department of Mechanical Engineering, Delhi Technological University, Delhi for the award of the ***Doctor of Philosophy*** degree in ***Mechanical Engineering***. The work presented in this thesis has not been submitted to any other university or institution for the award of any degree or diploma.

AJAY LAMBA
2K14/PhD/ME/09
Research Scholar
Department of Mechanical Engineering
Delhi Technological University

DELHI TECHNOLOGICAL UNIVERSITY

BAWANA ROAD

DELHI-110042 (INDIA)

SUPERVISOR'S CERTIFICATE

This is to certify that the Ph.D. thesis entitled "**Study and optimization of abrasive EDM process parameters with tool rotation"** being submitted by Mr. Ajay Lamba, Roll No. 2K14/PhD/ME/09 for the award of degree, Doctor of Philosophy in Mechanical Engineering, Delhi Technological University, Delhi, India, is a bonafide record of original research work carried out by him under my guidance and supervision. The work presented in this thesis has not been submitted to any other university or institution for the award of any degree or diploma.

Dr. VIPIN

Professor

Department of Mechanical Engineering

Delhi Technological University

ACKNOWLEDGEMENTS

First and foremost I am thankful to the almighty for keeping me fit, healthy and energetic during the entire course of my Ph.D. work.

I would like to express my gratitude to Prof. Jai Prakash Saini, Vice-chancellor, Delhi Technological University, Delhi for providing this opportunity to carry out this work in this prestigious institute.

I would like to convey my sincere gratitude to Prof. S. K. Garg, H.O.D., Department of Mechanical Engineering, DTU, Delhi for his valuable suggestions during this research work.

With pleasure, I would like to express my greatest gratitude to my supervisor Prof. Vipin, Department of Mechanical Engineering, Delhi Technological University, Delhi for his proficient guidance, intelligent approach, constructive critique, wholehearted and ever available help, which has been the primary impetus behind the research. He is not only the supervisor but also my guardian, without the wise advice and able guidance, it would have been impossible to complete. He is always on the stand by to bring me to positivity, hope and smiles when things didn't seem to favour. It has been an honor to be a Ph.D. scholar under his supervision. I respect all his contributions of time and ideas to make my Ph.D. productive. I am also thankful for the excellent example provided as a successful professor.

I would also like to sincerely acknowledge my gratitude to all faculty members of the Department of Mechanical Engineering, DTU, Delhi for their wholehearted cooperation in my research work.

My appreciation and deep sense of gratitude to Dr. Sachin Maheshwari, Prof., Department of MPAE, NSUT, Delhi, Prof. Abid Haleem, Department of Mechanical Engineering, Jamia Millia Islamia, Delhi, for giving valuable suggestions for the betterment of this work.

I sincerely thank the technical staff of Machine shop Mr. Pradeep Kumar and Mr. Amit and other laboratories of DTU Mr. Tek Chand, Mr. Virender, Mr. Sandeep for all the

support received during this work. I am also thankful to non-teaching staff of the Department of Mechanical Engineering, Central Library, Computer Centre, Administration and Academic Department for their timely help and coordination. I would also like to thank my senior and fellow researchers Dr. Mukesh Kumar, Mr. Deepak Sharma for extending help whenever I required it.

I would like to specially thank Dr. Dayanidhi Krishana Pathak, Assistant Professor, Department of Mechanical Engineering, G. B. Pant Engineering College (GBPEC), Okhla, Delhi for boosting my morale and extending help whenever I required it during my research. I also sincerely thank the technical staff Mr. Sewa Singh, Mr. Jai Prakash, Mr. Atul at GBPEC for providing me in-house support. I would also like to thank Expo tools private limited, Noida for providing graphite electrode free of cost for conducting this research.

Special mention is deserved for, who I am greatly indebted to my parents, my brother and sisters and in-laws for their love and blessings to see me scaling greater heights of life. My wife Mrs. Reena Lamba, without whose motivation and encouragement, the pursuit of this Ph.D. work would have never been possible. I thank her for care and supporting me throughout my research work. Last, but not the least I am thankful to my daughter Gaurvi Lamba and son Aariv Lamba whose single smile could remove all the tiredness of my work. Above all, I would thank the almighty for blessing such an affectionate and efficient people playing great asset for me.

Ajay Lamba

ABSTRACT

Electrical Discharge Machining (EDM) is largely accepted advanced machining method in the domain of subtractive manufacturing processes across the globe. It caters lot of manufacturing applications involving generation of intricate shapes and machining hard to machine alloys in aerospace, defence, medical, and automobile industries. In this era of increasing competition, the developers and researchers are heading towards improvements of the method through various attempts. The focus area has always been the improvement of response measures.

The literature reveals the successful attempts by researchers through modification to die-sinker electrical discharge machine by adding electrode rotation and with abrasive mixed dielectric fluid. The blend of these two alterations has been attempted through this research study.

Two primitive materials, EN31 and D3 steel along with graphite and copper tool were taken for analysis keeping in view their wide scope of application in die industry. The aim is to provide a modified method which could be accepted for industrial usage. For this, a full factorial experimentation with three parameters i.e. tool rotation, current on time, and peak current at three levels each was planned. Three prominent responses were focused as output measures i.e. surface finish, electrode wear rate and material removal rate (MRR). The statistical model was generated which is effective in forecasting the response values. Analysis of variance revealed important parameters along with their interactions affecting response measures. The samples were also tested with scanning electron microscopy for surface morphology analysis.

Abrasive mixed rotary electrical discharge machining (AREDM) enhanced the surface characteristics by attaining lower roughness values and recast layer thickness. In percentage terms, surface finish improved by 5.17% with variation of tool rotation from 1200 rpm to 1800 rpm while machining EN31 steel with graphite electrode. While with D3 steel, improvement in surface finish by 9.15% and 26.86% were recorded with graphite and copper electrode, respectively. For EN31 steel, a thin recast layer thickness of 32.29 μm was formed in AREDM compared to 62.25 μm in conventional EDM when machined with copper electrode. Comparing Recast Layer thickness (RLT) in

AREDM with graphite and copper, graphite outperformed copper tool with RLT of 6.12 μm. Surface modification was also seen with the help of sub-surface micro hardness results. The sub-surface micro hardness increased from 514.59 HV0.5 to 533.23 HV0.5 in EN31 steel with graphite electrode and from 503.55 HV0.5 to 523.54 HV0.5 with copper electrode. Further, the surface morphology results at mid values of parameters were compared with conventional electrical discharge machining to see the improvements with existing methodology.

Finally, multi-objective optimization was performed with grey relational method and optimum parametric settings were obtained.

CONTENTS

LIST OF FIGURES

LIST OF TABLES

LIST OF SYMBOLS AND ABBREVIATIONS

Pc	Peak current
Ton	Pulse on time
Toff	Pulse off time
EDM	Electric discharge machining
AREDM	Abrasive rotary electric discharge machining
SiC	Silicon carbide powder
MRR	Material removal rate
TWR	Tool wear rate
SR	Surface roughness
EDS	Energy dispersive spectroscopy
XRD	X-Ray diffraction
DSO	Digital storage oscilloscope
ANOVA	Analysis of variance
FESEM	Field emission scanning electron microscopy
RLT	Recast layer thickness
CAD	Computer aided design

CHAPTER-1

INTRODUCTION

1.1 Introduction

Electrical discharge machining is a preeminent subtractive machining method. All the traditional machining processes involve a physical connect between the electrode and piece to be worked upon. It involves harder tool to machine softer work materials. This necessity of harder tool becomes critical when hardest materials like tungsten carbide and composites are to be machined. This essentially increases the cost and time of machining as tool replacement time is added in between. The increase in tooling cost and total time of machining is a very big concern for manufacturing industries. These manufacturing constraints led to the development of indirect machining method i.e. electrical discharge machining (EDM). The term "indirect" here refers to "no contact between tool and work material". As it doesn't involve direct contact, a softer tool can be employed to process any hard material provided they are electrically conductive and are immersed in dielectric medium. The dielectric medium here bridges the space between electrode and the piece to be machined. On applying current, the sparks are produced which extracts the material taken away by continuously circulating media. The EDM process mostly finds applications in making contours that are toilsome to produce by regular machines.

1.2 Genesis of EDM process

The genesis of EDM goes back to the time of mid 17^{th} century when Benjamin Priestly identified the material removal between two electrodes in the year 1751 recognized as "footprints". Then after, in 1766, Joseph Priestly reported the generation of rings-marks from discharges while experimenting with "Leiden Jars". Around 164 years have passed without much progress until during 1930ties when an American company ELOX developed a machine called Disintegrator. This machine used intermittent arcs to remove broken taps from work pieces. These electrical discharges which were referred as arcs could not be controlled to get material removal until the pressure of World War II compelled the researchers to develop the circuit to control the arc for machining of metals, particularly in Russia. The researchers worked in this area to convert arcs into controlled sparks by developing the controller circuits. The main requirement at that time was to have a machining method which is successful in cutting hard materials.

B. R. and N. L. Lazarenko, two Russian scientists, were assigned a task in 1943 during World War II to find out the ways to minimize wear of electrical contacts due to sparking.

They didn't succeed but have identified a phenomenon that led to the development of EDM machine i.e. erosion can be controlled more precisely by dipping the electrodes into liquid medium. Immediately, they developed an apparatus and patented the idea for its practical implementation. It was patented on Sept 24, 1946. Dagobert W. Rudorff has patented the idea of machining with wire electrode. It is said to be first proposal of wire EDM. Later, he became founder of Sparcatron Co. in UK, an EDM manufacturing company. It's not that people in Soviet Union were only working on development of EDM but an independent American team including scientist Harold Stark, Victor Harding and Jack Beaver were also trying to develop an EDM machine. The years of fifties and sixties were attributed to spread of sparking technology from laboratory to workshops.

With the development of planer transistor in 1959 by Hoerni and Noyce and first microprocessor by Intel in 1971, an upsurge was seen in EDM development. Here, it becomes obligatory to mention that emerge of spark technology from laboratory to workshop is attributed to dual impact of "Science Push" and "Market Pull". It is pushed by research community and parallel development in science from one side and pulled by industry people for their vested interest to capture the market on other side. Apart from controller circuitry, researchers also worked on improvement of table positioning through changes in axes drive technology. The X and Y table movements were performed with 4-way servo valve drives till late sixties when it took a shift during years of seventies to servo controlled drive. The industry people have also urged to have a common tool for rough and finish cutting which led to the development of planetary electrode movement, at first an accessory device to an integrated unit. With the advent of technology in microprocessor and controller circuits, EDM machining became more efficient. The first wire EDM machine was developed in 1967 by Soviet Union. In USA, Andrew engineering developed a wire EDM capable of generating contour as per drawing. Later, in 1976, they developed the first CNC based wire EDM machine. Presently, EDM is an established technology recognised worldwide (Schumacher et. al 2013).

1.3 EDM process

EDM is a thermal erosion process involving dielectric medium. The machining zone is immersed in dielectric fluid inside the working tank. The space between machining entities

is known as inter-electrode gap (IEG) (5-100 μm)(Lin *et al* 2009). With the help of DC pulse generator, potential difference is applied which generates an electric field in the space. As a result of this, intermittent sparking takes place leaving craters on the work piece and tool surface. The formation of craters results in ejection of tiny material particles, often known as debris. The operation of EDM is such that work piece remains stationary while the tool moves up and down continuously. This up and down movement of tool is controlled precisely by servo controller which is an important part of the process helping in removal of debris. As the process is an intermittent sparking process, the upward movement of the tool happens during the non-sparking time, often known as pulse off time. During the upward movement, a void is created, as a result of removal of shock wave, which is filled by surrounding dielectric fluid. In this process, a little swirl is generated which takes away all the debris. After this, the dielectric fluid goes in the storage tank from which it is recirculated again after passing through a filter system with the help of a pump. The EDM machine also has a provision to feed pressurised dielectric fluid directly into the machining space with the help of a nozzle attached to a flexible pipe, as shown in figure 1.1. The figure 1.1 illustrates all the parts of an EDM setup.

1.4 Material ejection process

The mechanism of material ejection in EDM is expounded through the following sub sections.

1.4.1 Ignition

In this process, tool and work piece are exposed to a potential difference with the help of a controller. This applied voltage sets up an electric field between tool and work piece. This state is portrayed in figure 1.2(a & b).

1.4.2 Building of plasma channel

In EDM process, electrode and piece to be machined must be electrically conductive. The electrically conductive tool and work piece means that both have free electrons. Due to formation of electrical field, the free electrons are exposed to an environment of electrostatic forces. If the work function of tool material is less, electrons are ejected out from the tool towards the work material. This phenomenon is referred as “cold emission of

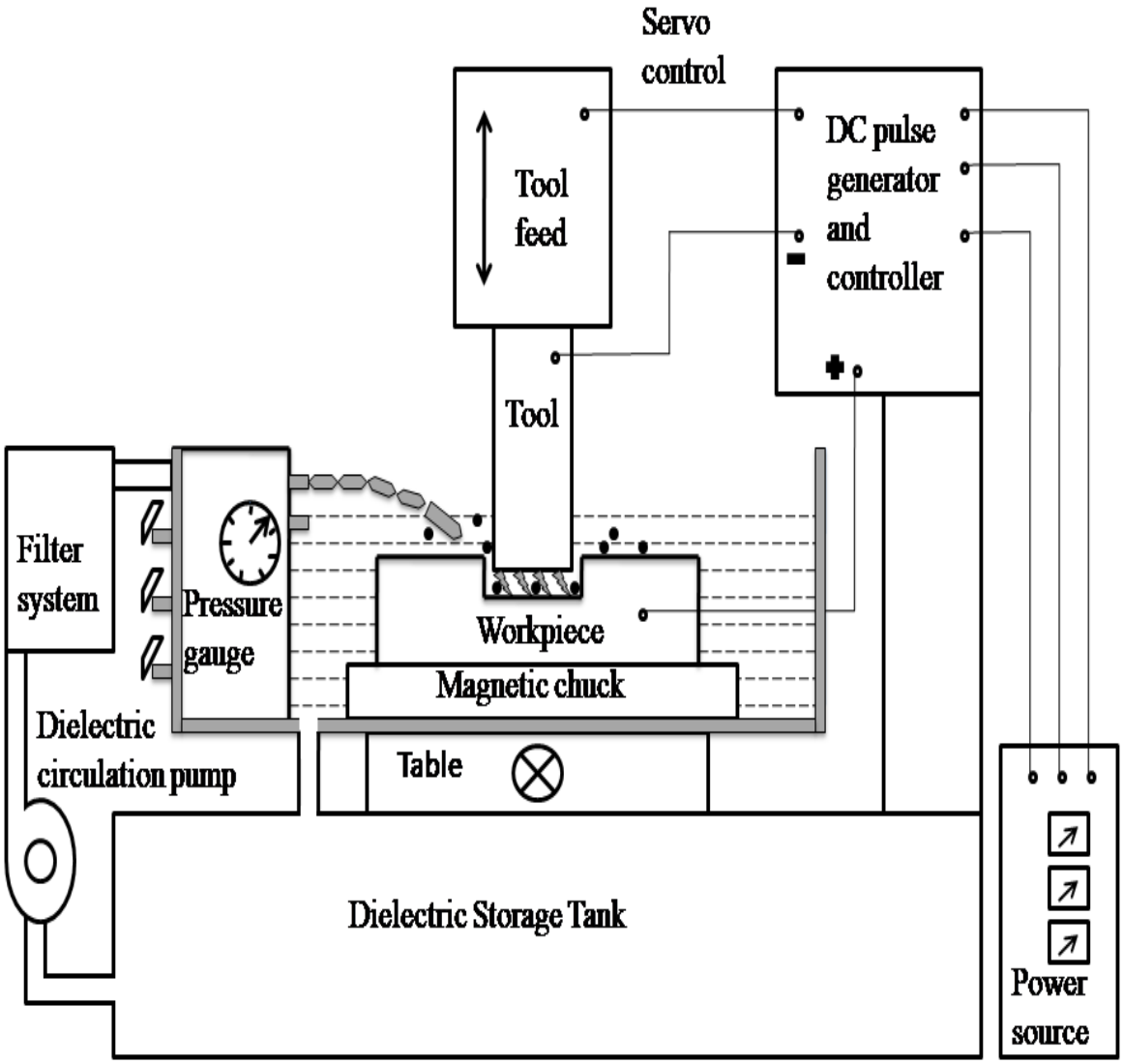

Figure 1.1. EDM setup.

electrons". The electrons travel through a liquid medium in which they strikes with the molecules of dielectric fluid. On collision, the high energy electrons ionize the dielectric molecules. As a result, additional ions and electrons are created. The electrons produced this way are again accelerated leading to further collision and formation of secondary and tertiary electrons. This process leads to formation of more and more ions and electrons. The ionization then reaches a stage where avalanche of electron movement takes place from electrode to piece and ions from piece to electrode. This avalanche action of electrons is referred as formation of plasma channel between tool and work piece, shown in figure 1.2(c).

1.4.3 Melting and evaporation

The building of plasma channel between electrode and work piece is a state wherein electrons moves fastest from tool to work piece as the path has minimum resistance at this level assuming tool as cathode. It is seen as spark between the two terminals. These high speed electrons impinge on the surface of work piece generating high heat. In this way, the kinetic energy of striking electrons gets converted into the thermal energy on the top of work piece. Such bombardment of electrons results in increase of temperature to a high value near 8000°C to 20000°C on the surface of work piece resulting in localised melting and vaporization of material, shown in figure 1.2(d) (Ho and Newman 2003).

1.4.4 Molten metal ejection and debris removal

The open circuit voltage is not supplied in EDM to avoid arcing; rather, the process applies the voltage in steps. It is applied for a definite time called as current on time and then after it is withdrawn. Current off time refers to the time for which voltage is withdrawn. The moment, voltage is withdrawn; a shock wave is generated resulting in ejection of material. This ejection of tiny material happens leaving voids on the work piece. These tiny particles disintegrated from the work piece are called debris, shown by black dots in figure 1.2(e). The debris removed from the space between tool and work piece by continuously flowing dielectric liquid. The inter-electrode gap reinstated to normal condition as shown in figure 1.2(f).

1.5 Classification of EDM

Electrical discharge machine is classified in figure 1.3. These different types are illustrated in the following sections.

1.5.1 Die-Sinker EDM – The Die-Sinker EDM employs the different variety of tool shapes to get the cavity. It is also known as Ram or Plunge EDM. Both rough and finish machining are used to get the final shape. It generally requires multiple passes. The Die-Sinkers are available with three axes i.e. Z, Y and X. The Y and X axis governs the work piece movement horizontally while the Z axis governs the tool movement vertically. Figure 1.1. shows a picture of Die-Sinker EDM for illustration.

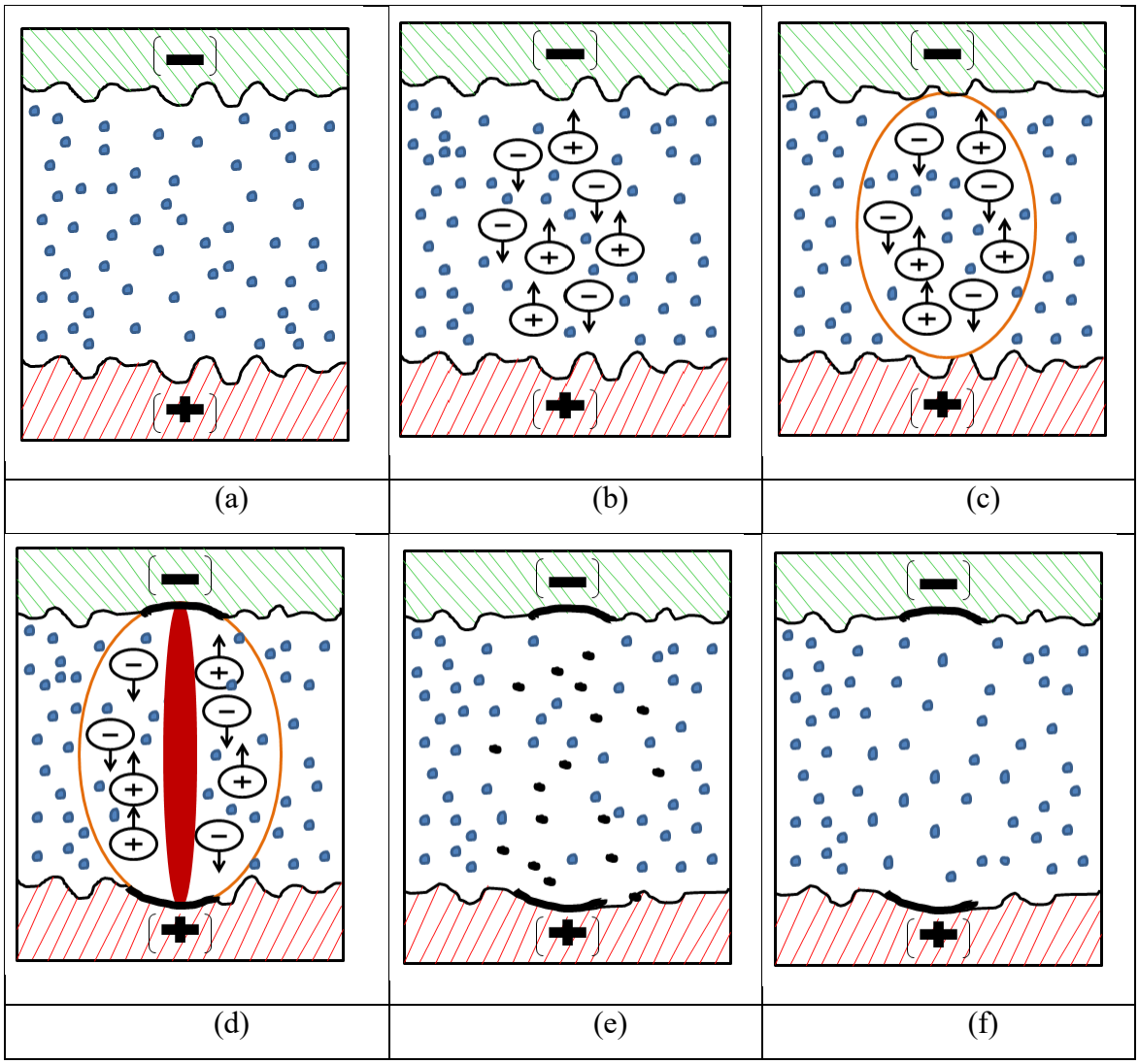

Figure 1.2. (a) Just before ignition (b) Ignition period (c) Formation of plasma channel (d) Melting and evaporation (e) Molten metal ejection and debris removal (f) Normal state after debris removal.

1.5.2 Wire EDM – Wire EDM is very popular EDM variant, largely used in industries for producing contours of any shape. In this EDM variant, a very fine electrically conductive wire is used to cut the material which gets consumed in the process of cutting. All wire EDM machines are equipped with a wire drive system which continuously replaces the old and used wire so that always fresh wire is available for cutting. The most common wire materials are copper and brass of diameter 0.015 to 0.3 mm. The widely accepted accuracy of wire EDM is ± 0.005 mm. The 5-axis CNC wire EDM machines are very capable in producing typical shapes in one set up. This saves the cost a lot.

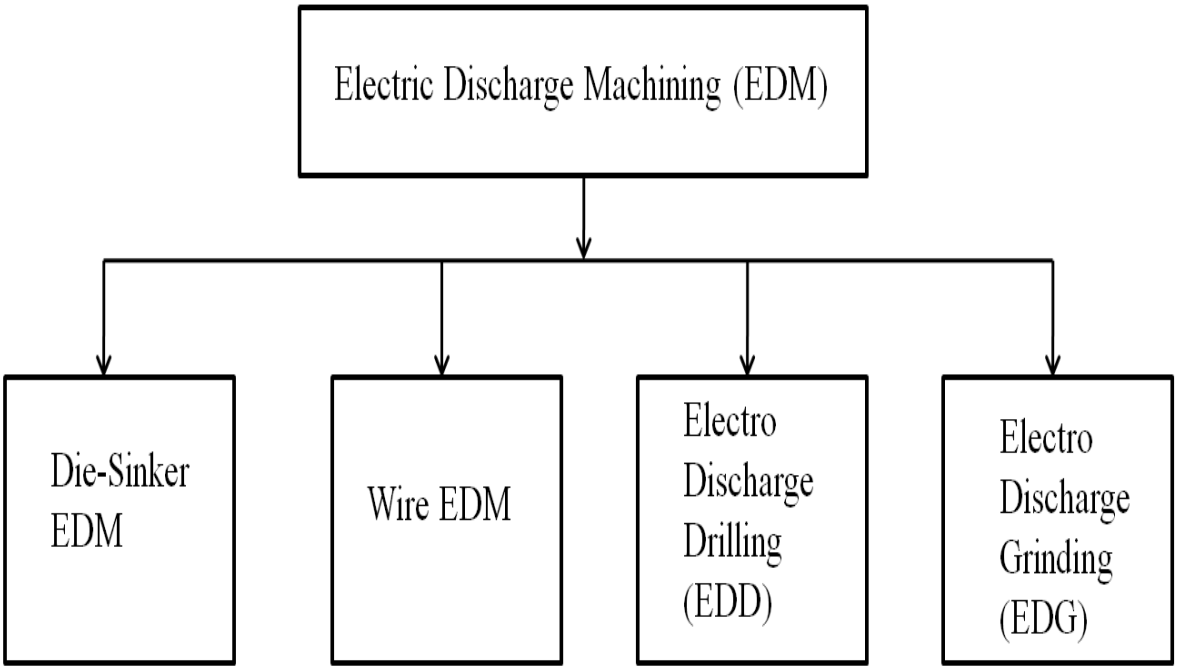

Figure 1.3. Classification of EDM.

1.5.3 Electro Discharge Drilling – Electro discharge drilling is a new and excellent variant of electrical discharge machining, specialized for making drilling job easier in extremely hard materials including composites, tungsten carbides etc which is beyond the scope of machining with twist drill. It is used for drilling of small holes of diameter up to microscopic dimensions in electrically conductive work pieces. The electrodes used are tubular which have provisions to pass dielectric fluid through them. It is an essential characteristic to flush away the debris generated during cutting. The generally used electrode materials are copper, brass and graphite of diameter ranging from 0.3 mm to 6 mm. It also has the capability to drill holes angled to the surface. The application areas include gas turbines, cooling holes in aero blades, cooling holes in lubrication and fuel systems of automobiles.

1.5.4 Electro Discharge Grinding – Electro discharge grinding is very similar to die-sinker electro discharge machining with just one change i.e. replacement of stationary electrode in die-sinker EDM with rotating wheel. This rotating wheel acts as an electrode in electro discharge grinding. The application areas include grinding of hardened die surfaces, inserts made of carbide, irregular cavities etc.

1.6 Configuration of the thesis

Chapter 1: It discusses the electrical discharge machine, its historical background and evolution, different stages of material removal mechanism and classification of the process. At last, the overall structure of the whole thesis is also presented.

Chapter 2: This chapter conveys information about contributions and development in the field of EDM by different researchers. It is tried to include the most important outcomes in the described papers in terms of information about the machine, method, process, parametric settings, output response, and the achievements of study. It also highlights the shortfalls in literature and accordingly, the objectives of the present study are showcased.

Chapter 3: It mainly caters to the development and fabrication of the experimental setup for conversion of conventional EDM to the proposed method. It presents a CAD model of die for better comprehension. Furthermore, it also caters the fabrication of electrodes, recording of voltage and current waveforms, powder characteristics, details of process parameters along with their levels, planning of experiments, information about workpiece and tool material, and chemical composition of parts.

Chapter 4: This chapter shows the experimental results. It reveals the input parametric settings and output responses. In addition, this chapter also shows the snapshots of cavity formed under different experimental conditions.

Chapter 5 and Chapter 6: These two chapters discuss the machining results and their analysis in detail for all four work tool material combinations taken in the study. It includes development of statistical models, validation, analysis of variance, surface morphology of the processed parts, recast layer estimation, Vickers hardness, and DSO waveforms analysis.

Chapter 7: It finally concludes the main findings of the present research study. Limitations of the study along with future scope of work is also presented in this.

Finally, the references are presented which were considered during this research work.

CHAPTER-2

LITERATURE REVIEW

2.1 Introduction

The researchers are very keen on exploring the different research capabilities on EDM since its inception. First and foremost thing which attracted the researchers is eroding process which doesn't involve direct contact between work piece and tool electrode. Since the commercialisation of the process, lot of literature is available from last 5 decades in EDM area but the recent research for the last 2 decades is focused the most. For this purpose, a large number of journals were referred on the subject of EDM. The extracts from meaningful reviewed papers are presented in the following section.

2.2 Literature review of EDM

Koshy et al (1993) – They investigated that the making of holes in the tool is impracticable, and flushing of the working gap poses a major problem. It is suggested that using a spinning disc tool is a more effective and precise method than using a regular tool. TWR, relative tool wear, MRR, corner accuracy, and SR were compared to those of a stationary tool. The electrode revolution effectively flushes the working gap, which greatly enhances MRR and produces surfaces with a superior finish.

Karthikeyan *et al* (1999) – They have reported the mathematical modeling of EDM with Al, SiC particulate composites. The models were evaluated using the analysis of Variance using a 3 level complete factorial design. While the TWR and the Ra were found to rise with an increase in the volume of SiC, the MRR was found to decrease as the % volume of SiC increased.

Chow *et al* (1999) – In this research paper, feasibility study of micro slit machining was done on conventional EDM with electrode in disk form to explore the effects of polarity, pulse duration, discharge current, and rotational speed on MRR, EWR, slit expansion, re-deposited material layer. The position of rotary disk electrode in RDE-EDM was different from conventional RDE-EDM in the way that in the former, the electrode was positioned below the work piece which is opposite in the latter. The biggest benefit of using the electrode beneath the work piece was easier removal of debris. The eroded debris were easily removed due to two reasons, firstly, due to rotation of electrode and secondly, due to

gravity. A thin copper rotary disk electrode of four different thickness (25, 50, 75, 100 μm) was used as electrode. The work piece used for experimentation was titanium alloy. The kerosene was employed as the circulating oil. The results showed that MRR initially increased, reached maximum value at 15 rpm and decreased at large rotational speed while the EWR increased monotonically with increase in rotational speed. Further, results also revealed that thicker tool helped in higher MRR. The MRR was also observed more with -ve polarity (workpart kept at -ve potential and tool at +ve). The maximum MRR reported in the study was 1.5 mm^3/min using optimum conditions at 15 rpm, 0.1 A current and 5 μm on-time pulse.

Wang and Yan (2000) – The investigation of drilling a Al2O3/6061Al composite utilising EDM electrode swirl was submitted by the authors. They asserted that, in contrast to solid electrodes, rotating eccentric through-hole electrodes produced higher MRR, but the measured electrode wear rate (EWR) was also higher. Additionally, they noted that while current intensity had an impact on EWR, electrode polarity mostly influenced SR and MRR.

Che Haron *et al* (2001) – Here, the investigators have seen the effects of current at two levels and change in electrode diameter on EDM of tool steel (230 HB). The copper with three different radius (i.e. 4.75, 6, 10 mm) was employed as the electrode. The machining on AISI 1045 tool steel was done at 2 levels i.e. 6.5 and 3.5 A to assess the effect on material ejection rate and rate of electrode wear. The investigation was accomplished on Mitsubishi model M35J. The machining was done for 20 minutes in which material ejection rate and electrode wear were calculated after every 5 minutes. The mass loss of work piece was found greater at 6.5 A, larger current than at 3.5 A, smaller current. The results inferred that the MRR is dependent on both the electrode diameter and current. The MRR with bigger diameter (20 mm) electrode was found more than the smaller diameter (9.5 and 12 mm) at 6.5 A current level. But, exactly opposite results were obtained at lower current level of 3.5 A i.e. smaller diameter electrode performed better than the bigger diameter electrode. The rate of electrode wear of smaller diameter was assessed more than the electrode with bigger diameter. The best performance was given at current level of 6.5 A and 20 mm diameter electrode achieving highest MRR and lowest EWR. The MRR and

EWR rate were found to be at same levels for first 5 minutes of machining. It was also concluded that small current is appropriate for smaller radius electrode and large current for bigger radius electrode.

Cogun and Akaslan (2002) – In this publication, work on edge wear of tool, TWR and MRR was reported**.** The inner radii was discovered to be rising with on-time pulse, pressure of EDM oil, and discharge current on electrode wear on the machining of 2080 die steel with a centre hole in Cu electrode.

Mohan *et al* (2002) – The authors have analyzed the variations of on-time pulse, current, polarity, tool material, and electrode swirl on the SR, EWR and MRR value in EDM with two volume percentage of silicon carbide. Cu and Br rods of ∅12 mm were employed as tool. The circulating oil was fed at a pressure of 3.5 kg/cm^2. The SR was assessed with the help of Surtronic three plus. The material removal rate was identified to be larger at +ve polarity juxtaposed to -ve polarity. It was observed that the MRR with Br was more than the Cu with more intensity of current irrespective of volume percentage of silicon carbide and polarity. They also claimed higher MRR with tool rotation compared to stationary electrode at all values of current levels. The authors also claimed less tool wear and better surface finish with rotary tool electrode compared to stationary electrode.

Simao *et al* (2003) – The modification of the surface was proposed using EDM by use of powder metallurgy (PM) tool with the use of powders suspended in the dielectric fluid, typically aluminum, titanium, and nickel. The surface alloying of AISI H13 hot work tool steel employing partly sintered WC/Co tools operating in a hydrocarbon oil dielectric is experimentally studied.

Fujun *et al* (2004) - They discussed the motion laws for machining rotary workpieces, the shaping concept of machining non-spheres with rotary tools, and a more in-depth analysis of the functions of machining non-sphere systems with rotary tools. These works serve as the foundation for studying the general rules of creating non-spheres using rotary tools to bevel circles and creating mathematical models.

Singh *et al* (2004) – The authors investigated the effects of changing the pulsed current with different tool electrode material on EWR, SR, MRR, and diameteral overcut on EDM of En 31 steel. The tool pieces taken for study were Cu, Cu-W, Br and Al. The radius of all the electrodes was 8 mm. The -ve polarity was employed throughout the machining. The machining depth was kept unchanged at 10 mm for all the work materials. The discharge current levels were 6, 7.5, 9, 10.5, 12 A. The experimental results showed that copper achieved the best MRR followed by aluminium, copper tungsten and brass. Further, copper also showed the persistent overcut with the rise in current. The tool wear was ascertained to be lowest with copper and copper tungsten followed by aluminium and brass. Hence, wear in brass electrode was maximum at all current levels. The surface roughness results showed that Cu-W gives low SR at higher current levels. It was also concluded that Cu and Al resulted in inadequate surface finish at large current levels. At last, authors have also highlighted future scope of work which can be done by combined study of effects of pulse on duration and current, re-deposited layer, micro-cracks, blocked stresses and deposition of carbon content. Finally, Cu was recommended as the best electrode material which results in higher MRR, less EWR, low diameteral overcut and better surface finish for the said material. The Al was graded next to Cu where surface finish can be overlooked.

Hewidy *et al* (2005) – They looked into the super alloy material and came to the conclusion that the TR, Ip, and duty factor all affect MRR, but only the Ip and duty factor together significantly affect Ra.

Kansal *et al* (2005) - In this research paper, the authors have presented an optimization of abrasive additive electrical discharge machining (AAEDM) by RSM. The effects of four factors namely, duty cycle, on-time pulse, concentration of silicon powder, peak current were investigated on SR and MRR of EN-31 tool steel. Cu rod of Ø25 mm was employed as tool. The attempts were conducted on EZNC fuzzy logic die-sinker EDM (Electronica Machine tools, India Ltd.). The experiments were performed with positive polarity and machining time was 60 minutes. The silicon powder size was in the range of 20-30 µm. A full factorial central composite design (CCD) was used which resulted in 30 experiments at 2 positions i.e. small and large. The range of process parameters namely, duty cycle, on-time pulse, concentration of silicon powder, and peak current were (0.7, 0.9), (50, 150 µs),

(0, 2 g/l), and (3, 12 A), respectively. The results concluded that inculcation of silicon powder improves the MRR. The behaviour of interaction terms obtained through response surface plot was explained. For MRR, two interactions were found significant, first, the interaction between pulse on time and peak current and, second, the interaction between peak current and concentration of silicon powder. The MRR increased with increase in peak current for any value of pulse on time. The maximum MRR resulted at high peak current (12 A) and high pulse on time (150 μs) and highest level of concentration of powder (2g/l). The regression equation for surface roughness indicated one significant interaction term i.e. the interaction between peak current and concentration of silicon powder. The surface finish was found to increase with increase in current up to 10 A, beyond which it decreased. The SR also increased with pulse on time. The best values of SR were obtained at low peak current (3 A) and pulse on time (50 μs). The confirmation tests were found in good agreement with predicted results from developed regression equations within ± 8% for MRR and -7.85% to 3.15% for SR. The authors also ended with future scope of increasing the concentration of silicon powder to achieve even higher MRR and some more improvements in SR.

Lin et al (2006) - They examined how the machining parameters of EDM (SR, TWR, MRR) affected the machining properties of SKH 57 steel. The L18 OA, which was used in some of the experiment, was based on the Taguchi technique. ANOVA and the F-test were also used to analyse the signal-to-noise ratios linked to the experiment's observed results.. The experiment showed that MRR rose with current. MRR first rose to a 100 μs on-time pulse, and then it started to fall.

Nizar *et al* (2006) – They reported thermal views of the EDM. The numerical observations showing the temperature distribution due to the EDM process were conveyed. The MRR and overall roughness were lowered from these thermal data and compared to experimental findings. The comparison demonstrated the significance of accounting for conductivity temperature change and provided superior correlations with experimental data.

Kansal *et al* (2007) - The authors worked on the machining of AISI D2 Die Steel with silicon powder of size 30 μm mixed in dielectric (kerosene oil) on EDM. The paper

effectively explains the phenomena of expansion of plasma and bridging effect concept in powder mixed electrical discharge machining. The experiments were performed on EZNC fuzzy logic die sinking EDM. A separate tank was prepared of 7 litres capacity to mix silicon powder. Two permanent magnets were used to separate the debris from the dielectric fluid. The material under study i.e. AISI D2 die steel was annealed to an average hardness of 59 HRC. The copper tool of 25 mm diameter was used as tool electrode. The input parameters taken in study were peak current, pulse on-time, pulse off-time, powder concentration, gain and nozzle flushing. The output performance measures were material removal rate (MRR) and surface roughness (SR). They have optimized the MRR and SR by Taguchi method. Further, ANOVA analysis was performed which showed that percentage contribution of peak current and powder concentration was found to be more among all the parameters for maximizing MRR. The authors highlighted the comparison between conventional EDM and powder mixed EDM and found that addition of silicon powder has considerably increased MRR. The machining time taken was 30 minutes. It was concluded that the effect of nozzle flushing does not significantly affect MRR. The optimum parametric settings (levels) found were peak current (10A), powder concentration (4 g/l), pulse on-time (100 μs), pulse off-time (15 μs) and gain (1 mm/s).

Dhar *et al* (2007) - In this paper, the effect of current, pulse on time and air gap voltage on metal removal rate (MRR), tool wear rate (TWR), radial over cut (ROC) on electrical discharge machining of Al-4Cu-6Si alloy-10 wt% SiC composites. The experiments were performed in a systematic manner with three successive trials using a PS LEADER ZNC EDM machine and a cylindrical brass electrode of 30 mm diameter. Three factors, three levels full factorial design was adopted for analyzing the results. A second order, non-linear mathematical model has been developed for establishing the relationship among machining parameters. Analysis of variance (ANOVA) has been performed to verify the fit and adequacy of the developed mathematical model.

It has been observed that the current has major effect on MRR followed by pulse duration and voltage. The MRR is found to increase non-linearly with increase in current for constant gap voltage and pulse on time. MRR is also found to increase slightly with increase in pulse duration. It is found that TWR also increases with increase in current as high current results in high thermal loading on both electrode (tool and work piece) leading

to higher amount of material being removed from either electrodes. It is generally found to first increase and then decrease for increasing amount of pulse duration within the scope of this experiment. The effect of gap voltage on TWR is negligible as compared to current. It is also found that an increase in current increases the radial overcut due to increase in MRR. An increase in pulse duration keeping all other factors constant also increases the radial overcut due to prolonged presence of spark thus producing an increase in energy per spark.

Shih and Shu (2008) – In this paper, machining ability of cold working tool steel AISI D2 by EDG (Electrical discharge grinding) was investigated. In this work, a rotary disk electrode was used. An EDM machine (P36+E50 model made by MAX SEE Industry Co. Ltd.) with CNC control was used. The dielectric fluid used was Castrol SPE oil having a hydrocarbon base. The parameters involved in this study were polarity, pulse duration, discharge depth, rotating speed, discharge direction, dielectric fluid and flushing direction. Taguchi's robust design methodology was used for designing the experiments. An L_{18} orthogonal array was designed for the experiments. It was found that both material removal rate (MRR) and surface roughness (SR) increases with respect to peak current and pulse duration in cases where polarity is either positive or negative. MRR and surface roughness both have a greater value while machining with a positive polarity. In order to obtain higher MRR on EDG, parameters such as positive electrode polarity, higher peak current and longer pulse duration are suggested. The machining parameters such as rotating speed, discharge current and flushing direction have no significant effect on MRR and surface roughness in this study. When using negative electrode polarity on EDG, the micro crater's crack density and micro hardness values were increased with the increase in pulse duration. Lower electrode wear rate was obtained with positive electrode polarity and with longer pulse duration machining parameters.

Khan (2008) – Through this research paper, the author has investigated the effects of peak current and voltage on the electrode wear and material removal rate on machining of aluminium and mild steel with copper and brass electrode. The experiments were performed on die-sink EDM (Mitsubishi EX 22 model C11EFP60E). The size of the electrode was 70 mm long, having a cross-section of 15 mm x 15 mm. The levels of the

input process parameters i.e. peak current and voltage were considered at (2.5, 3.5, 6.5 A) and (5, 10 V) respectively. The spark on time and duty cycle were kept constant at 3 μs and 62.5% respectively. The square holes were machined up to a depth of 3 mm. The electrode wear was measured in x and y direction. The x-direction was considered in the direction of cross-section of electrode and y-direction in the direction of tool length. The x and y-direction may also be understood as in the longitudinal and lateral direction respectively assuming tool electrode to be kept upright on table. The results showed that the electrode wear increased with increase in peak current and voltage. The wear in copper electrode was found to be less than that of brass electrode. The electrode erosion was more in the x-direction than that of y-direction. The electrode wear was also found to be more in mild steel compared to aluminium. The wear ratio was also analysed which found to increase with current and voltage. The high to low wear ratio of different work tool pair were in the order of steel-brass, aluminium-brass, steel-copper and aluminium-copper respectively. The material removal rate was also found to increase with current. The maximum MRR resulted with aluminium-brass pair.

Chow *et al* (2008) – In this paper, the authors presented a study using SiC powder in water for micro-slit EDM machining. A rotating thin disk of copper with diameter 42 mm, thickness of 25-50 μm was used as electrode. The work piece was Ti-6Al-4V alloy. The conventional die-sink EDM was modified for conducting experimentation in such a way that the work piece was installed above the electrode and dielectric fluid was supplied in the gap through a pipe. A digital oscilloscope was also used for recording the discharging waveform for detailed analysis. The results were presented with different polarity i.e. positive and negative polarity. The results have shown that higher MRR, lower EWR and surface roughness were obtained with negative polarity. The MRR was first increased and then decreased when plotted with increasing pulse on time values. The reason was attributed to the fact that when pulse duration was increased, it resulted in the expansion of discharge column, reduction of current density and discharge impact effect. The authors have also done the gap analysis when SiC powder was added. The gap was increased with lesser crater width with SiC powder in pure water. Typical waveforms obtained from digital oscilloscope have also shown that multiple peaks were observed on addition of SiC powder in pure water which resulted in increase of MRR. The surface roughness was also

found to be less with SiC powder. The addition of SiC powder also improved the machining burr compared to pure water.

Payal *et al* (2008) – They investigated EN-31 tool steel machined by EDM employing Br, Cu and Gr as tools and concluded that three specimens exhibited different pattern of heat affected zones.

Che Haron *et al* (2008) – In this research paper, the authors have tested the performance of copper and graphite electrode in electrical discharge machining of XW42 tool steel. The work material chosen was XW42 tool steel. The work material was machined with copper and graphite electrode of different diameters (10, 15, 20 mm) at two current levels of 3 and 6A. The objective was to find out a work tool combination with maximum MRR and minimum EWR. The machining was carried out for 20 minutes and mass loss was measured after every 5 minute. The result showed that wear rate of copper electrode was lower than that of graphite electrode. The mass loss of copper electrode was found to increase for smaller diameter on increasing the current from 3A to 6A. The ratio of mass loss percentage from 6A to 3A was up to ten times for graphite electrode and fifteen times for copper electrode. The MRR was found to be more with copper electrode than that of graphite electrode. It was also concluded that copper electrode is more suitable for roughing operation and graphite electrode for finishing operation.

Kung *et al* (2009) – A report on wear ratio of tool and MRR in the abrasive additive EDM was reported on cobalt bonded WC. RSM was used to get the experimental run order using CCD. Grain size, concentration of Al powder, on-time pulse and current were investigated. Study reported rise in MRR with Al powder.

Chattopadhyay *et al* (2009) – This paper presented the empirical model for predicting the output characteristics in electrical discharge machining of carbon steel (EN-8) with rotary copper electrode. The effects of process parameters namely, peak current, pulse on time and tool rotation were investigated on machining characteristics, material removal rate, electrode wear rate and surface roughness. The different levels of the process parameters, peak current, pulse on time and tool rotation considered for experimentation were (9, 18, 36

A), (50, 100, 200 μs) and (18, 32, 48 rpm) respectively. The experiments were performed on Charmilles EDM machine model-D20. A copper disk electrode was used having 6 mm thickness and 20 mm diameter. The rotation was provided to electrode with worm and worm wheel arrangement in which worm was rotated with a DC motor. Taguchi design of experiment was used to plan full factorial experiments with L 27 OA (3^3). The linear regression was used to develop the empirical models. The ANOVA was used for analysis of variance and to identify the significant and non-significant input factors. During the experiments, duty factor and side flushing pressure were kept constant at 50% and 0.5 bar respectively. The machining time was also kept fixed at 5 minutes. The results showed that material removal rate increased with increase in current. The maximum material was removed at 36 A, higher than that of 9 and 18 A. The tool rotation has resulted in decrease of MRR. The EWR increased with increase in current at all levels of pulse on time. The EWR was found to decrease with increase in tool rotation. The ANOVA results have revealed that the most significant parameters for MRR and EWR in order of importance were peak current, pulse on time and tool rotation respectively. The SR increased with both, increase in peak current and tool rotation. The most significant parameters for SR in order of importance were peak current, tool rotation and pulse on time respectively. The developed empirical models for MRR, EWR and SR predicted the output characteristics with 1.5%, 0.6% and 0.05% error respectively with 95% confidence level.

Satsangi and Chattopadhyay (2010) - The authors presented the work on rotary electrical discharge machining by taking EN-8 as work piece material and copper as tool electrode. The effects of three parameters namely, peak current, pulse on time and tool rotation were seen on material removal rate and surface roughness. The parametric settings for three parameters namely, peak current, pulse on time and tool rotation were (9, 18, 36 A), (100, 200 μs) and (10, 18, 32, 48 rpm) respectively. The duty cycle and side flushing pressure were kept fixed at 50% and 0.5 bar. The experiments were done with negative polarity. A copper electrode with 3 mm thickness and 12.7 mm diameter was used for machining. The experiments were conducted on Charmilles P25 EDM machine. The empirical models for MRR and SR were developed by linear regression analysis which conformed quite close to actual values. The results revealed that MRR increased with increase in current and decreased with increase in tool rotational speed and pulse on time. The surface roughness

also found to decrease with increase in current and tool rotational speed and decreased with increase in pulse on time. The authors have recommended high current, low pulse on time and low rotational speed for achieving high MRR and low current, high pulse on time, low rotational speed for achieving smooth surface finish.

Patel *et al* (2010) – The authors have worked on the optimization of process parameters in EDM of Al_2O_3 ceramic composite. They developed one material Al_2O_3-SiC_w-TiC for checking EDM machinability. The investigation of process parameters, namely, discharge current, pulse on time, duty cycle and gap voltage were conducted to observe collectively the effect on material removal rate and surface roughness. The electrolytic copper of diameter 8.5 mm was used as an electrode. The electrically conductive Al_2O_3 ceramic composite was used as the work piece, fabricated by hot pressing at 1700-1800°C a mixture of 30.9 volume% SiC wiskers, 23.0 volume% TiC powder and balance Al_2O_3. A square work piece of size 10 × 10 mm^2 having thickness 5 mm was used. The range of the discharge current, pulse on time, duty cycle and gap voltage were used as 3 to 7 A, 50 to 150 μs, 0.48 to 0.80 and 50 to 90 V respectively. The L_9 orthogonal array was used for conducting the experiments. The grey relational technique was used for multi response optimization. The ANOVA of grey relational grade was done which revealed that the discharge current and duty cycle were the most influential parameters. The percentage contribution of factors for discharge current, pulse on time, duty cycle and gap voltage on the grey relational grade were found to be 30%, 19%, 35% and 16% respectively. The largest value of grey relational grade was found for discharge current, pulse on time, duty cycle and gap voltage at 7A, 50 μs, 0.80 and 50 V respectively. These were the recommended values of process parameters which resulted in better material removal rate and surface roughness.

Jin et al (2012) –They investigated into the flow of debris and bubbles during EDM machining. It was discovered that the key element excluding the debris from the space/gap between the tool and the workpiece during a tool down-time was the bubble expansion. Finally, the results demonstrated that the tool jump speed had an impact on the degree of oil and debris mixing.

Bhattacharya *et al* (2012) – The authors have presented a study on three die steel materials during rough and finish electrical discharge machining in powder mixed EDM. They have also investigated the optimal parametric settings. The seven input process parameters were explored to see their effects on MRR, TWR and SF. Out of seven parameters, five were kept at three levels and two at two levels. The seven process parameters were work piece, dielectric, electrode, pulse off time, pulse on time, current and type of powder. The type and levels of parameters for work piece, dielectric, electrode, pulse off time, pulse on time, current and type of powder were (EN31, H11, HCHCr die steels), (kerosene, refined mineral oil (transformer oil)), (copper, tungsten-copper), (38, 57, 85 µs), (10, 50, 100 µs), (2, 5, 8 A) and (No, graphite, aluminium) respectively. The authors have also included three interactions which they have identified through pilot experimentation. These three interactions were interaction between work piece and electrode, between work piece and powder and between electrode and powder. The size of the work piece and tool were (100 x 50 x 10 mm) and (Ø20, length 50 mm) respectively. The experiments were carried out on Victory Electromech (model T-3822) EDM machine. The Taguchi's L_{27} orthogonal array was used to conduct the experiments. The results showed maximum MRR in EN31 followed by H11 and HCHCr die steels. The maximum MRR obtained with copper electrode and aluminium powder. The addition of graphite powder led to less MRR but good surface finish. The MRR was found to be affected by current, pulse on and off time (significant factors). The electrode material found to be insignificant when considered alone, but it had a significant effect while considering the interaction with suspended powder in the dielectric.

Aliakbari and Baseri (2012) – The authors in this research paper have presented an optimization study in rotary electrical discharge machining (REDM) by Taguchi method. Three parameters were investigated at three levels to access their effect on MRR, EWR, SR and overcut. The three machining parameters were peak current, pulse on time and tool rotational speed of electrode. The levels of peak current, pulse on time and tool rotational speed of electrode were (6, 9, 12 A), (35, 100, 150 µs) and (400, 800, 1200 rpm) respectively. The X210Cr12 (SPK) (application in die manufacturing) and copper were used as work piece and tool electrode. A cylindrical bar shape work piece was used with 15 mm diameter 25 mm length. Three copper electrodes of different configuration (one-solid,

second-with one eccentric hole of Ø3, third-with two symmetric eccentric holes) with outer diameter (Ø10) were used. The experiments were conducted on Tehran Ekram304H/60A EDM machine. A separate arrangement for tool rotation mounted on the Z-axis was used in this work. The experiments were conducted with L9 orthogonal array for all three types of electrodes. The experimental results were analyzed with Qualitek-4 software. ANOVA results were presented in this paper for each output characteristics with all three types of electrodes. The multi response optimization was also presented with weight method. The results showed less overcut with electrode having two symmetric eccentric holes than that of other two. The increase in MRR and decrease in EWR were reported with increased number of holes i.e. with third type of electrode.

Gurule and Nandurkar (2012) – This article claimed that using electrode swirl improved MRR. They tested the die steel using 7 variables in 3 different places. They asserted that flushing had no positive impact on MRR. At 900 rpm of electrode spin and 4 g/l powder mix, the maximum MRR was attained.

Teimouri and Baseri (2012) – They examined how different external magnetic field strengths and electrode swirl affected EDM. Investigations into the effects of process variables on Ra and MRR outputs were conducted. The Ra and MRR were found to be improved by introducing a rotating magnetic field around the cutting gap. Due to improved explusion of debris from the cutting area, the use of electrode swirl in conjunction with a rotating magnetic field improves machining performance.

Gopalakannan *et al* (2013) - They used Taguchi-based grey analysis to analyse the EDM variables used in the machining of aluminium metal matrix composite and found that current and Ton are the main factors influencing the quality of the composite. Ton is regarded as the key factor.

Srivastava and Pandey (2013) – The authors have done a comparative study of conventional EDM and ultrasonic assisted cryogenically cooled electrode electrical discharge machining (UACEDM) by taking input process parameters namely, discharge current, pulse on time, duty cycle and gap voltage on performance measures namely, electrode wear rate, material removal rate and surface roughness. The copper was used as tool material and M2 grade HSS as work piece. The work piece was having a hardness of

35 HRC with dimensions of 15 mm x 15 mm x 15 mm. In this work, authors designed a holding fixture to support the ultrasonic generator along with a holding attachment for cryogenic cooling of the electrode through which liquid nitrogen was passed. The range of controllable factors namely, discharge current, pulse on time, duty cycle, gap voltage were (3, 4, 5, 6, 7 A), (100, 200, 300, 400, 500 μs), (0.24, 0.40, 0.56, 0.72, 0.88), (50, 55, 60, 65, 70 V) respectively. The CCRD (Central composite rotatable design) of second order was used for conducting 31 experiments of 4 parameters at 5 levels. On comparison, they found that EWR and SR were significantly lower in UACEDM and MRR was at par with conventional EDM.

Anirban Bhattacharya *et al* (2013) – This research work dealt with surface modification of die steel by using different powders in dielectric fluid of electrical discharge machining i.e. through powder mixed EDM. The surface roughness and micro hardness of three different die steels were investigated with three powder combinations (silicon, graphite and tungsten) mixed in dielectric fluid. The work piece materials used in study were H11, HCHCr (high carbon high chromium) and AISI 1045 die steels. The seven process parameters were taken out of which, six were at three levels and one at two levels. These parameters were dielectric (kerosene and EDM oil), workpiece (H11, HCHCr, AISI 1045 die steel), electrode (graphite, brass, tungsten-copper), powder concentration (0, 5, 10 gm/l), peak current (3, 5, 7 A), pulse on time (20, 50, 100 μs), and powder type (Si, Gr, W). The parameters like open circuit voltage (135 V), machining time (10 min), pulse off time (85 μs), and reverse polarity were kept constant throughout the experiments. The tool electrodes were cylindrical in shape with 20 mm diameter. The experiments were conducted on T-3822 Victory Electromech EDM machine. The experiments were designed using L18 orthogonal array. The results revealed that powder concentration and current were the most significant factor affecting surface roughness. In case of micro hardness, powder concentration, current and pulse on time were found to be significant factors. For both surface roughness and micro hardness characteristics, work piece material and dielectric were found to be insignificant. The authors claimed 50% improvement in surface finish in powder mixed EDM than that of conventional EDM at a powder concentration of 10 gm/l. Better surface finish was resulted with tungsten powder and brass electrode. The surface finish decreased by 63% on increase of current from 3 A to 7A and by 52% on

increase of pulse on time from 20 µs to 100 µs. Brass electrode resulted in best surface finish followed by graphite and W-Cu. The W-Cu resulted in higher micro hardness than graphite and brass. The addition of tungsten powder in dielectric fluid of EDM resulted in better surface finish than graphite and silicon. There was no effect found on surface roughness due to dielectric. Further from SEM and EDS analysis, the authors found the deposition of carbon, powder and electrode material on all work materials.

Bai *et al* (2013) – In this research paper, a novel powder mixed near dry electrical discharge machining (PMND-EDM) was tried with different combinations of work piece and tool electrode. The single factor experiment method was used to see the effect of peak current, pulse on time, pulse off time, flow rate, tool rotational speed, air pressure and powder concentration on material removal rate. In single factor experiment method, the effect of each process parameter on MRR was obtained by varying one factor at different levels keeping all other factors as fixed. The experiments were conducted on SF201 CNC die-sinking EDM machine made by Agie Charmilles. The copper and brass electrodes were used in the experiments to machine 45 carbon steel and W18Cr4V as work piece. The outer and inner diameter of copper tubular electrode was 4 mm and 2 mm respectively. A rotary spindle with centre flushing capability was used. Having eleven gears, it was able to rotate the spindle from 0 rpm to 2000 rpm. The minimal quantity lubrication (MQL) device was used to fed dielectric medium into the inter electrode gap between tool and work piece. The range of driving pressure was 0.4 MPa to 0.8 Mpa which provided a flow rate of 0 to 2.68 cm^3/min. The negative tool polarity was used during the experimentation. The levels of each factor namely, peak current, pulse on time, pulse off time, flow rate, tool rotational speed, air pressure and powder concentration was (3.2, 9.4, 25.6, 37, 50, 64A), (1.8, 32, 130, 240, 420, 560µs), (2.4, 32, 75, 180, 320, 560, 750µs), (1.502, 1.11, 0.722, 0.398, 0.066ml/min), (2000, 1600, 1000, 600, 200 rpm), (0.4, 0.5, 0.6MPa) , (0, 3, 6, 9, 12, 15g/l) respectively. The ionization mechanism was explained in this paper. The machining results revealed that material removal rate increased with increase in current but, at higher current values, copper outperformed brass. The MRR was initially found to increase but later on it decreased on higher values of pulse on time. The MRR decreased with increase in pulse off time. The MRR increased with increase in flow rate. The MRR first increased and then decreased with increase in powder concentration. The MRR with brass was more than

copper. The MRR also increased with increase in air pressure. The MRR with brass was more than copper. The MRR decreased with increase in tool rotational speed. Although it decreased with both electrodes, but, brass material removal rate was more than copper. It was concluded in the context of improving MRR of W18Cr4V that brass should be used as tool electrode.

Beri et al (2014) – A comparative study of microhardness of the surface produced by powder metallurgy processed Cu-W electrode in EDM with traditional EDM was reported on Inconel 718. XRD investigation validated the results of surface betterment. Micro-hardness was also rose be proposed tooling from 380.9 HV to 496.7 HV.

Singh *et al* (2015) – In this research paper, the authors have investigated the effect of addition of graphite powder in the dielectric on the surface properties of super alloy Super Co 605 in electrical discharge machining process (PMEDM). The polarity, peak current, pulse on-time, pulse off-time, discharge voltage and flushing pressure were used as the input parameters and their effects were seen on micro-hardness in conventional EDM and powder mixed EDM i.e. without and with graphite powder in the dielectric fluid. The selected levels of parameters namely, polarity, peak current, pulse on-time, pulse off-time, discharge voltage and flushing pressure were (positive, negative), (3, 6, 9 A), (20, 50, 100 µs), (20, 40, 60 µs), (25, 30, 35 V) and (0.5, 0.75, 1 kg/cm^2) respectively. The experiments were conducted on Electronica ELEKTRA EMS 5535 model. A separate tank with dielectric circulation arrangement and a special fixture to hold the work material was used in this research work. The super alloy, Super Co 605 was used as it is extensively used in gas turbine blade manufacturing. The graphite electrode (Ø16) was used as the tool electrode in this paper. The powder concentration taken was 10 gm/l. The Taguchi's L_{18} orthogonal array was used for experimental runs. The experimental results showed increase in micro hardness from 320.82 to 1608.30 HV in conventional EDM and from 320.820 to 1315.2 HV in graphite powder mixed EDM. The conventional EDM lead to more micro-hardness than powder mixed EDM. The surface finish showed improvement from 2.23 to 1.99 µm. The ANOVA results showed peak current, polarity and pulse on time as the significant factors with 56.41%, 34.85%, 5.29% contribution in conventional EDM, while in powder mixed EDM, peak current, polarity and pulse on time were found to be significant with 73.23%, 14.25% and 6.83% respectively. The optimum results were

obtained at negative polarity, peak current (9 A) and pulse on time (20 µs), pulse off time (40 µs), discharge voltage (35 V) and flushing pressure 0.75 kg/cm^2.

Dewangan et al (2015) – They conducted the EDM experiments on the AISI P20 tool steel using Ø12 mm Cu electrode and investigated the surface integrity characteristics such as the re-deposited material thickness, SR and surface crack density. The discharge current was discovered to be the second most important element determining the surface integrity characteristics after on-time pulse.

Muthuramalingam and Mohan (2015) – Authors reviewed the electrical variables to enhance the thermal energy developed in the EDM process. The variation of electrical variables, discharge energy and pulse shape were focused on Ra, TWR, and MRR. The electrical process parameters, empirical connections between process parameters, and process parameter optimization in the EDM process were also covered.

Choudhary *et al* (2015) – In this study, effect of machining parameters like tool polarity, current, pulse on-time and voltage has been investigated on surface roughness of Nimonic75 alloy using Taguchi's experimental design technique.

Nimonic75 is one such alloy which belongs to the family of Nickel super alloys. It is widely used in manufacturing of turbine blades, aerospace fasteners and heat treatment equipments. The experiments were performed on Sparkonix Die-Sinking EDM. The tool used is of pure copper and of cylindrical cross section of dimension 10 mm and 100 mm diameter. The work piece used is Nimonic75 alloy of dimension 75 mm X 35 mm X 8 mm. Tool polarity was found as dominating factor for surface roughness followed by pulse on time and current. The minimum surface roughness was observed at negative tool polarity, 8 A current, 60 µs pulse on-time and 40 V gap voltage.

Torres *et al* (2015) - In this paper, researchers have taken Inconel 718 alloy as work piece material which is a hard to machine alloy having widespread applications in aeronautical, nuclear and automotive sector and modelling of three response variables namely surface finish, electrode wear and material removal rate was done. The parameters considered under study were current intensity, pulse time, duty cycle and open circuit voltage. The DOE was applied with 2^4 factorial design (4 factors at 2 levels each). The experiments

were performed on die sinking EDM machine ONA Datic type D-2030-S with jet flushing system at a pressure of 30 kpa. An electrolytic copper electrode with rectangular section (12 mm x 8 mm) was used. The work piece material dimensions were 32 mm x 28 mm x 10 mm. The second order models were generated through regression for MRR, EW and SR. It was found that the peak current was the most influential factor for material removal rate followed by duty cycle, open circuit voltage and pulse time. For surface roughness, current intensity proved to be the most influential factor followed by open circuit voltage and duty cycle.

Younis et al (2015) – To prevent residual stresses, SR, and fractures, researchers evaluated the impact of two types of electrodes, namely Dura graphite 11 and Poco Gr EDMC-3 electrode material on EDM of tool steel. It was revealed that POCO Gr EDMC-3 electrode imparted higher residual stresses compared with Dura Graphite 11 electrode.

Mandaloi *et al* (2016) – Crystalline structure of AISI M2 steel was investigated by using tungsten–thorium electrode through EDM. The SR, TWR and MRR of tool steel was done with 3 input process parameters. Following that, using various characterisation methods such as SEM, Atomic Force Microscopy (AFM) and Optical Surface Profiler (OSP), the surface topography of the treated material was evaluated. OSP and AFM studies yielded the lowest Ra values of 1.12 m and 2.18427 nm, respectively.

Dwivedi *et al* (2016a) – As per authors' analysis, the electrode swirl mechanism boosted the MRR by improving spark efficiency and debris clearance. They demonstrated how the occurrence of tool rotation considerably raised the average Ra and MRR by 11% and 41%, respectively. In addition, compared to the fixed tool EDM, the end surface has a more homogeneous structure, fewer microcracks, and a thinner recast layer.

Dwivedi *et al* (2016b) – The authors have worked on improvement of performance of EDM process with tool rotation. A rotary setup was used with permanent magnet direct current motor on Electronica Z-axis numerical control EDM machine. The experiments were performed on AISI D3 steel specimen (5 mm thick) using rotary copper tool (10 mm diameter) on electrical discharge drilling (EDD). The experiments were performed in two sets. In first set, the effect of change of current (10, 15, 20, 25 amperes) on MRR and SF were seen without tool rotation i.e. at 0 rpm. Then, in second set, the experiments were

performed at 1000 rpm. The constant parameters were voltage (75V), Ton (150 μm), Toff (58.33 μm), polarity (positive), feed rate (0.88mm/sec), dielectric (paraffin oil). The final machined surface with tool rotation was found to be more uniform in structure with less number of micro cracks and thinner recast layer as compared to stationary tool EDM. The authors achieved improvement in MRR and SF by 41% and 12% respectively.

Singh *et al* (2017) – A study of the argon gas assisted rotary EDM process variables was reported by the authors. The results indicated that rotary EDM (REDM) and air aided EDM (AAEDM) had larger wear of electrode and SR over argon gas assisted EDM (AGAEDM). AAEDM was said to have a larger MRR than REDM and AGAEDM. In addition, it was discovered that AAEDM included more re-deposited material thickness than REDM and AGAEDM.

Tanjilul *et al* (2018) – EDM process was used for drilling holes in Nickel-based super alloys. Significant information about the sizes of the debris particles under various machining settings is revealed by the study. Better Ra was seen in the case of suction-assisted drilling.

Patel *et al* (2018) – In this research paper, the authors have investigated the machining characteristics in powder mixed electrical discharge machining (PMEDM). The Inconel 718 was used as the work piece material and copper-tungsten as the tool electrode. The work piece and tool electrode size were 25 mm x 25 mm x 5 mm and 10 mm respectively. The EDM kerosene dielectric fluid was mixed with aluminium oxide (Al_2O_3) powder to find out the effects on material removal rate, tool wear rate and surface roughness. The effects of five process parameters namely, sparking gap, peak current, slurry concentration, pulse on time, duty cycle were seen on MRR, TWR and SR respectively. The levels of different process parameters namely, sparking gap, peak current, slurry concentration, pulse on time, duty cycle considered for experimentation were (50, 62 V), (9, 17, 28 A), (0.5, 1, 1.5 gm/l), (50, 100, 150 μs) and (0.4, 0.5, 0.6) respectively. The other fixed parameters during experimentation were inlet flushing pressure (3.5 kgf/cm^2), outlet flushing pressure (2 kgf/cm^2) and tool rotation speed (300 rpm). An attachment for providing rotation to tool was designed. A separate tank of dimensions 580 mm (L) x 440 mm (B) x 250 mm (H) was also used for sparking the job. Taguchi's L18 orthogonal array

was used for conducting experiments. A linear regression models were developed for MRR, TWR and SR with Minitab 16. The ANOVA results revealed peak current as the most significant factor for MRR as well as SR. The pulse on time was the most significant factor for TWR.

Beravala and Pandey (2018) – The authors have evaluated the effect of magnetic field on air and argon gas assisted EDM process. They have used liquid-cum-gaseous dielectric i.e. magnetic field- air assisted EDM (MF-AAEDM) and Magnetic field-Argon gas assisted EDM (MF-AGAEDM). They have considered five process parameters namely, pulse duration μs (100, 200, 300, 400, 500), duty cycle % (40, 50, 60, 70, 80), peak current A (3, 4, 5, 6, 7), air/argon gas pressure mm of Hg (1, 2, 3, 4, 5) and magnetic field density T (0.1, 0.2, 0.3, 0.4, 0.5). The work piece material was SAE 304 steel. The experiments were conducted on die-sinking EDM machine (Savita machine tools, ZNC EDM-3250). The setup used was consisting of two attachments, one for tool rotation and second with fixtures for magnets. During the experimentation, the electrode rotational speed was kept constant at 500 rpm. The gap voltage and machining time were also kept at 45 V and 15 minute respectively. The authors used central composite design and multi-objective optimization was done with genetic algorithm to obtain the optimum parametric levels. The findings of their study revealed that magnetic field increased the material removal rate by 21-41% and electrode wear rate by 7-14% in EDM process using liquid-air mixed dielectric.

Bhagat et al (2019) – On H13 die steel, they described the importance of the EDM process variables. The kind of tool material and the Ton have very little bearing on the MRR. Ip was the most significant element determining both the TWR percent (using Cu tool) and MRR. The best set of variables with Cu electrode were 14 A Ip and 150 μs Ton, for the highest MRR; 2 amp Ip and 150 μs Ton.

Kumar *et al* (2019) – In this research paper, a comparative study has been presented between the conventional EDM and nanopowder mixed EDM (NPMEDM). The term NPMEDM has been coined by mixing alumina nanopowder (Al_2O_3) in the dielectric fluid of EDM. The size of nanopowder was 45-50 nm. The dielectric fluid in conventional EDM and NPMEDM were deionised water and mixture of 1% of alumina powder in one litre of deionised water respectively. The effects of three process parameters namely, peak current,

pulse on time and gap voltage were investigated on material removal rate, surface roughness, surface morphology, recast layer thickness, surface topography and induced residual stresses. The levels of different process parameters i.e. peak current, pulse on time, gap voltage were (2, 5, 8 A), (8, 14, 20 µs) and (10, 30, 50 V) respectively. The other parameters kept fixed were spark timing at 3 µs, duty cycle at 50%, bypass current at 1A and tool surface area at 75 mm^2. The work piece and tool material were Inconel 825 and copper respectively. The experiments were conducted on Sparkonix ZNC EDM machine. The response surface method was used and conducted 15 experiments in each case i.e. conventional EDM and NPMEDM. The second order regression equations were developed using Minitab 17 software. The mechanism of NPMEDM was explained by authors with the help of recorded pulse waveform. The results showed that NPMEDM process results in increased gap distance, no arcing and uniform sparking. The MRR and SF were found to be better in NPMEDM than that of conventional EDM. The 57% increase in MRR and 63% decrease in SR were claimed in this paper. The less recast layer thickness (1 -2 µm) was measured in NPMEDM process declared to be one third than that of conventional EDM. The less micro holes, cracks, holes were seen in NPMEDM process. The less residual stresses were seen in work piece machined with NPMEDM process.

Bajaj et al (2020) – Authors reported blending of multi-wall carbon nanotube with EDM circulating media. The investigation was performed on EN31 steel. An improvement of 46.17% in MRR and 45.43% in SR was reported over traditional EDM. Surface topography was also claimed to be better by the blending in this research paper.

Deepak and Vipin (2020) – This paper reported study on EN31 steel with 3 variables at 3 positions in EDM with electrode swirl. The investigation was reported on SR. Variables taken were electrode swirl, concentration of powder, and current. They reported best surface conditions at 12A current, 1800 rpm electrode swirl, and 80g/l concentration of powder.

2.3 Summary of Literature review

The literature review revealed that lot of work has been done on different EDM directions, including, understanding the mechanism of material removal, optimization of input process parameters for certain output characteristics, study of different variants of EDM such as

electrical discharge grinding (EDG), electrical discharge drilling (EDD), electrical discharge turning (EDT), powder mixed EDM (PMEDM), nanopowder mixed EDM (NPMEDM), ultrasonic vibration assisted EDM, magnetic assisted EDM, ultrasonic vibration and magnetic field assisted EDM, EDM with tool rotation, vibro-rotary EDM, powder mixed EDM with tool rotation, near dry EDM etc. These dealt with the analysis of various machining and non machining parameters i.e. peak current, pulse on time, pulse off time, duty cycle, gap voltage, concentration of powder, positive (straight or normal polarity) & negative polarity (reverse polarity), electrode material, tool rotation and output responses have been seen on MRR (material removal rate), TWR (tool wear rate) and SR (surface roughness). However, the studies related to recast layer thickness, study of micro-cracks, micro-holes were also seen which included surface morphology and surface topography studies. The various researchers have reported experimental results on different materials such as high carbon steel, EN8 Carbon steel, EN31 tool steel, D3 Die steel, AISI H13 tool steel, Mild steel, Inconel 718, Inconel 825, SAE 304 steel, Nimonic 75 alloy, 45 carbon steel, M2 grade HSS, Al_2O_3-SiC_w-TiC composite, XW42 tool steel, Ti-6Al-4V alloy, aluminium, AISI D2 tool steel, AISI 1045 tool steel, Al-SiC metal matrix composite (MMC) etc. The different tool materials used as electrode were copper, copper-tungsten, brass, graphite, aluminium etc. The researchers have investigated the effects of mixing silicon, SiC, aluminium, chromium, nickel, copper, graphite etc. to the dielectric fluid of EDM as the abrasive powder on MRR, TWR and SR.

2.4 Research gap

The study of literature suggested that lot of in-depth work on different variants of EDM has been investigated for various electrical and non electrical parameters. Further careful exploration of EDM variants has come up with two powerful yet independently explored areas. The first area is electrical discharge machining with tool rotation i.e. rotary EDM (REDM). The second variant is powder mixed EDM i.e. identifying the effects of mixing abrasive powder in dielectric medium of EDM on machining characteristics such as material removal rate (MRR), tool wear rate (TWR) and surface roughness (SR). These two areas focused at maximizing MRR, minimizing TWR and surface roughness are combined in this research work for investigating the potential benefits of both. So, a combined study

of abrasive mixed electrical discharge machining with tool rotation is taken up as a research topic.

2.5 Objectives of present research

Electrical discharge machining is widely used in stamping tools, mould cooling slots, micro-pins, micro-cavities, die making, automobile and aerospace industries etc. The major performance measures in electrical discharge machining are MRR, TWR and SR. Now, it is a well known fact that EDM process gives low machining rate and poor surface finish. From productivity aspects, higher MRR is always desired with better surface quality. Tool life also plays an important role while aiming higher MRR and better surface quality as it affects the dimensional accuracy as well as tooling cost. The longer tool life also minimizes machining interruptions ultimately increasing productivity. So, from industrial point of view, engineers always intend to achieve multiple goals such as maximum material removal rate (MRR), minimum tool wear rate (TWR) and surface roughness (SR). Hence, it becomes utmost important to study all three output characteristics. As a result, in this research work, all three are taken up for analysis i.e. MRR, TWR and SR. Further the literature review has revealed that peak current and pulse on time are the two most important electrical parameters which affect MRR, TWR and SR. Tool rotation is the third parameter which is added to these two for combined study to analyse its impact on machining performance. So, three input process parameters are finalized for study in this research work i.e. peak current, pulse on time and tool rotation. Further, from literature review, D3 die steel and EN-31 tool steel are selected which are widely used materials in the application areas of EDM. Next, copper and graphite are selected as tool electrode materials. The SiC powder is selected as abrasive powder to be mixed with dielectric fluid of EDM as it has moderate density with high thermal conductivity. After the finalization of output performance measures, input process parameters, work piece and tool electrode material, abrasive powder, the following are the laid down objectives for this research work.

- To investigate the effect of different input process parameters on MRR, TWR and SR in abrasive mixed rotary EDM.
- To study the effect of rotation of tool electrode on MRR, TWR and SR.
- To optimize the cutting conditions for maximizing MRR, minimizing TWR and SR.

CHAPTER-3

MATERIALS AND METHODS

3.1 Conventional EDM machine

Figure 3.1. Conventional EDM machine (Sparkonix 35A).

The conventional EDM machine is shown in figure 3.1. This machine was used for conducting experiments after necessary modifications for tool rotation.

3.1.1 Sparkonix EDM machine specifications

The experimental research work was completed on Sparkonix 35A EDM machine available in machine shop of Mechanical Engineering department of DTU. The particulars of the machine are showcased in table 3.1.

Table 3.1. Particulars of Sparkonix 35A EDM machine.

Size of Table (mm)	550 x 350
Size of Tank (mm)	775 x 450 x 325
Movement, X (mm)	200
Movement, Y (mm)	200
Quill travel, Z (mm)	200
Maximum work piece height (mm)	300
Maximum weight of work piece (kg)	400
Maximum weight of electrode (kg)	35
Dielectric fluid tank capacity (litres)	260
Pump motor (H.P.)	1
Range of current variation (A)	1-35

3.2 Die design

The purpose of die is to provide tool rotation which is not available as a feature on conventional EDM machine. For this, two cast iron rods were purchased from the market. The radius and length of first rod was 45 mm and 60 mm respectively, while the second rod had radius and length as 20 mm and 70 mm respectively. The complete die consisted of below mentioned different parts:

1. Main body
2. Bearing (Two number)
3. C-clip
4. Step cylindrical part
5. Sprocket
6. Allen screw (Two number)

3.2.1 Main body

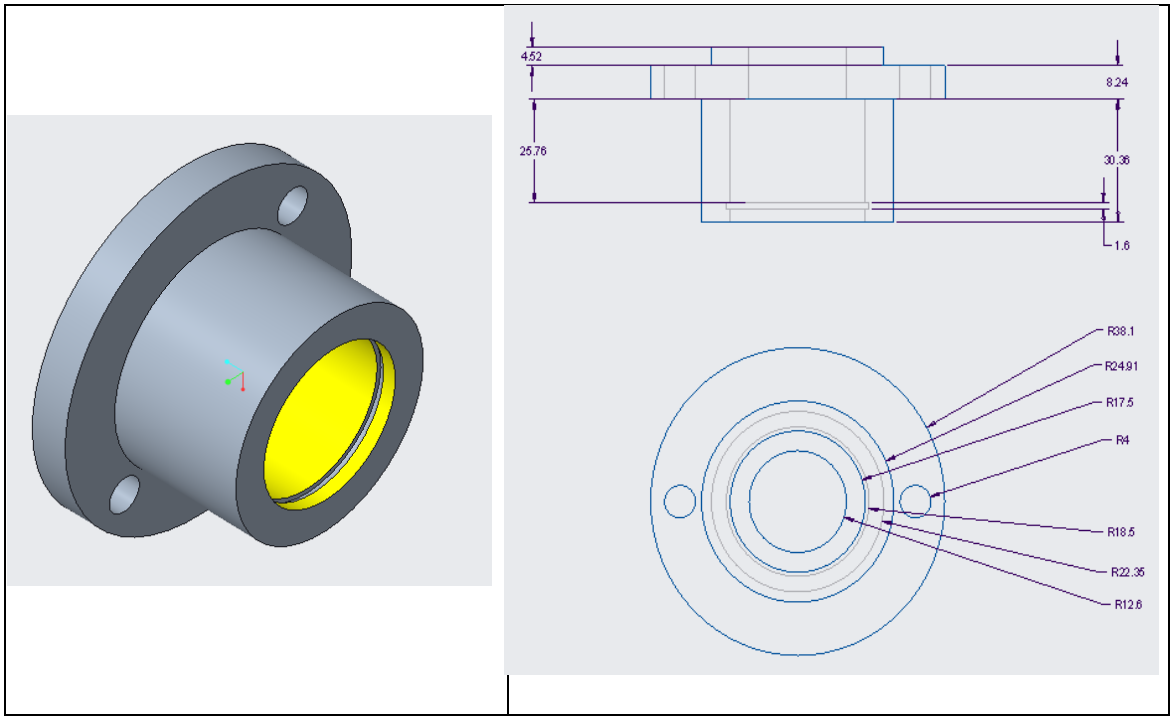

Figure 3.2. CAD model of Hub and its front and top view.

3.2.2 Bearing

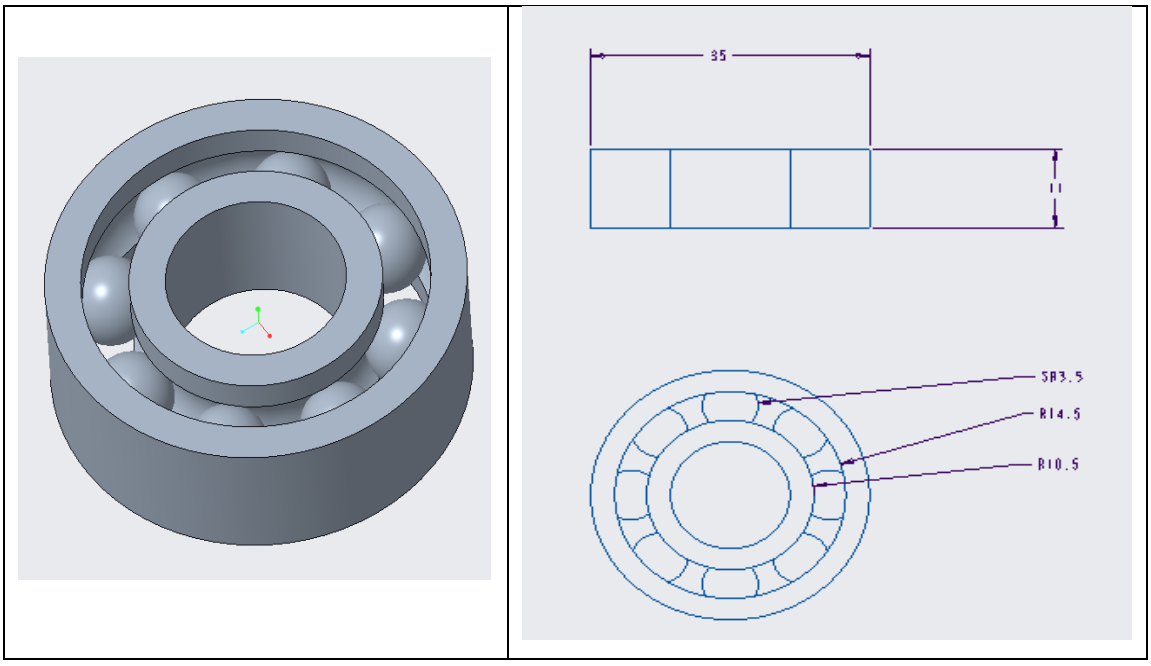

Figure 3.3. CAD model of Bearing and its front and top view.

3.2.3 C-Clip

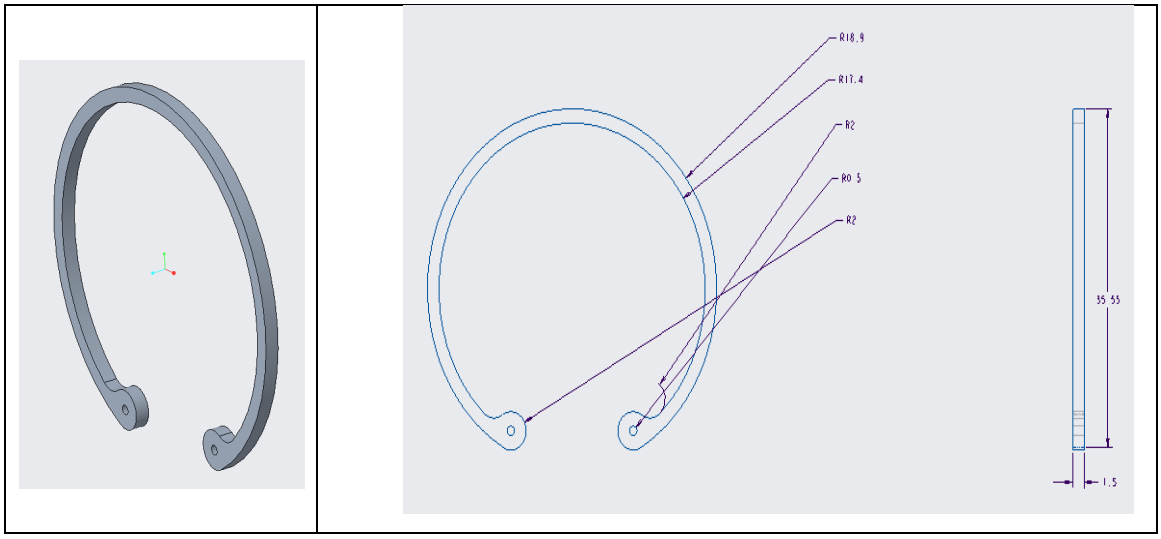

Figure 3.4. CAD model of C-clip and its front and side view.

3.2.4 Step cylindrical part

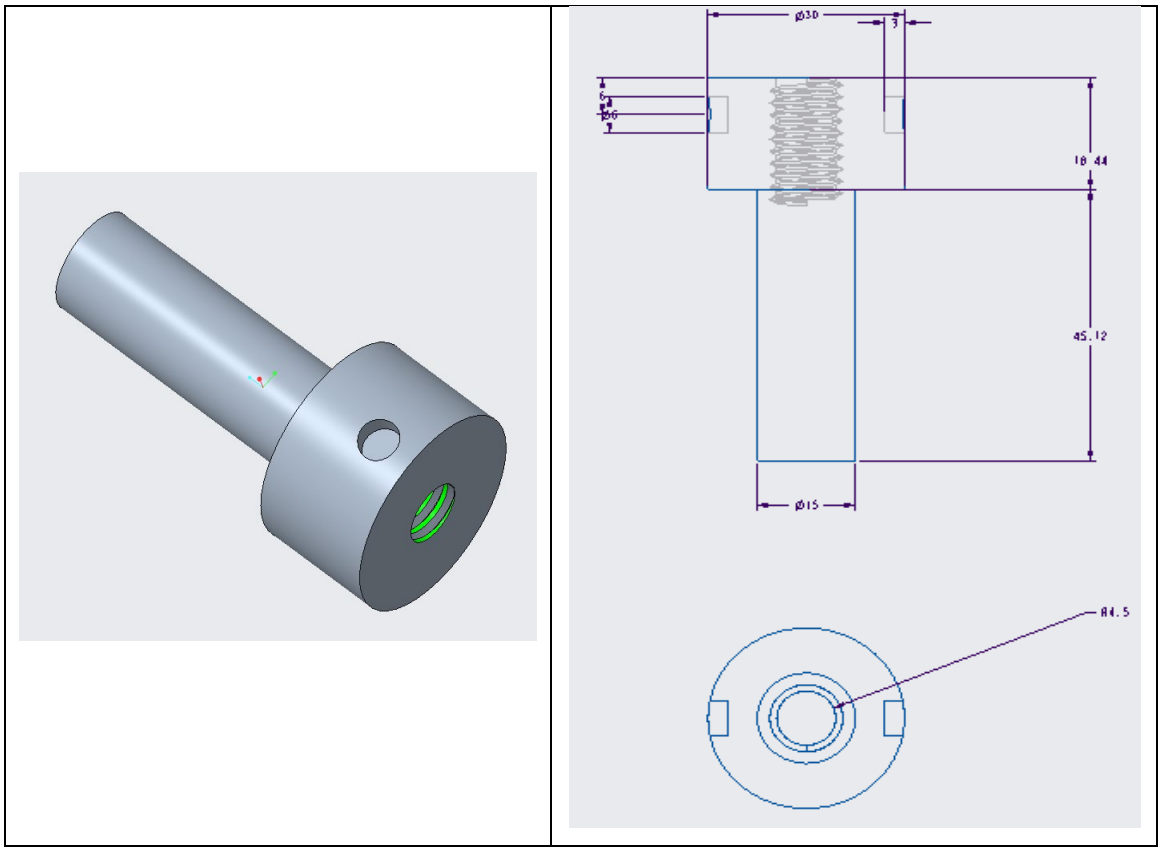

Figure 3.5. CAD model of step cylinder and its front and top view.

3.2.5 Sprocket

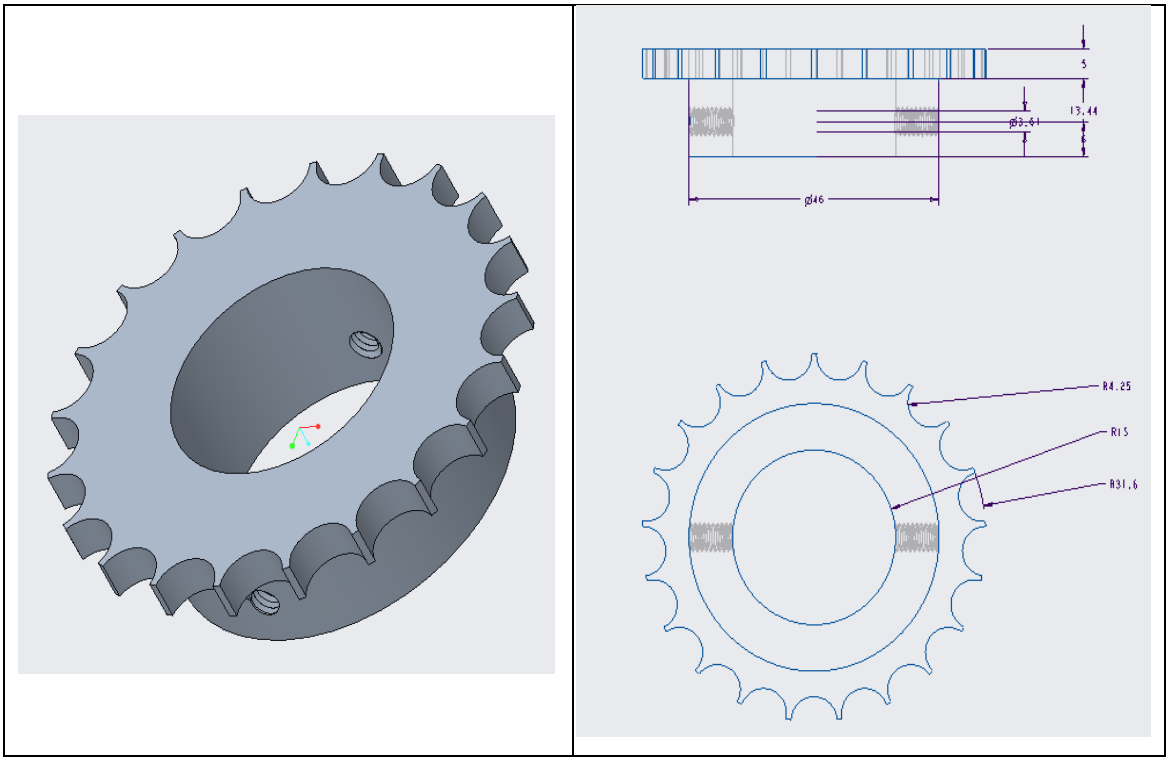

Figure 3.6. CAD model of sprocket and its front and top view.

3.2.6 Allen screw

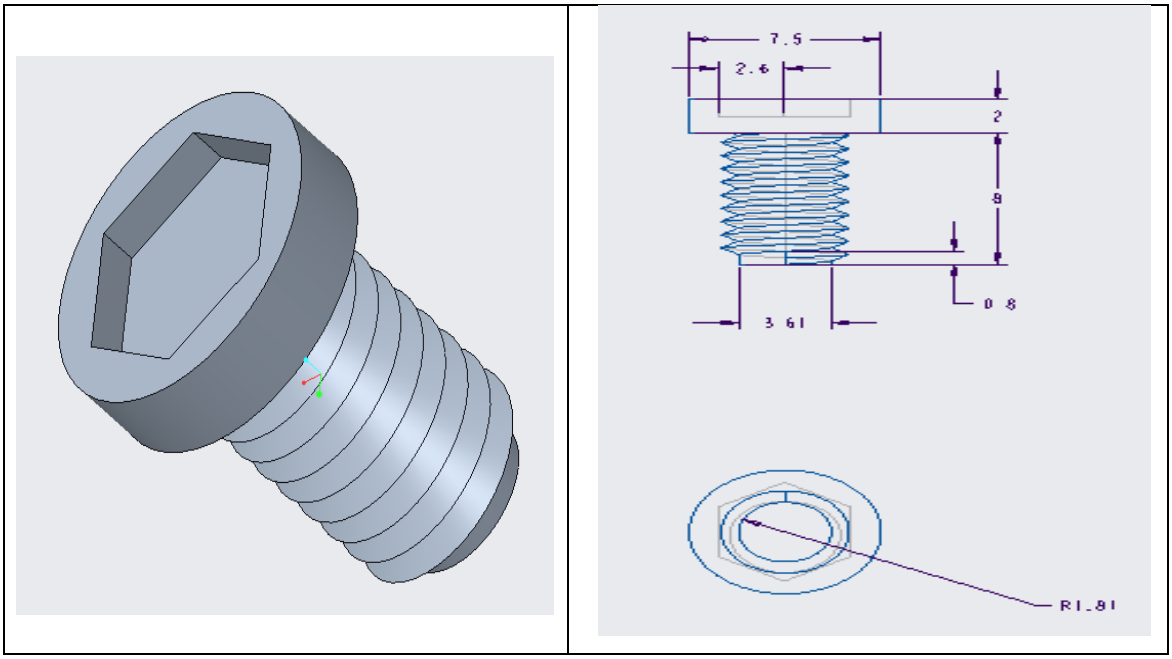

Figure 3.7. CAD model of allen screw and its front and top view.

3.2.7 Die assembly

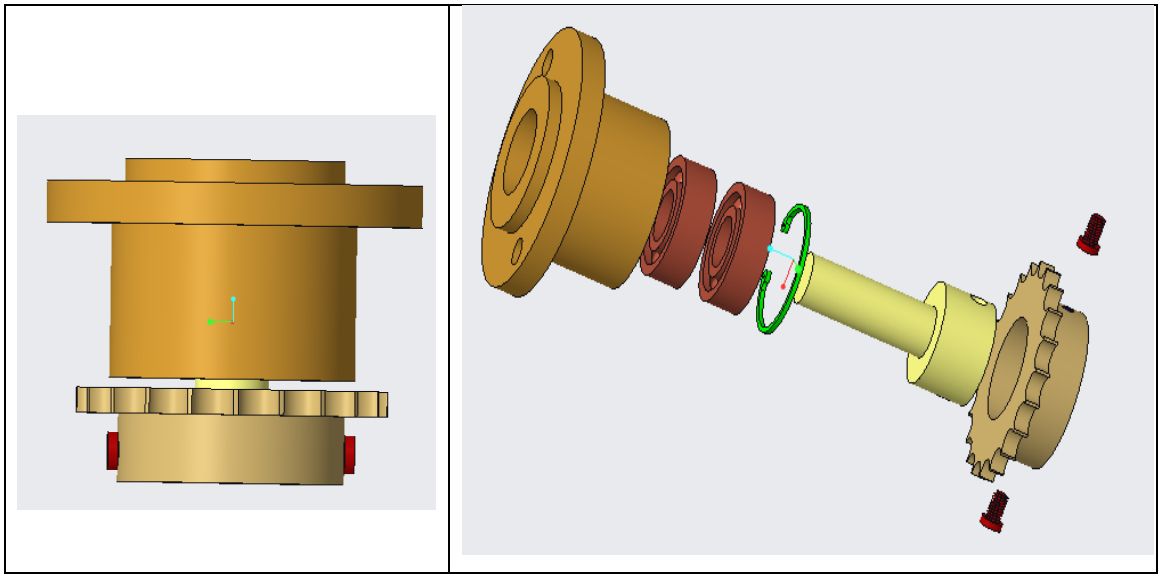

Figure 3.8. CAD model of complete rotary die and its exploded view.

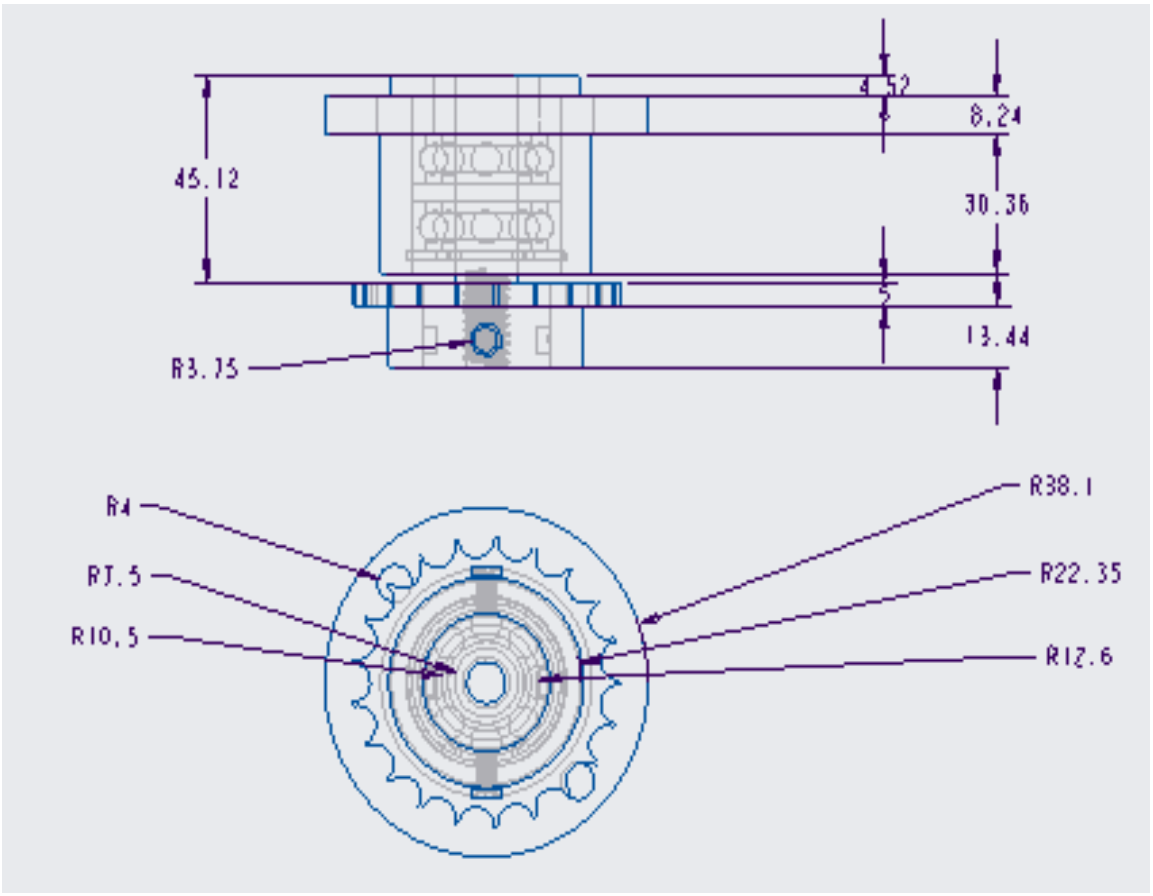

Figure 3.9. Front and top view of complete die.

3.3 Tool fabrication

Tool fabrication was done to fit the tool electrode into the rotary die. For this, it was essential to have thread on one side as it has to go inside the threaded portion of rotary die. As the study involves the investigation of tool wear rate of copper and graphite tool, initially, two raw electrolytic copper and graphite rods were taken and machined on lathe to cut to a size of 96 mm length (33 mm threaded portion and 63 mm remaining length of 20 mm diameter). The raw and fabricated copper tool are displayed in figure 3.10. Table 3.2 summarizes the properties of graphite and copper.

Figure 3.10. Before and after images of copper tool.

Table 3.2. Properties of graphite and copper tool.

Property	Unit	Graphite	Copper
Bulk density	Mg/m^3	1.78	8.96×10^9
Tensile strength	MPa	46	210 Ultimate, 33.3 Yield
Hardness	HSD, Vickers	76 HSD	50 Vickers
Flexural strength	MPa	65	218
Electrical resistivity	μΩ ·m	15	0.01673
Thermal expansion coefficient	10^{-6}/K	5.6	16.8
Young's modulus	GPa	12	116
Thermal conductivity	W/(m·K)	70	385
Compressive strength	MPa	135	206.84

In case of graphite electrode, selection of proper grade is very important. For this, different graphite grades were studied and finally, ISO 63 graphite grade was finalized for the experimental work, taken from Expo tools pvt. Ltd, A-19, Sector-5, Noida, U.P. The properties of this grade are mentioned in table 3.2 for reference. As graphite is a soft material, an extension was fabricated first which consisted of tapped hole on one side and tapped rod on the other. This extension was essentially made to safeguard the graphite electrode from braking due to frequent opening and closing of tool from die in each experimental run as the before and after weight have to be taken for measurement of tool wear. The diameter used was 20 mm. The raw and fabricated graphite tool are shown in figure 3.11. FESEM micrographs illustrated in figure 3.12 were used to perform an examination into the detection of pores in graphite tool. It was done to ensure surface quality of graphite tool as it has a direct impact on the surface roughness of the machined parts. For this, a sample of 10 mm diameter was prepared. Following that, facing was done to acquire the same surface condition as it had prior to each experiment in order to represent the right surface condition. Figure 3.12 depicts micrographs captured at low and high magnification ranging from 125x to 10kx. It may be clearly elucidated from figure 3.12 that overall quality of graphite is adequate, with few micro-pores with mean size of 24.87 μm (Image J software) as evident in figure 3.12(a). Some graphite flakes are seen as bright spots in figure 3.12(b), which is more obvious in figure 3.12(c& d). Table 3.2 further shows that the properties of the graphite tool utilised in this study are in moderate range, with adequate bulk density, hardness, and compressive strength. The machining time was kept constant for a period of 2 minutes for each experiment. The current off time was fixed at 30 μs. The experiments were repeated three times on same levels of the parameters (Lamba and Vipin 2022).

3.4 Method of rotation

Tool rotation requires additional setup as the conventional EDM available in lab doesn't have this facility. So, a die as explained in section 3.2 was fabricated in house. After the fabrication of die, an AC servo motor was used with speed controller as shown in figure 3.13. The selection of this particular servo motor was primarily due to its successful application in industrial sewing machines. The torque of the motor was upto 3 Nm which was sufficient to move a rotary die.

Figure 3.11. Before and after images of graphite tool.

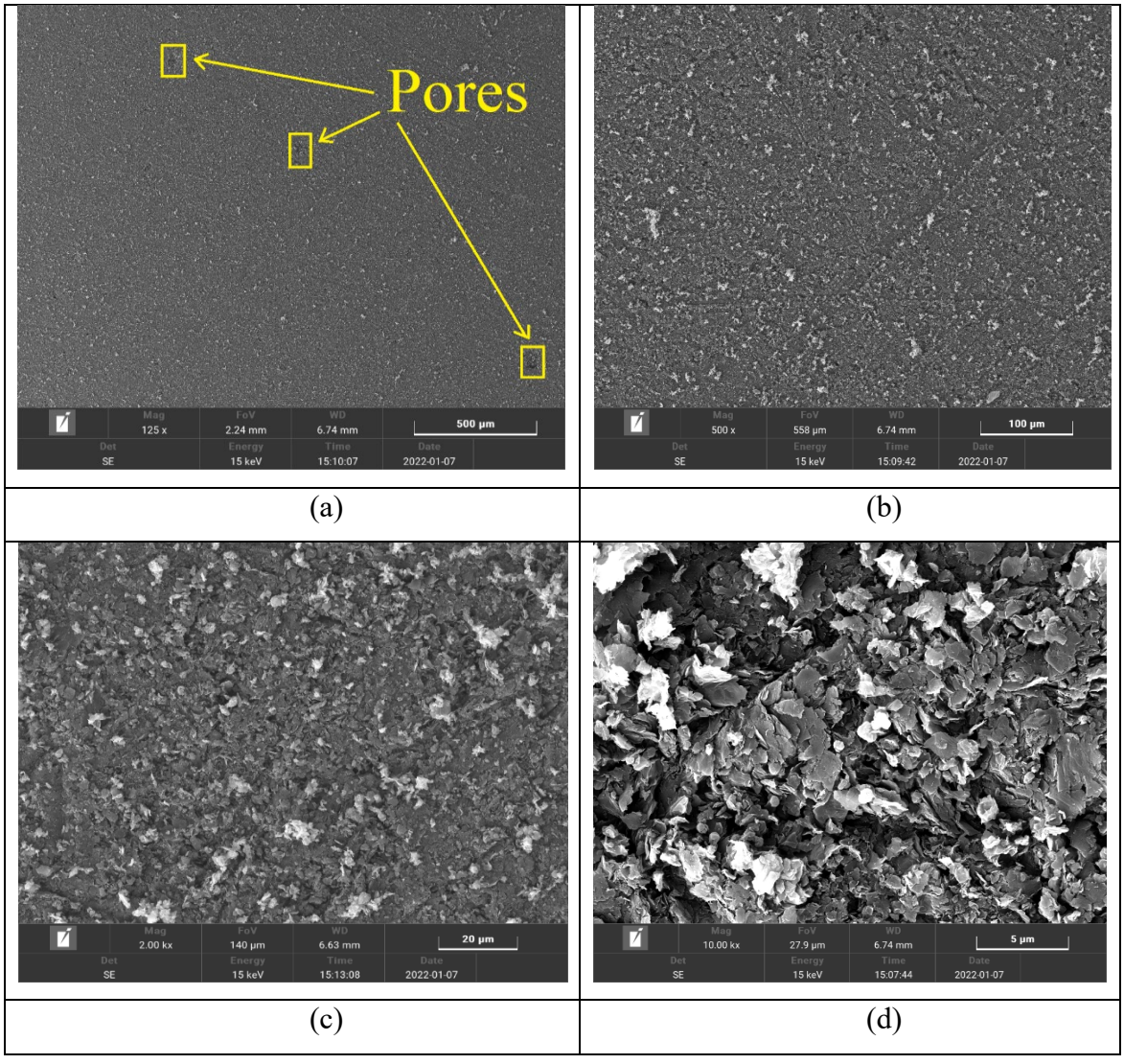

(a) (b)

(c) (d)

Figure 3.12. FESEM pictures of graphite tool at (a) 125x; (b) 500x; (c) 2kx; (d) 10kx.

This servo motor was capable of providing a large range of electrode speed, starting from 100 rpm to 5000 rpm in both clockwise and anticlockwise direction. The output shaft of motor initially consisted of a pulley while was replaced by sprocket having 24 teeth. One more sprocket having same number of teeth was fixed to the die. These two were then connected with the help of a chain. So, the drive feed from servo motor to die was connected with sprocket and chain arrangement. The detailed specifications of the servo motor and controller are listed in table 3.3.

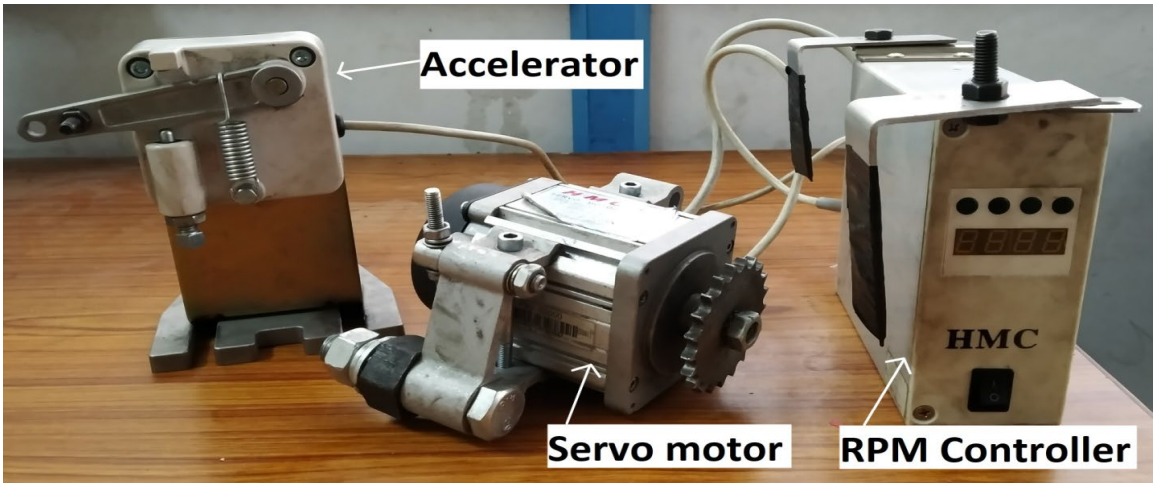

Figure 3.13. Servo motor with speed controller.

Table 3.3. Servo motor and controller specifications.

Motor type	HMC AC Servo motor WR 561-1
Volts	220 V
Frequency	50 Hz
Output	550 W
Speed range	100 – 5000 rpm
Torque	Upto 3 Nm

3.5 Auxiliary tank fabrication

The present research work involves mixing of SiC powder into the EDM oil. So, an auxiliary tank was fabricated in house so as to maintain constant concentration of abrasive powder into the EDM oil. The fabricated tank dimension was 510 mm (L) x 285 mm (B) x 160 mm (H) (refer figure 3.14). It can take 17 litre of oil in it during machining. A machine

vice was also fitted at bottom to hold the work piece. In order to arrest degree of freedom of tank w.r.t. original tank table, a slight extension of sheet on one side was given with two holes over it. The holes were used to fix it with the help of nut and T bolt.

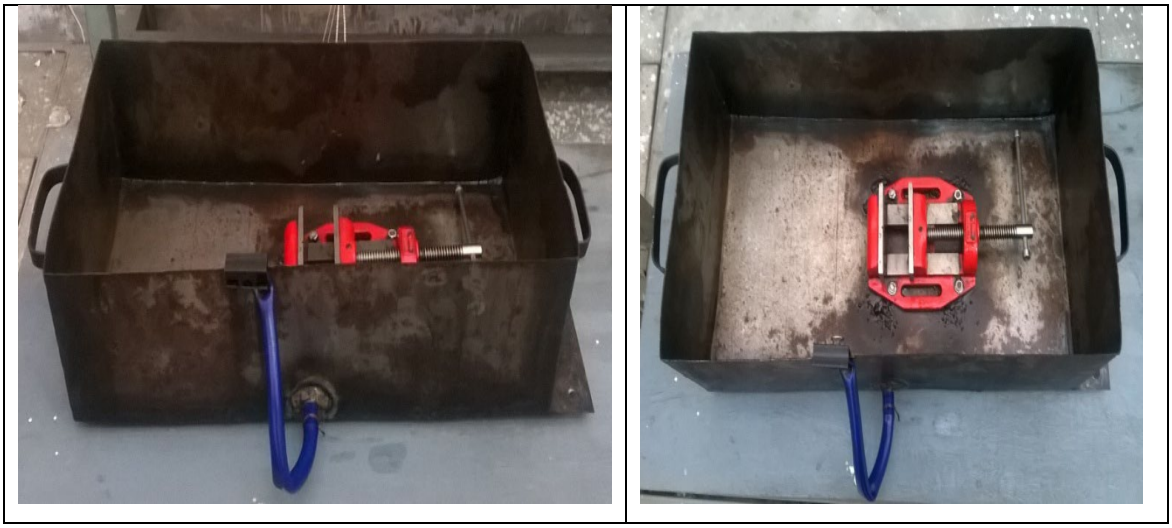

Figure 3.14. Fabricated auxiliary tank.

3.6 Stirrer motor

The stirrer motor used in this study is single phase ac electric motor shown in figure 3.15. The motor specifications were single phase, 50 Hz frequency and 220-240 Voltage. It is a table fan electric motor which is designed to overcome air resistance. But, in this study, the same is used to rotate the fluid in the auxiliary tank. As the fluid resistance was more than the air, the motor started heating up. The machining time was fixed at 2 minutes. Then after, a gap of 5 minutes was given between experimental runs. The motor was tested in the trial experiments which yielded successful results. The rotational speed was measured with DT-2234B tachometer which was found to be 565 rpm during experimentation.

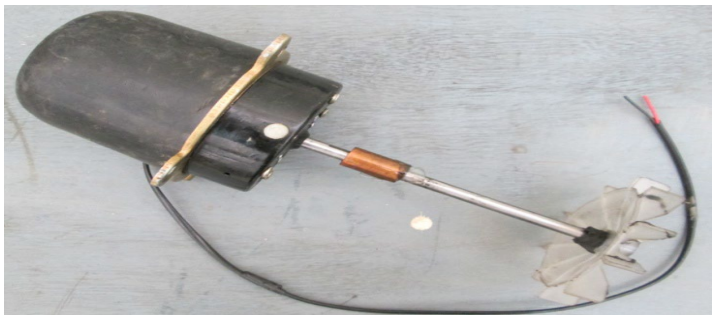

Figure 3.15. Stirrer motor.

3.7 Modified conventional EDM for abrasive rotary EDM

The modified conventional EDM from the abrasive mixed rotary EDM is shown in figure 3.16. The parts used for the conversion are rotary die, fabricated tool, chain and sprocket, two mild steel L plates (fabricated in house in welding lab), AC servo motor and controller, nut and bolts, auxiliary tank, stirrer motor and machine vice. All these parts fitted on the conventional EDM like rotary attachment was fixed to the machine head while the auxiliary tank placed in the main tank of machine. The stirrer motor was placed on the auxiliary tank for continuously mixing of abrasive powder in dielectric fluid of EDM.

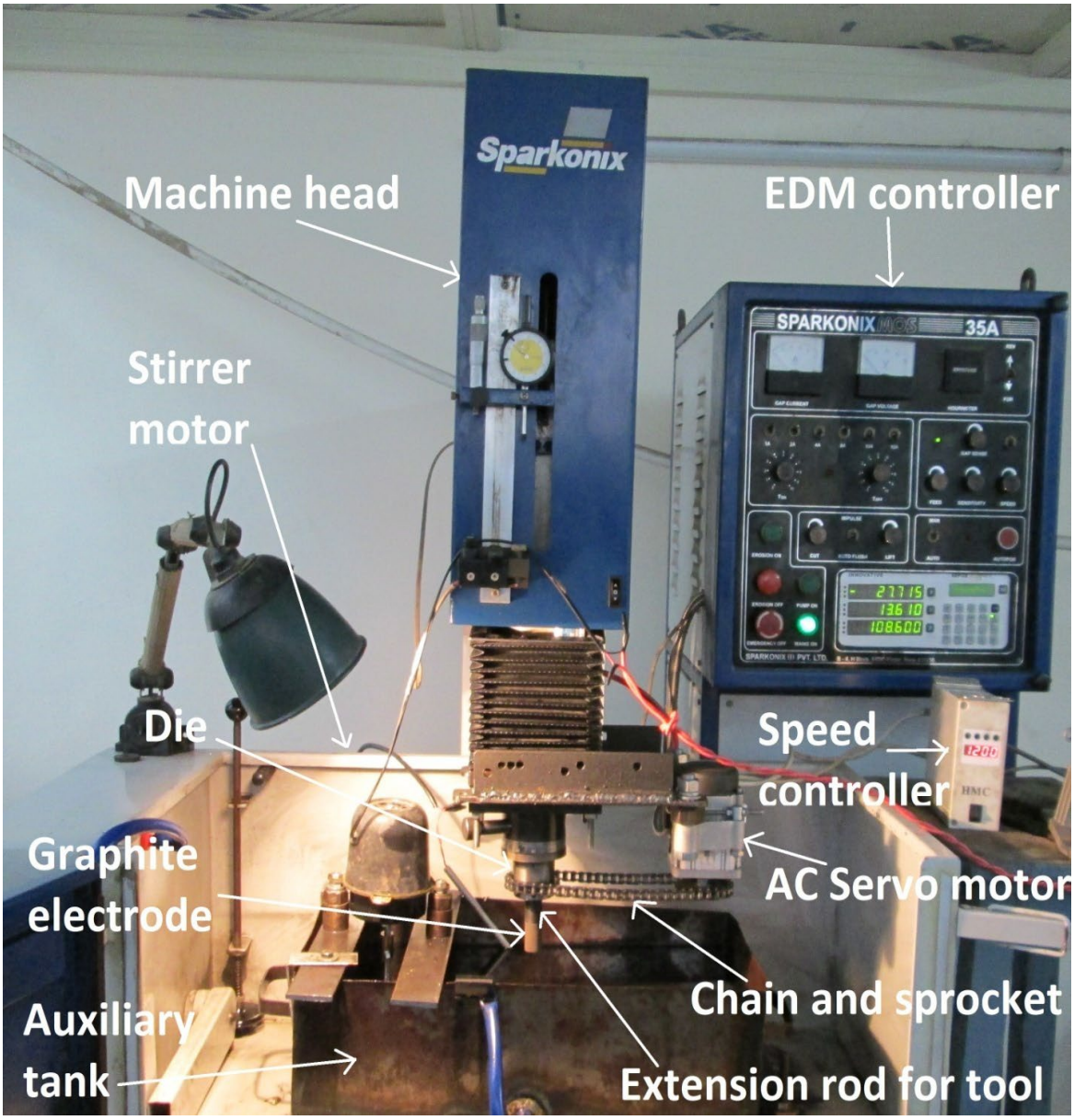

Figure 3.16. Abrasive mixed rotary tool EDM setup.

3.8 Experimental setup and circuit with DSO

A keysight Infinii Vision DSO-X 2022A digital storage oscilloscope (DSO) was employed to capture the current and voltage waveforms during machining. It is done to understand the sparking phenomenon in detail and to correlate with the response measures. The experimental setup with DSO is shown in figure 3.17. Furthermore, an illustrative circuit diagram is also presented in figure 3.18 along with schematic of abrasive rotary EDM setup with better understanding.

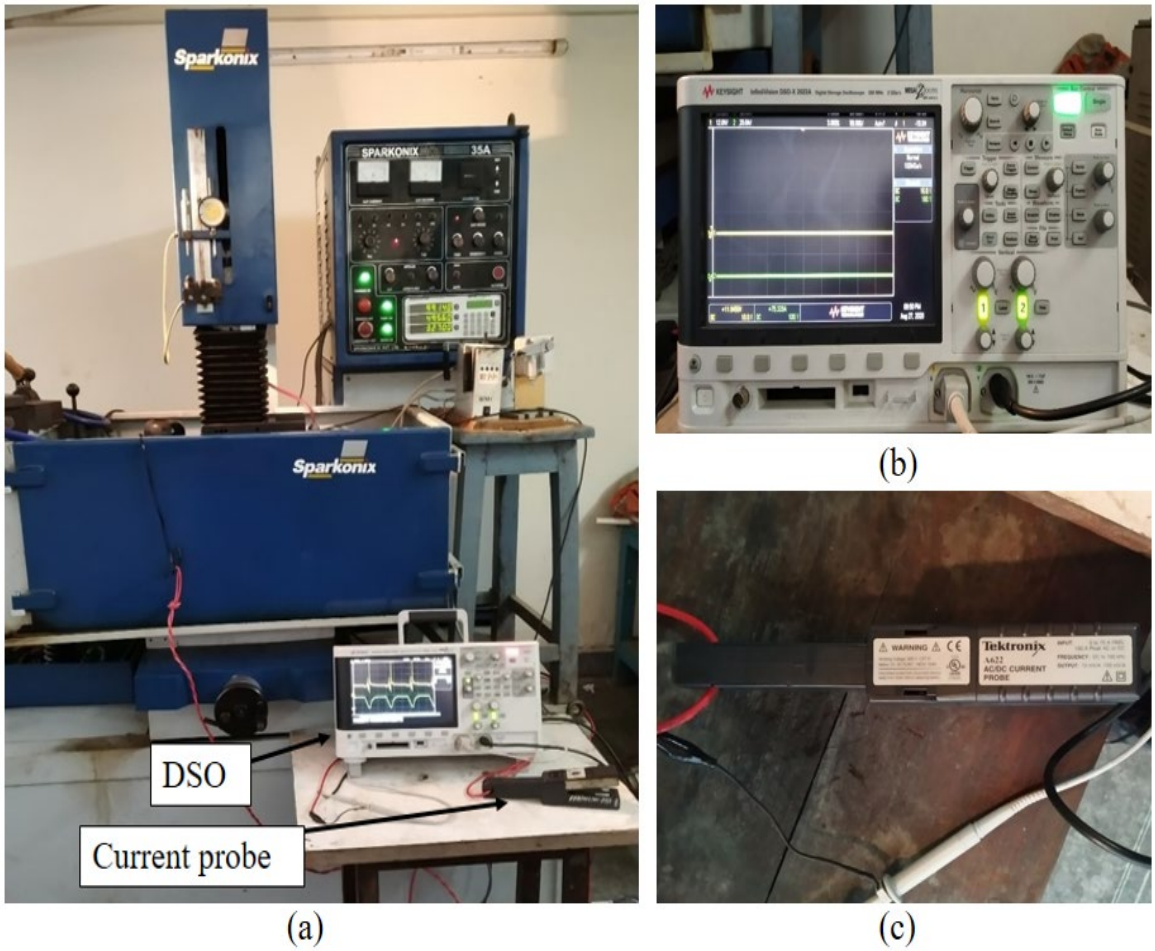

Figure 3.17. (a) Experimental setup with DSO; (b) DSO; (c) current probe.

3.9 Silicon carbide powder characteristics

Out of many available options in powder type, silicon carbide powder was selected with focus on physical properties, availability and cost. These factors favours easy adaptability of proposed change in EDM to industries. Silicon carbide powder exhibits high melting point (2975℃) and electrical conductivity (1×10^7 μΩ·m) which makes it suitable for the

present work as it involves large intensity of current and current on time leading to higher temperatures in machining.

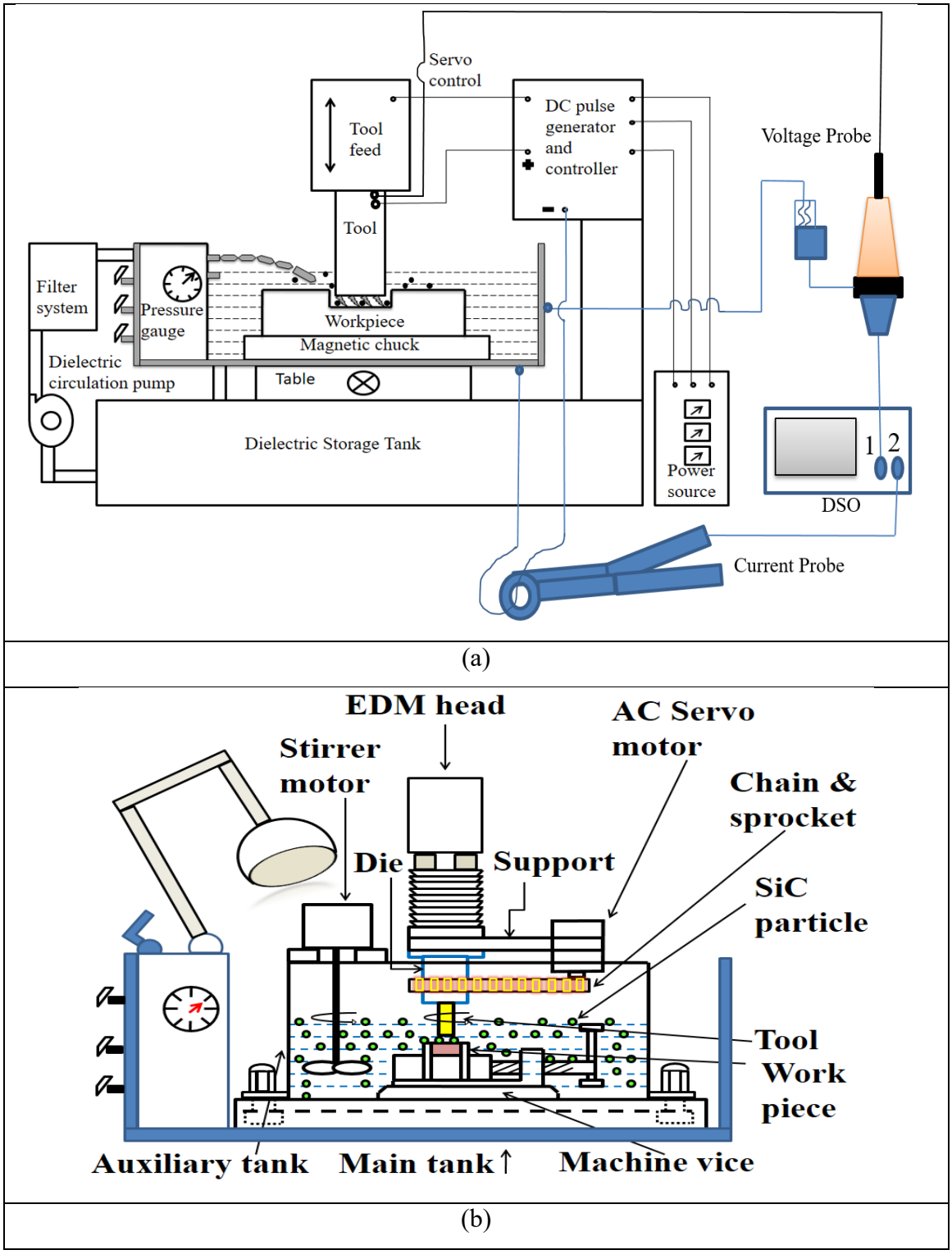

Figure 3.18. (a) Circuit diagram with DSO; (b) schematic diagram of AREDM setup.

Furthermore, the researchers have presented results favouring this selection. Chow *et al* (2008) claimed that silicon carbide powder gained higher MRR compared with aluminium powder. Kung *et al* (2009) also highlighted the improvements in MRR, TWR and SR with silicon carbide powder. It is also stated that macro-sized silicon carbide powder was chosen over nano-sized powder because the larger the size of the powder, the greater the inter-electrode gap. Because this study proposes integrating tool rotation with PMEDM, the larger gap, together with swirl impact of tool rotation to the dielectric, may result in improved surface integrity. Literature review of research in the micro range revealed that powder in the range of (10-50 µm) has shown improvements, yet the higher size has not been yet covered (Surani 2020). To fill the gap, a range of 60-100 µm was initially taken in trial experiments with powder sizes of 60, 80 and 100 µm. Out of these, initial results favoured the selection of 60 µm particle size. The size of the powder was calculated as 60 µm by Image J software based on recorded SEM images of 'as received' powder. Figure 3.19 depicts the relevant images. It can be elucidated from figure 3.19(a, b, c & d) that the size of powder particles was not homogenous. It varied from microns for larger particles to nano for smaller ones (refer figure 3.19(a)). As seen in figure 3.19(b), several smaller nano particles were discovered laying atop the larger ones. The variation of size can be better viewed from figure 3.19(c & d). EDS spectra of 'as received powder' is depicted in figure 3.19(e) (Lamba and Vipin 2022).

3.10 Work piece and tool material

The EN-31 and D3 steel were chosen as the work piece material. These are extensively used in manufacturing divisions for die-making, mould making etc. The elemental constitution of these are mentioned in tables 3.4 and 3.5. The hardness measured on Brinell hardness tester resulted in 52 HRC and 59 HRC for EN31 and D3 steel respectively. The EN31 and D3 steels were hardened using the following procedure (Lamba and Vipin 2022): (i) Preheating of the material was done at 750°C for 3 hours, an essential step to avoid cracking (ii) Material was then dipped in salt bath oil fired furnace (Neutral salt) at 1020°C for 90 minutes. (iii) Quenching in oil was done for 60 minutes. (iv) At last, tempering was done at 400°C for 4 hours.

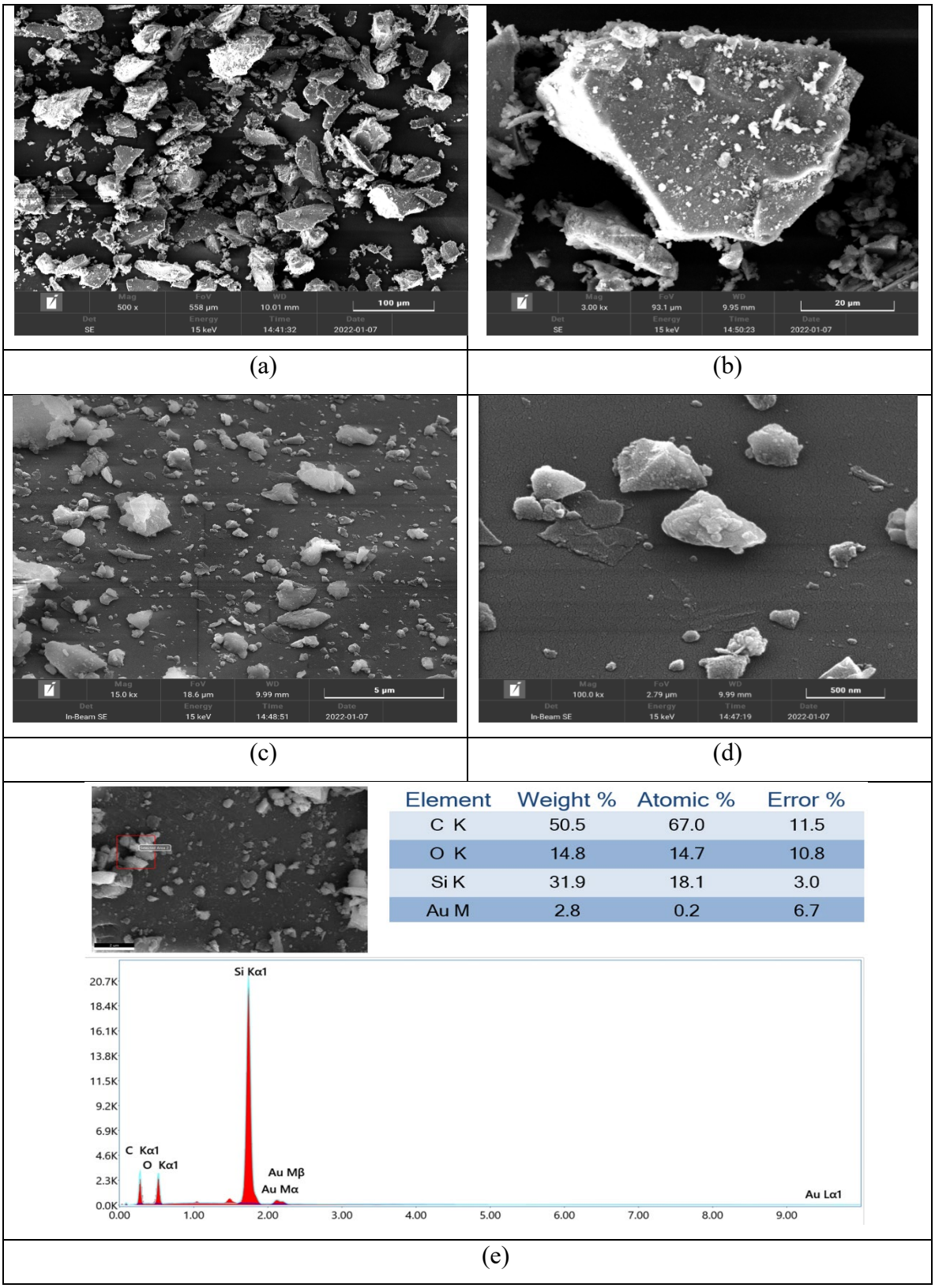

Figure 3.19. FESEM pictures of silicon carbide powder particles at (a) 100 microns; (b) 20 microns; (c) 5 microns; (d) 500 microns, and (e) EDS of SiC.

Table 3.4. Elemental constitution (wt.%) of EN31 steel.

C	O	Si	P	S	Cr	Mn	Fe
1.05	1.57	0.26	0.05	0.11	1.55	0.64	Rest

Table 3.5. Elemental constitution (wt.%) of D3 steel.

Cr	C	O	Si	Mn	S	P	W	V	Fe
13.40	2.23	2.0	0.41	0.40	0.03	0.05	0.15	0.08	Rest

3.11 Process parameters

The selection of process parameters is the most vital step in any research. The EDM researchers have explored many electrical and non-electrical parameters. The electrical parameters includes pulse on time, pulse off time, peak current, servo voltage etc. and non-electrical parameters includes workpiece rotation, flushing of dielectric, tool rotation, electrode design etc. In this research work, three process parameters, namely, peak current, pulse on time and tool rotation were selected based on literature survey and pilot experimentation. It was seen that most of the research focused on low range of peak current, which can be used as finish cut. Now, as we know that EDM suffers from low MRR, so, machining with rough cut becomes an open scope for research as exploring this area with supportive surface analysis including recast layer formation and sub-surface microhardness can reveal the intensity of peak current for finish cut as per the surface finish requirements of the workpiece. Considering this, it was further identified that published work in EDM has a research gap from mid to higher range of these selected parameters as most researchers have published work in low range of peak current (1-10 A), pulse on time and tool rotation (up to 1000 rpm). It is also mentioned that level selection for pulse on time to 100, 400, 1000 µs was actually limited by the available panel options on EDM machine (Sparkonix 35A). Considering literature and machine constraints, rough cut machining in the range of 12-24 A for peak current, 100-1000 µs for pulse on time and 1200-1800 rpm for tool rotation was focused in this study (Lamba and Vipin 2022).

During experimentation, off-time pulse, size and concentration of powder were kept constant during machining on EN31 and D3 die steels in this research work on abrasive

rotary electrical discharge machining. Machining variables with their levels are displayed in table 3.6.

(i) Peak current (A)

(ii) Pulse on-time (μs)

(iii) Tool rotation (rpm)

(iv) Off-time pulse (μs) (constant)

(v) Size of powder (micron) (constant)

(vi) Concentration of powder (g/l) (constant)

(i) Peak current (A) – It is the intensity of current supplied between electrode and piece to be machined. Peak current has been the factor that had the greatest influence on machining output, according to literature. Hence, in this research study, peak current was considered as one machining variable to be studied with tool rotation to investigate its effects on machining outputs with tool rotation.

(ii) Pulse on time (μs) – It is the interval of time for which current is supplied into the space between electrode and piece to be processed. Since electrical discharge machining is an intermittent process having current on and off cycle for certain duration, pulse on time is referred as "current on time". It was considered as an input parameter as its duration significantly affects the machining performance which can't be neglected.

(iii) Tool rotation (rpm) – Tool rotation refers to the rotational speed of the electrode. In this research work, tool rotation was taken as an input parameter to investigate its effects on different response measures.

(iv) Off-time pulse (μs) – It is the interval of time for which current remains off between electrode and piece to be processed. Pulse off time is referred as "current off time" or "cooling period". During this period, the debris generated during pulse on time are removed by dielectric fluid from the inter-electrode gap. This parameter was kept constant during experimentation for all combinations of tool and work piece at 30 μs.

(v) Size of powder (micron) – It refers to powder's particle size. The silicon carbide powder of 60 micron size was taken as fixed parameter throughout this research study. The size was finalized by conducting trial experiments on three particle size of powder i.e. 60, 80, 100 micron. The trial experiments with 60 micron particle size resulted in better machining characteristics than other two.

(vi) Concentration of powder (g/litre) – The concentration of powder refers to the amount of powder to be mixed per litre of dielectric fluid. The powder concentration was also finalized by conducting trial experiments. The concentration was varied at 0, 3, 6 and 9 g/litre where 6 g/l resulted in maximum MRR. The concentration of powder was kept fixed at 6 g/l throughout this research work.

Table 3.6. Process parameters and their levels.

Process parameters	Symbol	Unit	Selected levels		
			I	II	III
Peak current	P_c	A	12	18	24
Pulse on time	T_{on}	µs	100	400	1000
Tool rotation	T_{rpm}	rpm	1200	1500	1800

3.12 Planning of experiments

A full factorial experimentation was planned with three factors at three levels. So, 27 experiments were planned for each work-tool material combination.

3.13 Measurement of output responses

Three output characteristics were chosen for response measurement. They were material removal rate (MRR), tool wear rate (TWR) and surface roughness (SR). All three were selected as complete EDM analysis couldn't have been possible without proper addressing of these characteristics. As the first two characteristics i.e. MRR and TWR involves accurate measurement of material loss from work piece and tool, selection of precise weight measurement machine becomes very important. The following sub-sections give more insight about weighing machine and measurement of characteristics.

3.13.1 Weighing machine

Sartorius BSA 224S-CW weight estimation scale was employed for measurement of pre and post machining weight of electrode and work piece, shown in figure 3.20. The maximum capacity of weight measurement was 220 gm.

3.13.2 Measurement of MRR

MRR was estimated by taking the difference of weight of workpiece pre and post EDM, and then dividing it by machining time. The measurement was taken in standard unit in mg/min (Dhar 2007).

Material removal rate=(Wi-Wf)/Tm

Where, Wi= weight of the work piece before EDM, mg

Wf= weight of the work piece after EDM, mg

Tm=Total machining time, minutes

3.13.3 Measurement of TWR

TWR was estimated by taking the difference of weight of electrode pre and post EDM, and then dividing it by machining time. The measurement was taken in standard unit in mg/min (Dhar 2007).

Tool wear rate=(Wi-Wf)/Tm

Where, Wi= weight of the tool before EDM, mg

Wf= weight of the tool after EDM, mg

Tm=Total machining time, minutes

3.13.4 Measurement of SR

Tesa Rugosurf 10G roughness checker was employed for measurement of surface roughness of EDM processed surfaces, shown in figure 3.21. The cut off length for movement of stylus was set at 0.8 mm. In order to reduce variability, three readings inside cavity were taken at different locations and then, average value was considered in each experimental run.

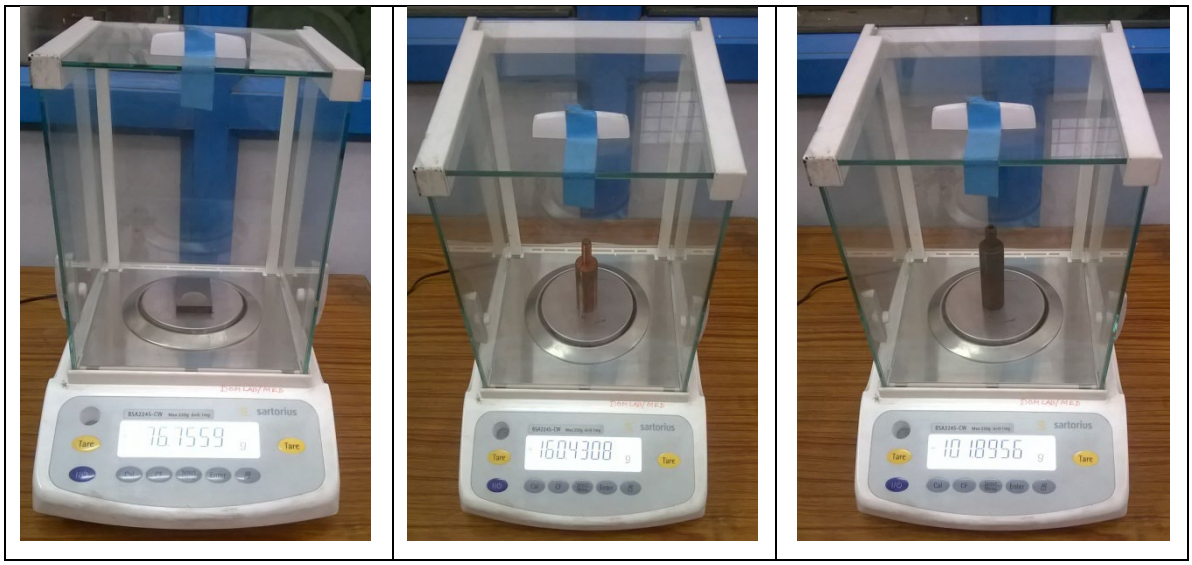

Figure 3.20. Weight measurement machine for work piece and tool.

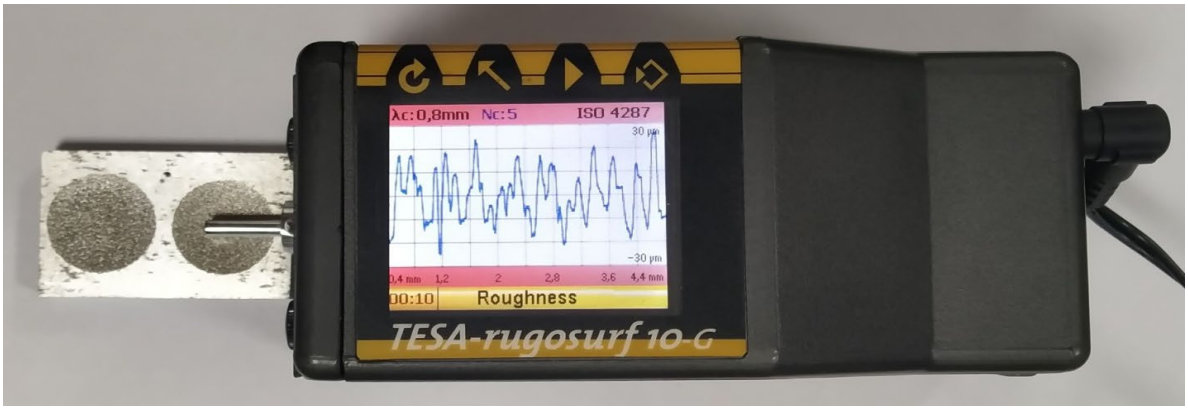

Figure 3.21. Surface roughness tester (Tesa-rugosurf 10-G).

CHAPTER-4

EXPERIMENTAL RESULTS

4.1 Introduction

The experiments were performed on EN31 and D3 steel wokpiece material machined by graphite and copper. The parametric settings and their levels are once again re-iterated here in Table 4.1 for better understanding and reference. In this research work, three process parameters, namely, peak current, pulse on time and tool rotation were selected to record MRR, TWR and SR of EN31 and D3 steel with graphite and copper electrode. The upshots are portrayed in tables 4.2-4.5. Further, figures 4.1-4.4 shows the experimental images of machined samples.

Table 4.1. Process parameters and their levels.

Process parameters	Symbol	Unit	Selected levels		
			I	II	III
Peak current	P_c	A	12	18	24
Pulse on time	T_{on}	µs	100	400	1000
Tool rotation	T_{rpm}	rpm	1200	1500	1800

4.2 Experimental data and machined samples of EN31 steel and graphite

Table 4.2. Experimental results of EN31 steel and graphite.

Run order	Factor levels			Output measures		
	Pc (A)	Ton (µs)	Trpm (rpm)	MRR (mg/min)	TWR (mg/min)	SR (µs)
1	18	100	1200	632.5	73.2	8.942
2	24	1000	1800	227.8	33.95	10.568
3	12	100	1500	333	107.4	8.237
4	12	400	1200	373.1	43.7	12.454
5	24	400	1200	502.4	17.4	13.263
6	24	400	1800	500	70.2	12.159
7	12	400	1800	390.8	117.4	10.468
8	18	100	1800	701.7	147.7	8.258
9	18	1000	1800	266.4	43.1	10.183
10	24	1000	1500	216.8	26.4	11.428

11	18	400	1500	547.9	73.3	11.59
12	24	100	1500	823.3	100.4	8.344
13	18	400	1200	544.4	46.9	11.842
14	12	1000	1200	245.9	29.4	11.178
15	24	100	1200	783.8	64.4	8.371
16	18	1000	1200	262.9	11.7	11.569
17	12	1000	1800	255.9	95.5	9.254
18	18	400	1800	545.3	98.5	11.23
19	18	100	1500	716.9	84.3	8.723
20	12	100	1800	308.5	151.3	7.859
21	24	1000	1200	204.7	8.8	11.835
22	24	100	1800	710.8	102.6	8.262
23	12	100	1200	326.6	57.7	8.368
24	12	1000	1500	190.2	55.7	9.815
25	24	400	1500	543.9	34.5	12.881
26	18	1000	1500	292.9	27.2	10.979
27	12	400	1500	302	73.1	11.487

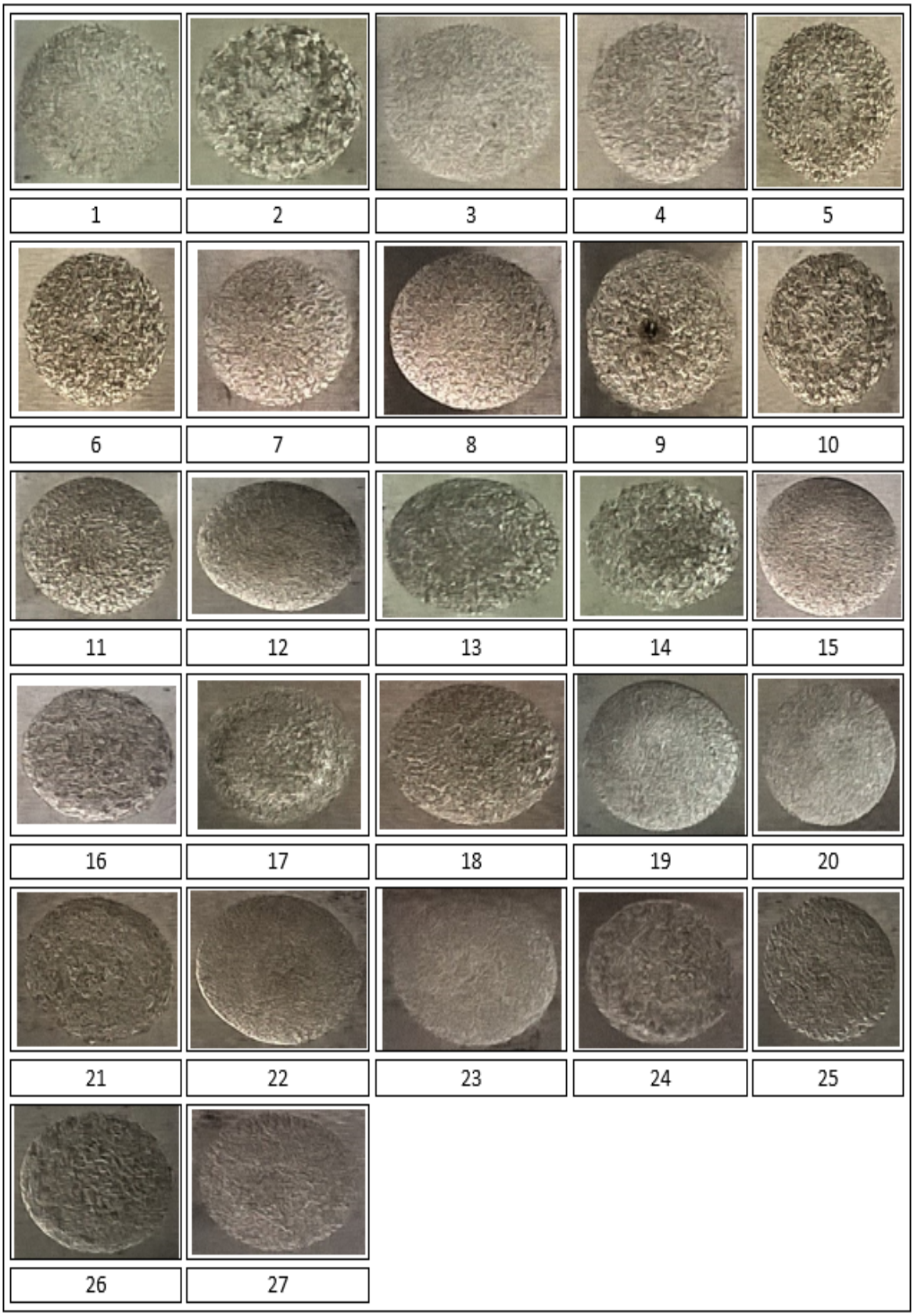

Figure 4.1. Machined samples of EN31 steel and graphite.

4.3 Experimental data and machined samples of EN31 steel and copper

Table 4.3. Experimental results of EN31 steel and copper.

Run order	Factor levels			Output measures		
	Pc (A)	Ton (µs)	Trpm (rpm)	MRR (mg/min)	TWR (mg/min)	SR (µs)
1	24	100	1500	549.45	254.6	10.583
2	18	100	1500	189.15	115.9	7.115
3	24	400	1800	588.1	151.4	17.003
4	12	1000	1800	282.65	34.1	11.835
5	18	1000	1200	540.55	21.6	12.545
6	18	400	1500	410.7	102.45	12.508
7	12	400	1200	385.4	49.9	10.392
8	12	1000	1200	337.6	37.9	10.64
9	24	400	1500	641.5	135.6	14.809
10	18	1000	1800	347.1	18.65	14.374
11	12	100	1200	162.8	76.5	9.583
12	24	1000	1200	685.2	69.7	18.46
13	12	100	1800	130.7	56.2	5.944
14	18	400	1200	630.75	68.65	12.917
15	24	1000	1800	402.95	55.65	18.323
16	18	100	1200	440.35	160.55	10.141
17	18	100	1800	284.45	170.5	8.23
18	24	400	1200	890.7	158.45	17.613
19	18	400	1800	496.65	94.1	14.58
20	24	100	1800	468.35	272.4	6.858
21	24	1000	1500	347.4	18.1	20.655
22	12	1000	1500	205.05	32.8	8.047
23	12	400	1500	260.25	49.15	10.786
24	18	1000	1500	293.5	20.56	16.758
25	12	400	1800	180.4	39.4	12.256
26	24	100	1200	665.8	267.6	7.501
27	12	100	1500	118.5	61.25	7.499

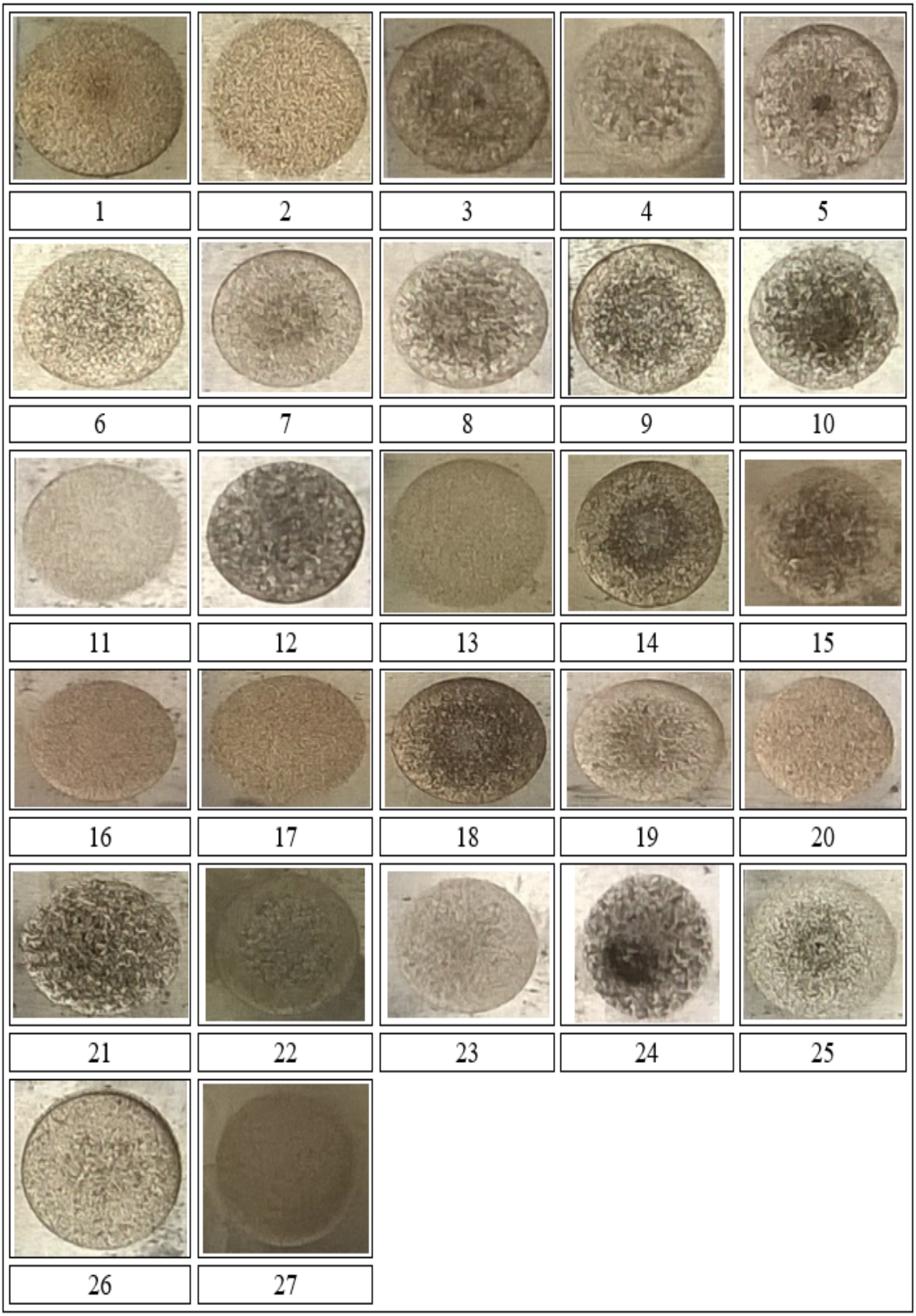

Figure 4.2. Machined samples of EN31 steel and copper.

4.4 Experimental data and machined samples of D3 steel and graphite

Table 4.4. Experimental results of D3 steel and graphite.

Run order	Factor levels			Output measures		
	Pc (A)	Ton (µs)	Trpm (rpm)	MRR (mg/min)	TWR (mg/min)	SR (µs)
1	18	1000	1500	258.05	28.8	8.158
2	24	1000	1800	198.55	42.95	9.254
3	12	400	1500	276.5	78.34	8.941
4	24	400	1200	523.54	38.5	15.009
5	24	400	1500	573.45	56.245	13.256
6	12	100	1200	296.15	70.9	8.235
7	12	100	1500	332.65	125.9	8.14
8	24	100	1800	806.3	106.3	9.321
9	24	1000	1200	178.25	14.35	10.545
10	12	100	1800	361.1	159.1	6.885
11	18	400	1800	522.95	89.5	11.17
12	12	1000	1800	121	67.6	4.523
13	18	1000	1200	224.55	19.75	8.856
14	12	1000	1200	112.45	10.7	7.776
15	24	100	1500	759.1	98.5	10.401
16	18	400	1500	481.15	63.65	11.858
17	24	1000	1500	170.25	17.4	9.147
18	18	1000	1800	188.45	46.05	7.704
19	18	100	1800	660.75	147.5	8.256
20	18	400	1200	457.85	42.85	12.295
21	24	100	1200	743	72.5	10.654
22	12	400	1800	339.65	99.55	8.256
23	24	400	1800	510.23	57.55	13.053
24	12	400	1200	255.89	33.75	10.42
25	18	100	1500	698.9	90.85	8.419
26	18	100	1200	676	57.55	9.208
27	12	1000	1500	183.6	47.9	5.188

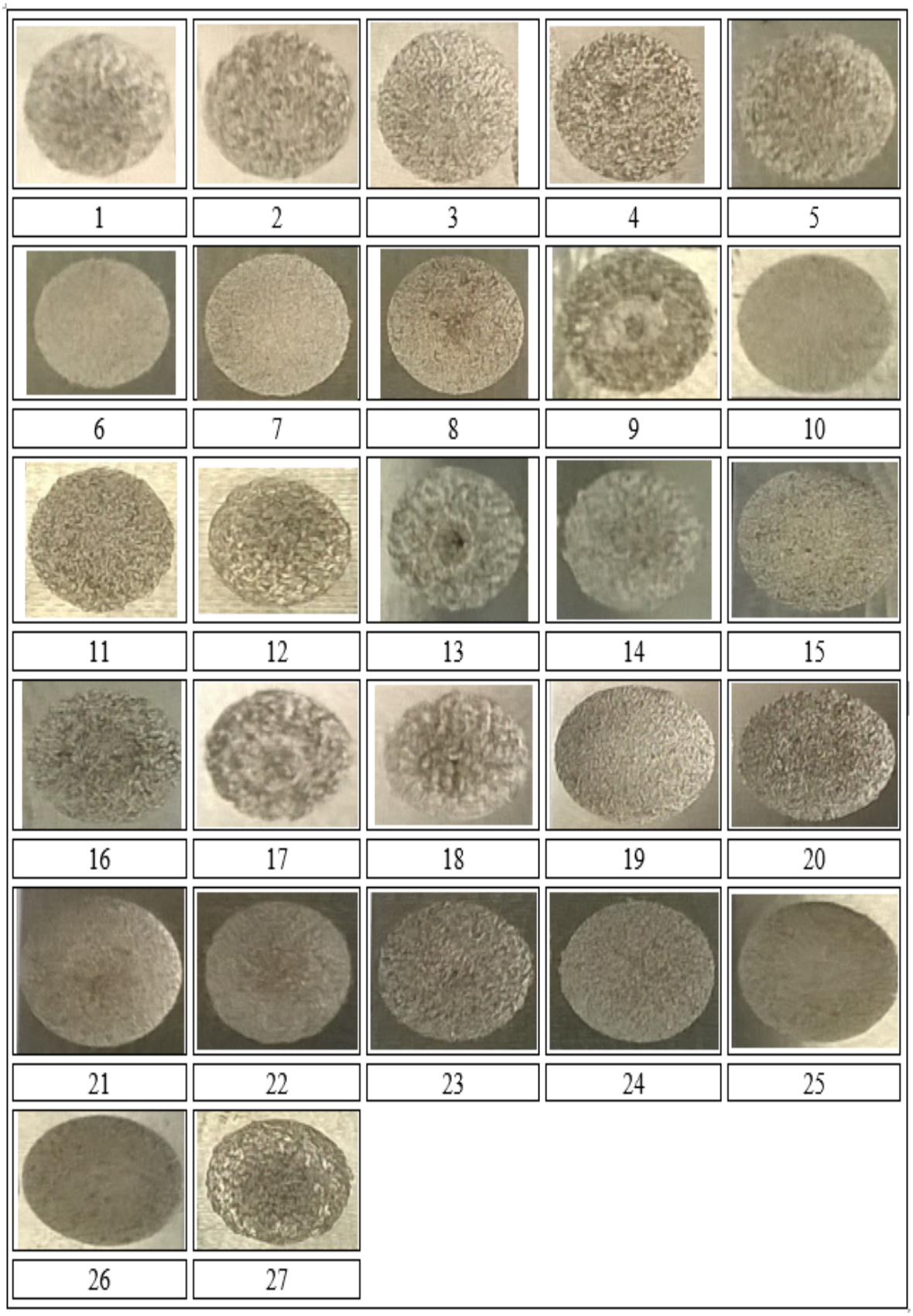

Figure 4.3. Machined samples of D3 steel and graphite.

4.5 Experimental data and machined samples of D3 steel and copper

Table 4.5. Experimental results of D3 steel and copper.

Run order	Factor levels			Output measures		
	Pc (A)	Ton (µs)	Trpm (rpm)	MRR (mg/min)	TWR (mg/min)	SR (µs)
1	12	1000	1500	161.5	15.15	5.91
2	18	100	1200	516.6	118.55	9.75
3	18	100	1500	493.9	116.5	8.01
4	12	100	1500	279.9	62.3	7.09
5	24	400	1800	602.35	92.33	9.82
6	12	400	1800	334.25	26.1	6.64
7	18	100	1800	348.65	148.5	5.74
8	18	400	1200	654.15	43.5	10.87
9	18	1000	1800	181.55	9.2	5.65
10	24	1000	1500	459.4	49.79	8.32
11	18	400	1500	532.95	76	10.32
12	24	100	1500	571.6	217.15	8.79
13	12	1000	1200	240.7	26.05	6.86
14	12	1000	1800	110.45	21.45	5.21
15	18	400	1800	431.9	80.25	7.95
16	12	100	1800	160.9	50.25	4.81
17	18	1000	1200	342.9	9.6	7.98
18	24	1000	1200	538.95	24.3	8.49
19	24	100	1800	561.1	191.25	6.44
20	12	100	1200	323.2	55.1	7.85
21	24	400	1500	686.75	106.25	11.12
22	24	400	1200	821.7	79.2	11.99
23	24	100	1200	664.85	195.6	11.41
24	12	400	1500	348.8	28.25	7.89
25	24	1000	1800	399.65	24.6	7.99
26	18	1000	1500	379	30.9	7.1
27	12	400	1200	386.9	28.3	9.3

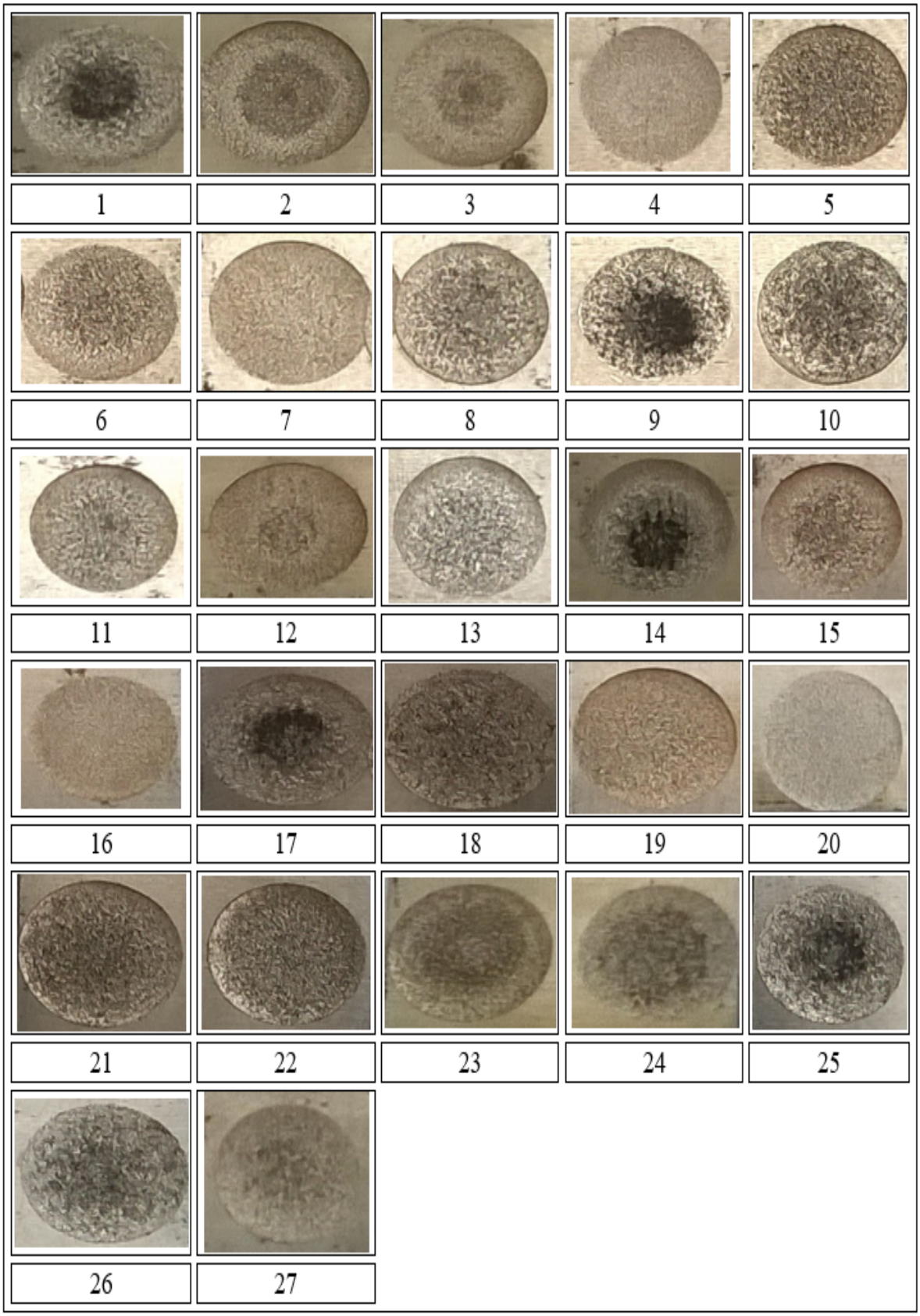

Figure 4.4. Machined samples of D3 steel and copper.

CHAPTER-5

AREDM OF EN31 STEEL WITH GRAPHITE AND COPPER ELECTRODES

5.1 Introduction

This section displays the analysis of variance, regression equations, interactions curve, surface plots, morphology results on EN31 steel machined with graphite and copper electrode. The parametric settings and their levels are once again re-iterated here in Table 5.1 for better understanding and reference. In this research work, three process parameters, namely, peak current, pulse on time and tool rotation were selected to record MRR, TWR and SR of EN31 steel with graphite and copper electrode.

Table 5.1. Process parameters and their levels.

Process parameters	Symbol	Unit	Selected levels		
			I	II	III
Peak current	P_c	A	12	18	24
Pulse on time	T_{on}	µs	100	400	1000
Tool rotation	T_{rpm}	rpm	1200	1500	1800

5.2 Regression equations and ANOVA results

ANOVA was done to quantify the variance due to process parameters and uncontrollable factors along with the percentage share of different parameters on machining responses. A confidence interval of 95% was used. The statistical models were generated for MRR, TWR and SR in machining of EN31 steel with graphite and copper electrode through regression equations with the help of Minitab 17 software. The uncontrollable factors during experimentation led to the difference between the model output and experimented data.

5.2.1 AREDM of EN31 using Graphite Electrode

ANOVA results for SR, TWR and MRR while processing of EN31 steel with graphite electrode are shown in tables 5.2, 5.3 and 5.4, respectively. These tables consist of data after removing insignificant interactions and square terms. Equations (1), (2) and (3) are regression equations for MRR, TWR and SR, respectively. The $R^2_{adjusted}$ for SR, TWR, and MRR are 94.32%, 92.39%, and 94.45%, respectively which showed good fit for model.

Table 5.2. ANOVA table for SR (EN31&Gr) (after removing insignificant interactions and square terms).

Origin	DOF	Adj. SS	Adj. MS	F	P
Regression	5	68.5389	13.7078	87.28	0.000
Pc	1	3.5476	3.5476	22.59	0.000
Ton	1	28.9963	28.9963	184.63	0.000
Trpm	1	0.4201	0.4201	2.68	0.117
Ton × Ton	1	44.1502	44.1502	281.11	0.000
Ton × Trpm	1	0.7750	0.7750	4.93	0.037
Error	21	3.2982	0.1571		
Total	26	71.8370			

F: Fisher's value. Adj. MS: adjusted mean square; Adj. SS: adjusted sum of squares; DOF: degree of freedom; P: Probability of acceptance based on confidence level.

Table 5.3. ANOVA table for TWR (EN31&Gr) (after removing insignificant interactions and square terms).

Origin	DOF	Adj. SS	Adj. MS	F	P
Regression	6	37503.8	6250.6	53.59	0.000
Pc	1	531.4	531.4	4.56	0.045
Ton	1	359.2	359.2	3.08	0.095
Trpm	1	4701.5	4701.5	40.31	0.000
Ton × Ton	1	1174.9	1174.9	10.07	0.005
Pc × Trpm	1	1145.6	1145.6	9.82	0.005
Ton × Trpm	1	603.7	603.7	5.18	0.034
Error	20	2332.6	116.6		
Total	26				

F: Fisher's value. Adj. MS: adjusted mean square; Adj. SS: adjusted sum of squares; DOF: degree of freedom; P: Probability of acceptance based on confidence level.

Table 5.4. ANOVA table for MRR (EN31&Gr) (after removing insignificant interaction and square terms).

Origin	DOF	Adj. SS	Adj. MS	F	P
Regression	5	961673	192335	89.45	0.000
Pc	1	107735	107735	50.11	0.000
Ton	1	29142	29142	13.55	0.001
Trpm	1	53	53	0.02	0.877
Pc × Pc	1	58826	58826	27.36	0.000
Pc × Ton	1	147325	147325	68.52	0.000
Error	21	45152	2150		
Total	26				

F: Fisher's value. Adj. MS: adjusted mean square; Adj. SS: adjusted sum of squares; DOF: degree of freedom; P: Probability of acceptance based on confidence level.

$$\begin{aligned} MRR = &-864.0 + (135.7 \times P_c) + (0.3343 \times T_{on}) \\ &+ (0.0057 \times T_{rpm}) - (2.750 \times P_c^2) \\ &- (0.04030 \times P_c \times T_{on}) \end{aligned} \quad (1)$$

$$\begin{aligned} TWR = &-167.1 + (5.62 \times P_c) - (0.0785 \times T_{on}) + (0.2174 \times T_{rpm}) \\ &+ (0.000079 \times T_{on}^2) - (0.00543 \times P_c \times T_{rpm}) \\ &- (0.000052 \times T_{on} \times T_{rpm}) \end{aligned} \quad (2)$$

$$\begin{aligned} SR = &\ 6.518 + (0.0740 \times P_c) + (0.02230 \times T_{on}) \\ &- (0.000850 \times T_{rpm}) - (0.000015 \times T_{on}^2) \\ &- (0.000002 \times T_{on} \times T_{rpm}) \end{aligned} \quad (3)$$

5.2.2 AREDM of EN31 using Copper Electrode

ANOVA results for SR, TWR, and MRR while processing of EN31 steel with copper electrode are shown in tables 5.5, 5.6 and 5.7, respectively. The regression equations for MRR, TWR and SR are shown in equations (4), (5) and (6), respectively. The $R^2_{adjusted}$

for SR, TWR and MRR are 84.99%, 94.14%, and 90.91%, respectively which showed good fit for model.

Table 5.5. ANOVA table for SR (EN31&Cu) (after removing insignificant interactions and square terms).

Source	DOF	Adj. SS	Adj. MS	F	P
Regression	5	379.103	75.8206	30.43	0.000
Pc	1	0.541	0.5407	0.22	0.646
Ton	1	19.084	19.0838	7.66	0.012
Trpm	1	0.008	0.0084	0.00	0.954
Ton × Ton	1	64.353	64.3529	25.83	0.000
Pc × Ton	1	48.827	48.8268	19.6	0.000
Error	21	52.317	2.4913		
Total	26				

DOF: degree of freedom; Adj. SS: adjusted sum of squares; Adj. MS: adjusted mean square; F: Fisher's value; P: Probability of acceptance based on confidence level.

Table 5.6. ANOVA table for TWR (EN31&Cu) (after removing insignificant interactions and square terms).

Source	DOF	Adj. SS	Adj. MS	F	P
Regression	5	145427	29085.5	84.50	0.000
Pc	1	67886	67886.3	197.23	0.000
Ton	1	28	27.6	0.08	0.780
Trpm	1	19	18.9	0.05	0.817
Ton × Ton	1	3178	3177.7	9.23	0.006
Pc × Ton	1	25127	25127.1	73.00	0.000
Error	21	7228	344.2		
Total	26				

DOF: degree of freedom; Adj. SS: adjusted sum of squares; Adj. MS: adjusted mean square; F: Fisher's value; P: Probability of acceptance based on confidence level.

Table 5.7. ANOVA table for MRR (EN31&Cu) (after removing insignificant interactions and square terms).

Source	DOF	Adj. SS	Adj. MS	F	P
Regression	6	933087	155514	44.31	0.000
Pc	1	380009	380009	108.28	0.000
Ton	1	169531	169531	48.31	0.000
Trpm	1	77209	77209	22.00	0.000
Ton × Ton	1	126493	126493	36.04	0.000
Trpm × Trpm	1	66115	66115	18.84	0.000
Pc × Ton	1	43988	43988	12.53	0.002
Error	20	70190	3509		
Total	26				

DOF: degree of freedom; Adj. SS: adjusted sum of squares; Adj. MS: adjusted mean square; F: Fisher's value; P: Probability of acceptance based on confidence level.

$$\begin{aligned} MRR = {} & 2506.0 + (40.42 \times P_c) + (1.353 \times T_{on}) \\ & - (3.788 \times T_{rpm}) - (0.000821 \times T_{on}^2) \\ & + (0.001166 \times T_{rpm}^2) - (0.02202 \times P_c \times T_{on}) \end{aligned} \quad (4)$$

$$\begin{aligned} TWR = {} & -115.9 + (17.08 \times P_c) + (0.0173 \times T_{on}) - (0.0034 \times T_{rp} \\ & + (0.000130 \times T_{on}^2) - (0.01664 \times P_c \times T_{on}) \end{aligned} \quad (5)$$

$$\begin{aligned} SR = {} & 4.83 + (0.048 \times P_c) + (0.01436 \times T_{on}) \\ & - (0.00007 \times T_{rpm}) - (0.000019 \times T_{on}^2) \\ & + (0.000734 \times P_c \times T_{on}) \end{aligned} \quad (6)$$

5.3 Validation of Statistical Model

Validation of statistical model is a crucial step before processing to detailed analysis of results. A regression model validation is presented in table 5.8. The regression equations (1), (2), (3) and (4), (5), (6) were used to predict the results for EN31&Gr and EN31&Cu, respectively. The percentage error between experiment and predicted values were within 10% which showed good approximation. In addition, Figure 5.1 depicts the validation graphs between response predictor equation obtained through

Table 5.8. Model validation.

W/p & tool	Run order	Machining parameters			MRR (mg/min)		TWR (mg/min)		SR (microns)	
		Pc (A)	Ton (µs)	Trpm (rpm)	Experiment	Predicted, Residual, % Error	Experiment	Predicted, Residual, % Error	Experiment	Predicted, Residual, % Error
EN31 &Gr	18	18	400	1800	545.3	542.0, 3.27, 0.60	98.5	93.61, 4.89, 4.97	11.23	11.45, -0.22, -1.99
	22	24	100	1800	710.8	756.3, -45.54, -6.41	102.6	108.23, -5.63, -5.48	8.262	8.51,-0.25, -2.97
	27	12	400	1500	302	317.8, -15.81, -5.24	73.1	79.03, -5.93, -8.11	11.487	11.49, 0.00, 0.00
EN31 &Cu	6	24	400	1800	588.1	636.38, -48.28, -8.21	151.4	155.88, -4.48, -2.96	17.003	15.68, 1.32, 7.78
	8	18	100	1800	284.45	282.84, 1.61, 0.57	170.5	158.48, 12.03, 7.05	8.23	8.14, 0.09, 1.09
	11	18	400	1500	410.7	428.29, -17.59, -4.28	102.45	94.34, 8.11, 7.91	12.508	13.65, -1.14, -9.14

regression and experimental findings in machining EN31 steel with graphite and copper electrode. The graphs also reveals a closer match with experimented values proving its efficacy.

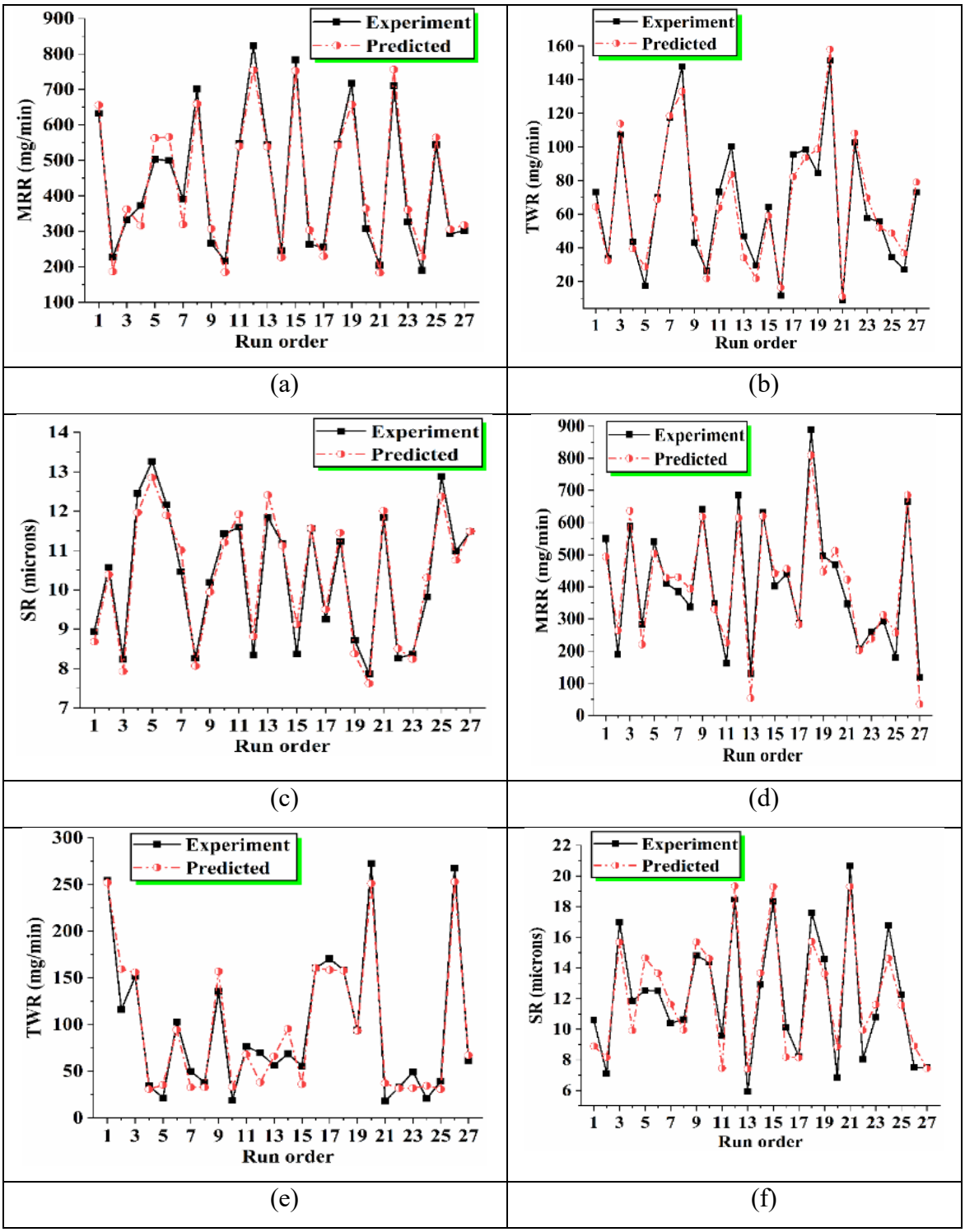

Figure 5.1. Regression model validation for MRR, TWR and SR in EN31&Gr (a, b, c); and in EN31&Cu (d, e, f).

5.4 Effect of machining variables on output

The following segment explains the result of different machining variables and their interactions on the output. Figures 5.2, 5.3 and 5.4 show the actual plot and percentage share by each parameter on material removal rate, electrode wear rate and surface roughness in EN31&Gr and EN31&Cu, respectively.

5.4.1 Findings on MRR

Figure 5.2(a, b, c) and Figure 5.5(a, b, c) exhibits the mutation in MRR with change in machining variables while processing EN31 steel with graphite and copper electrode, respectively. For both electrodes, the rate of material ejection increased as current rose. At high current, energy density of spark increases resulting into more intense heating. As a result, the rate of material removal rises. The material removal rate with graphite was found to be more during current interval from 12 to 18 A but copper takes over from 18 to 24 A in which the graphite electrode showed a flat response. In the first half, the graphite electrode performs better than the copper electrode due to its low thermal conductivity (70 W/m·K) and high melting temperature. Due to this, a stable arc is formed as the sideways dissipation of heat is less. With copper electrode, thermal conductivity being high (385 W/m·K), heat dissipation is more than that of graphite. Hence, for same current, less heat is transferred to work surface leading to less MRR. In the second half i.e. during high current interval, the electrical conductivity of copper (5.96×10^7 S/m at 20 ℃) which is very high than that of graphite (2 to 3×10^5 S/m at 20 ℃) outperforms the thermal conductivity effects. Because of high electrical conductivity, copper tool effectively conducts the electric charge leading to high MRR. On the contrary, graphite fails to apprehend MRR at high current because at high current, temperature becomes high which reduces the electrical conductivity owing to more vibration and movement between molecules which obstructs in the route of current flow. Figure 5.2(e) shows that peak current was the most influencing factor in MRR with a percentage of 55.86% with copper electrode.

On-time pulse is the time for which current flows into the circuit. In the first interval, MRR decreased with graphite electrode i.e. from 100 to 400 µs and increased with copper electrode. Then, in the second interval i.e. from 400 to 1000 µs, the value decreased in both

cases but the rate of decrease was more rapid with graphite electrode. At low pulse on time i.e. at 100 µs, arc is highly stable (cylindrical arc) with both electrodes but low MRR was recorded for copper electrode owing to its high thermal conductivity, less heat goes into the work leading to less MRR whereas graphite electrode recorded a high MRR because of its low thermal conductivity leading to more heat transfer to work and hence higher MRR. At 400 µs, cylindrical arc changes to convex arc because of considerably higher pulse on time than off time which is the reason for its expansion in the longitudinal direction (longitudinal direction here refers to the direction parallel to the machine bed) due to more heat (Chow *et al* 2008). Hence, heat loss increases in longitudinal direction compared to cylindrical arc. Now, at this value, MRR reduced for graphite electrode because of this additional heat loss due to convex arc. On the other hand, MRR increased for copper electrode because of its high electrical conductivity which encompasses the loss done by convex arc in longitudinal direction. At 1000 µs, pulse off time (30 µs) became very small compared to on time. At this stage, short circuiting was noticed with both electrodes. This might be because the dielectric fluid doesn't have enough time to deionize. Figure 5.2(d) show that on-time pulse is the most influencing factor in MRR with a percentage of 57.41% in graphite electrode.

Tool rotation refers to different rotational speeds of tool electrode. The material removal rate remained almost same at different rotational speeds of graphite electrode while in case of copper, it decreased in the first interval i.e. from 1200 to 1500 rpm and then increased in second interval i.e. from 1500 to 1800 rpm. The graphite electrode being less thermally conductive was not sufficiently augmented by tool rotation and hence recorded no appreciable improvements in MRR. The decrease of MRR with copper electrode is again attributed to its high thermal conductivity (5.5 times greater than graphite electrode). The high thermal conductivity of copper was augmented by tool rotation effects leading to more sideways heat dissipation. This led to less heat transfer rate to work and hence recorded less MRR, although small increase was noticed beyond 1500 rpm.

5.4.2 Findings on TWR

Figures 5.3(a, b, c) and Figure 5.6 (a, b, c) exhibits the mutation in TWR with change in machining variables while processing EN31 steel with graphite and copper electrode, respectively. The TWR decreased with rise in current intensity with graphite electrode

while it increased with copper electrode. Figure 5.3(d) showed that the pulse on time contributed maximum (40.59%) for TWR with graphite. On careful observation of table 4.2, it is inferred that set of high current (24 A) and on-time pulse (1000 μs) resulted in very low TWR particularly for graphite. As explained earlier, graphite underwent more erratic cycling and short circuiting which led to material deposition on its surface and hence, reduced TWR.

The TWR of both electrode was found to decrease with pulse on time. The reason was reduction in tool tip temperature as a result of enlargement of plasma at higher on-time pulse. Moreover, it was observed during experimentation that carbon deposits increased on high pulse on time, particularly on 1000 μs. The carbon decomposition from dielectric fluid on tool surface provided the protection against wear under pyrolysis process (Beravala and Pandey 2018). Hence, reduction in tool tip temperature and added carbon layer led to less TWR at high on-time pulse.

Enhancement in tool rotation resulted in increase of TWR with graphite electrode while the effect with copper electrode remained same as that of graphite i.e. increased in first half but, later on, recorded a small decline.

Figures 5.3(d, e) shows the percentage share by each parameter on TWR in EN31&Gr and EN31&Cu, respectively. The on-time pulse and electrode rotation were discovered to be highest influencing variables with 40.59% and 35.85%, respectively for graphite electrode. In case of copper electrode, on-time pulse and peak current were discovered to be highest influencing variables with 44.12% and 32.59%, respectively.

5.4.3 Findings on SR

Figures 5.4(a, b, c) and Figure 5.7(a, b, c) exhibits the mutation in SR with change in machining variables while processing EN31 steel. The SR increased with increase in current for both the electrode, however, the increase with copper electrode was more compared to graphite electrode. At high value of current, energy density of spark is high and hence crater formed in the workpiece is larger. The surface roughness value therefore rises.

The pulse on time is also critical parameter affecting SR. The SR increased with increase in pulse duration; however, it decreased from 400 to 1000 μs in case of graphite electrode. The cumulative effects of current and on-time pulse were seen on SR by observing a clear dark circle near centre indicating carbon deposit with copper electrode. This deposited carbon resulted in high surface roughness. It was also observed during experimentation that the extent of carbon deposition increased from mid to large value of peak current and on-time pulse.

Surface roughness increased with increase in electrode rotation with a minor dip at 1500 rpm for copper electrode and reduced for graphite electrode. Tool rotation has contributed in better flushing with graphite electrode contributing to enhanced surface finish.

The on-time pulse was highly influencing variable for graphite and copper electrode with percentage of 20.83% and 35.77%, respectively (refer figures 5.4(d, e)).

5.5 Interaction effect in EN31&Gr

The interaction effects of Pc and Ton on MRR, Pc and Trpm on TWR, Ton and Trpm on TWR, Ton and Trpm on SR were found to be significant in EN31 steel machined with graphite electrode.

5.5.1 Interaction effect on MRR

Figure 5.8 depicts the surface and interaction plot of Pc and Ton on MRR. The low level of Ton and high level of Pc resulted in maximum MRR. The reason is attributed to the fact that combination of these two levels makes the arc highly concentrated over the workpiece leading to maximum heat input into the workpiece and, hence, high MRR.

5.5.2 Interaction effect on TWR

Figure 5.9 shows the surface and interaction plot of Pc and Trpm on TWR. The current intensity affected TWR in inverse proportion for all tool rotation value. The effect of increase in peak current resulted in reduction of TWR. With increase in tool rotation, slope of the line was also increased. The lowest TWR occurred at high value of Pc and low value of Trpm as at high value of Pc, energy density of spark is high but at the same time tool rotation changes the concentricity of spark column to formation of bulge at the centre making the distribution of temperature uneven at ends and at centre. Due to this

phenomenon, tool tip temperature decreases leading to less wear of surface and, hence, less TWR.

Figure 5.10 illustrates the surface and interaction plot of Ton and Trpm on TWR. The pulse on time also showed the inversely proportional effects on TWR for given tool rotation values. The lowest TWR was found on high value of Ton and low value of Trpm. The reason for low TWR is reduction in tool tip temperature as a consequence of enlargement of plasma channel at high levels of Ton.

5.5.3 Interaction effect on SR

Figure 5.11 illustrates the surface and interaction plot of Ton and Trpm on SR. The surface roughness increased in first half then decreased in second half with rise in Ton for all stages of tool rotation. The lowest surface roughness recorded at low level of Ton and high level of Trpm. The reason is attributed to low intensity of spark at low level of Ton and effective debris removal with higher rotation. The higher tool rotational speed helped in cleaning the inter-electrode gap. Due to this effective cleaning, re-solidified spots were not formed which otherwise would have been formed and would have increased roughness.

5.6 Interaction effect in EN31&Cu

The interaction effects of Pc and Ton on MRR, Pc and Ton on TWR, Pc and Ton on SR were found significant in machining of EN31 steel with copper electrode.

5.6.1 Interaction effect on MRR

Figure 5.12 elucidates the surface and interaction plot of Pc and Ton on MRR. The current intensity affected MRR in direct proportion as MRR increased with increase in Pc for all settings of Ton. The largest slope was recorded on 100 µs, then reduced on 400 µs and lowest on 1000 µs. The maximum MRR was recorded on high level of Pc and intermediate level of Ton. The reason for decrease in slope with rise in Ton is the expansion of plasma in longitudinal direction which decreases the energy density of spark.

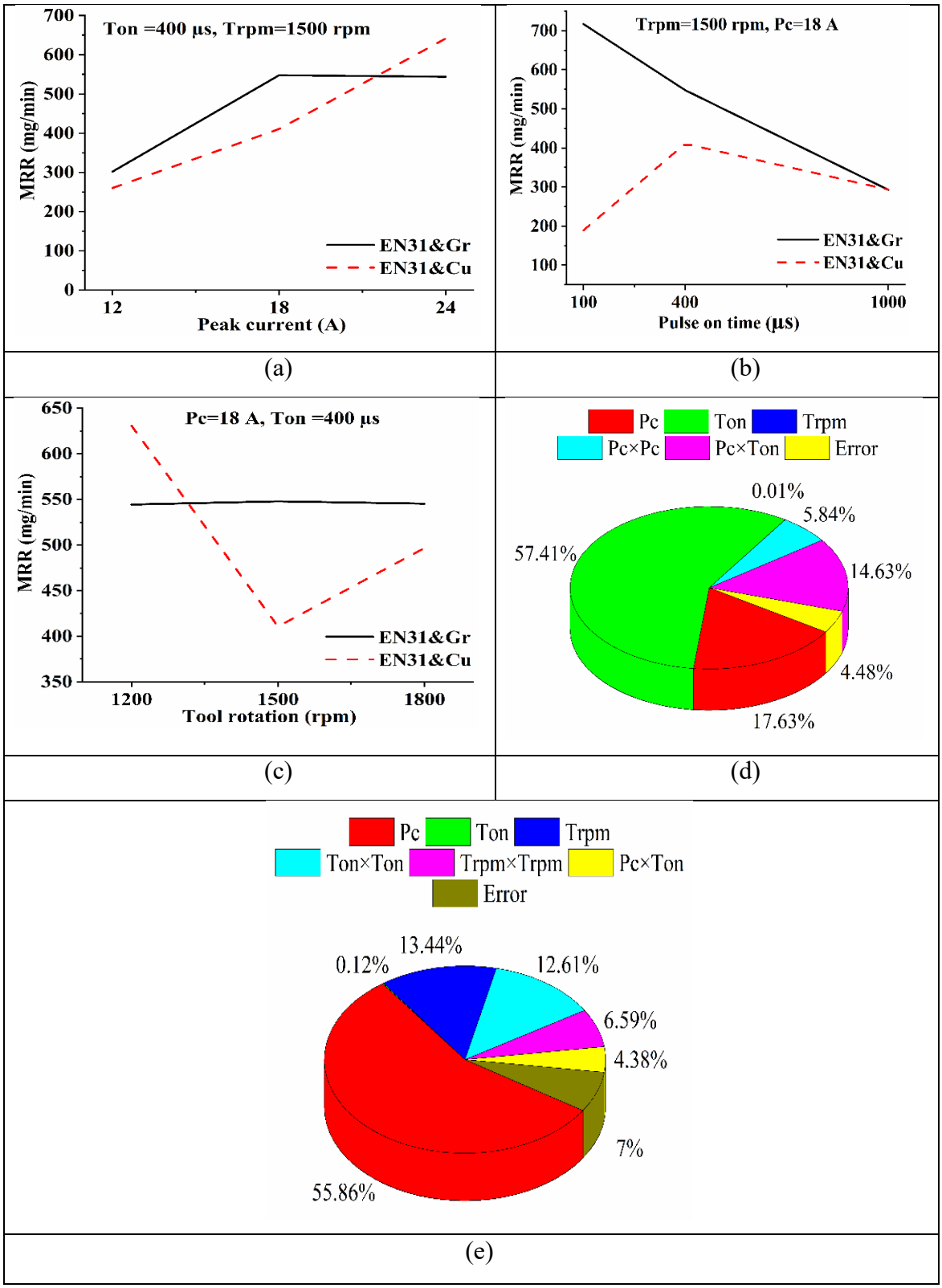

Figure 5.2. Actual plots showing variation of (a) Pc; (b) Ton; (c) Trpm on MRR in EN31&Gr and EN31&Cu; (d) parameters percentage share on MRR in EN31&Gr; (e) parameters percentage share on MRR in EN31&Cu.

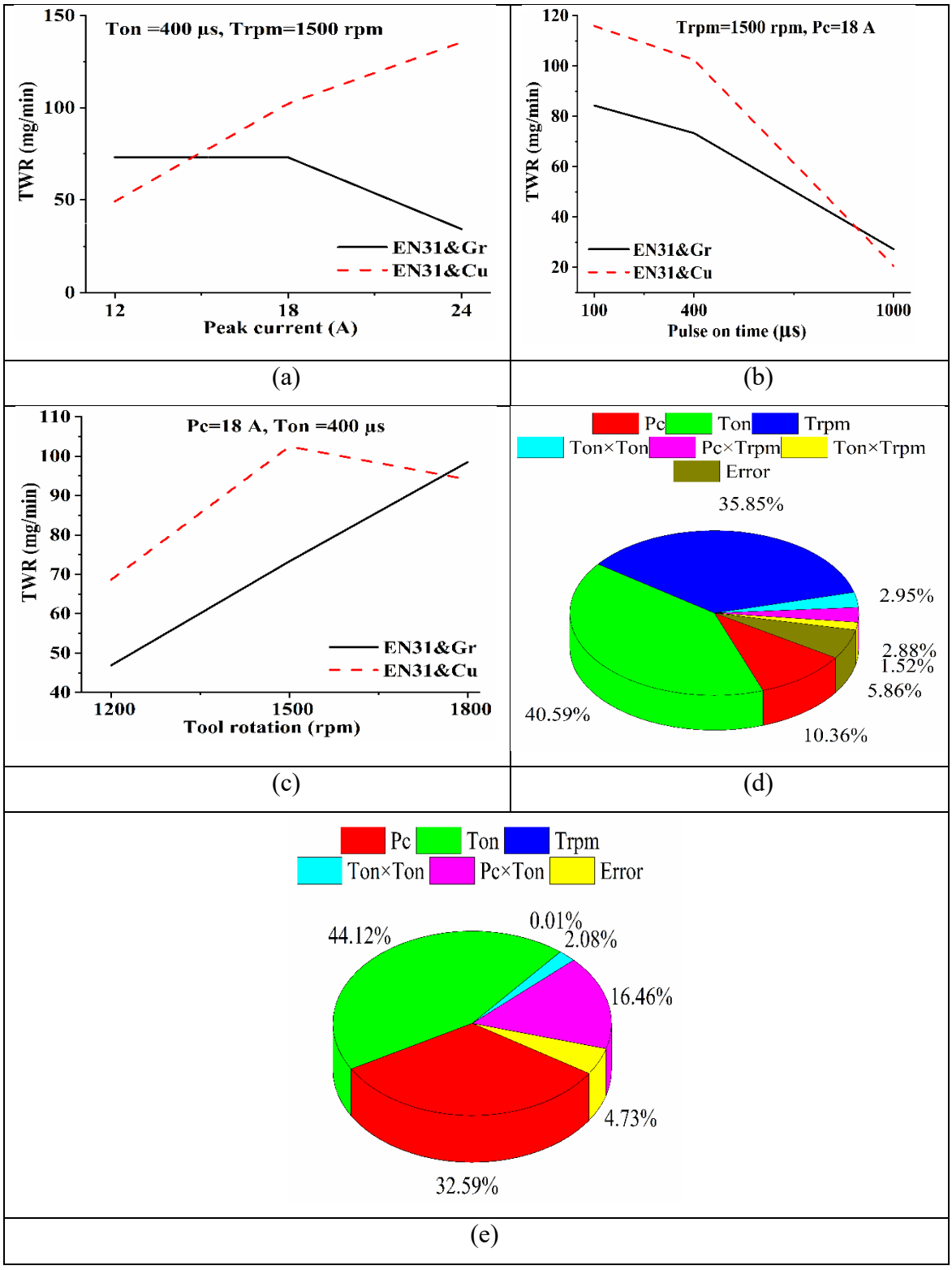

Figure 5.3. Actual plots showing variation of (a) Pc; (b) Ton; (c) Trpm on TWR in EN31&Gr and EN31&Cu; (d) parameters percentage share on TWR in EN31&Gr; (e) parameters percentage share on TWR in EN31&Cu.

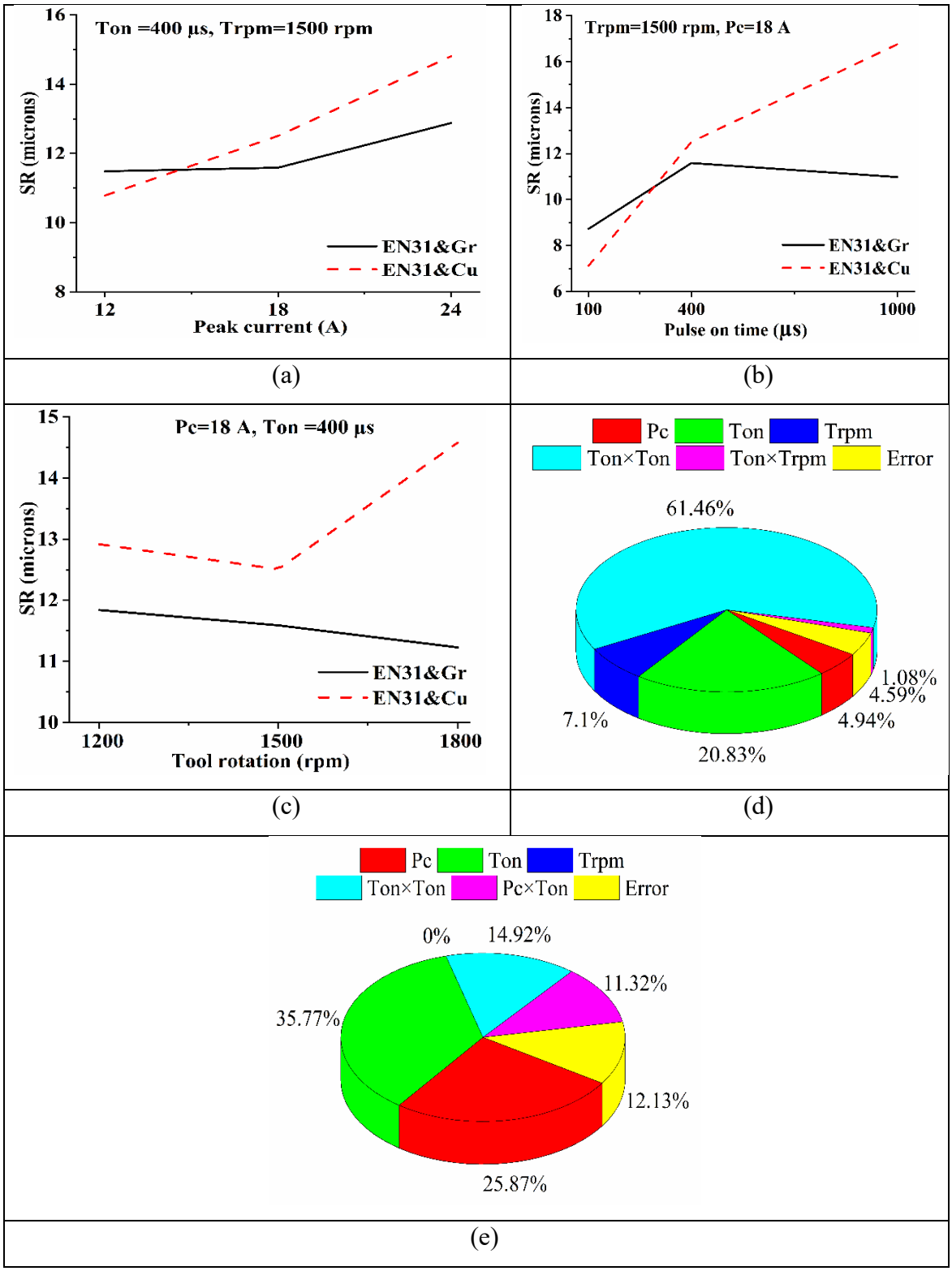

Figure 5.4. Actual plots showing variation of (a) Pc; (b) Ton; (c) Trpm on SR in EN31&Gr and EN31&Cu; (d) parameters percentage share on SR in EN31&Gr; (e) parameters percentage share on SR in EN31&Cu.

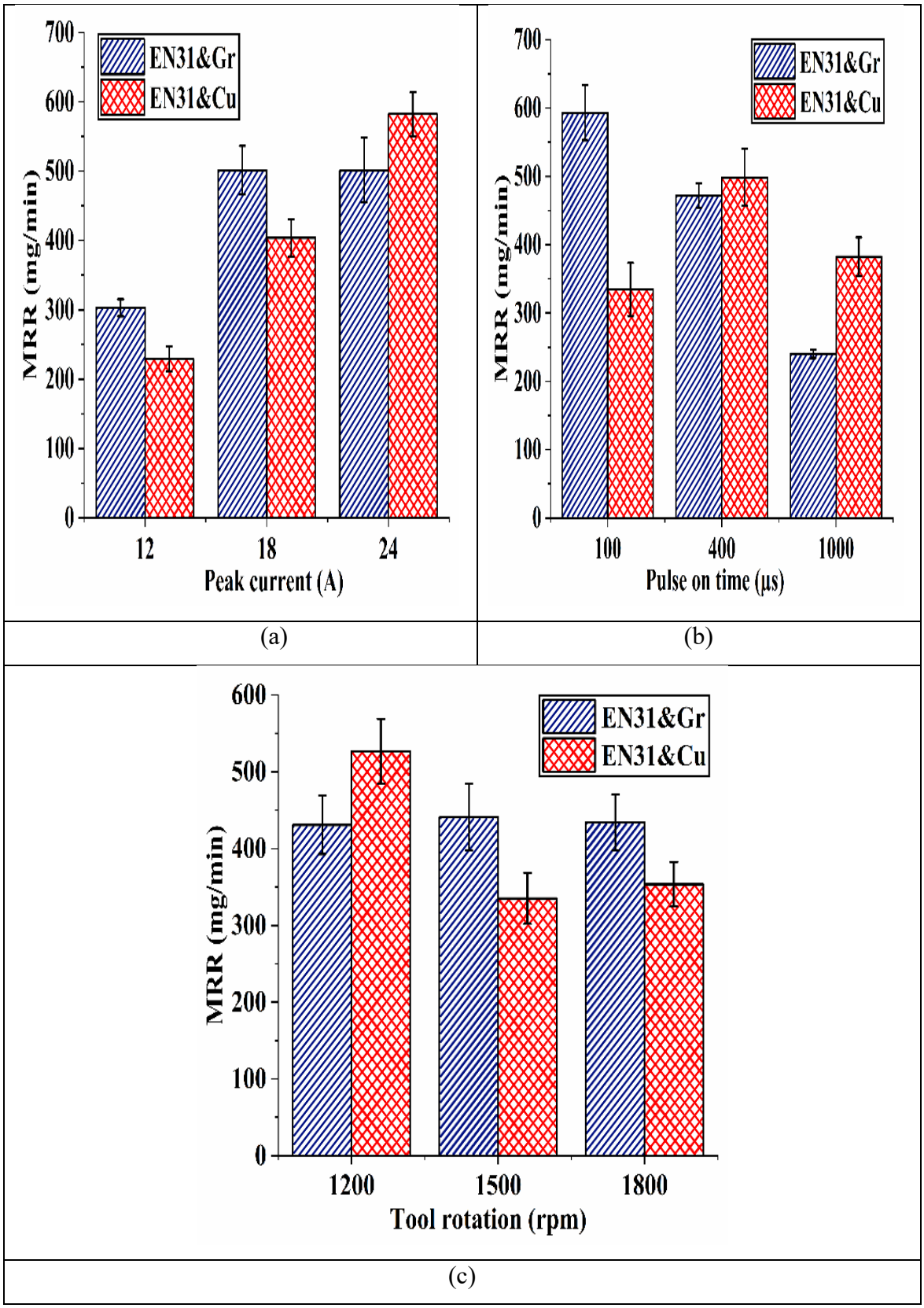

Figure 5.5. Bar graph showing effect of (a) peak current; (b) pulse on time; (c) tool rotation on MRR of EN31 steel machined with graphite and copper electrode.

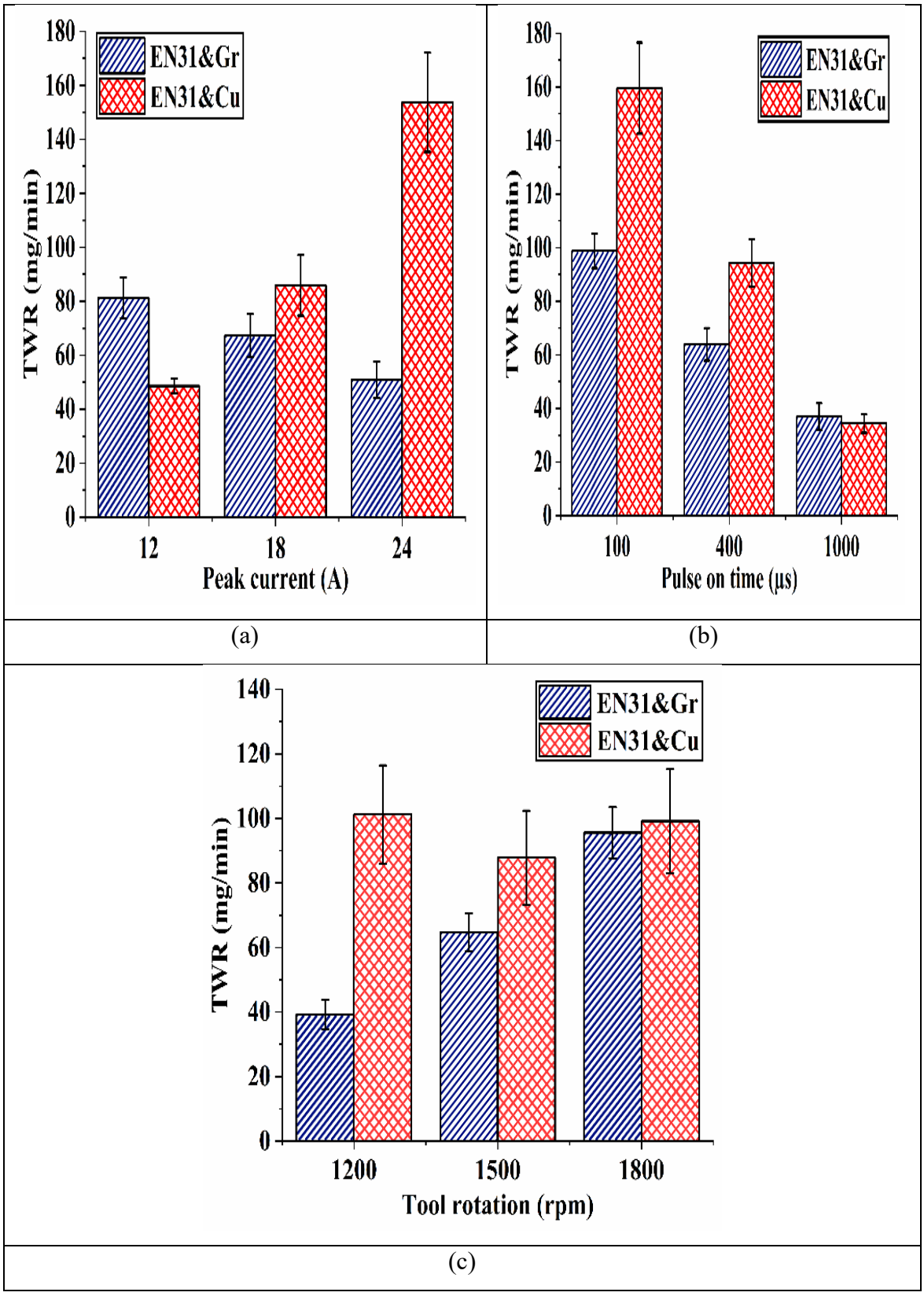

Figure 5.6. Bar graph showing effect of (a) peak current; (b) pulse on time; (c) tool rotation on TWR of EN31 steel machined with graphite and copper electrode.

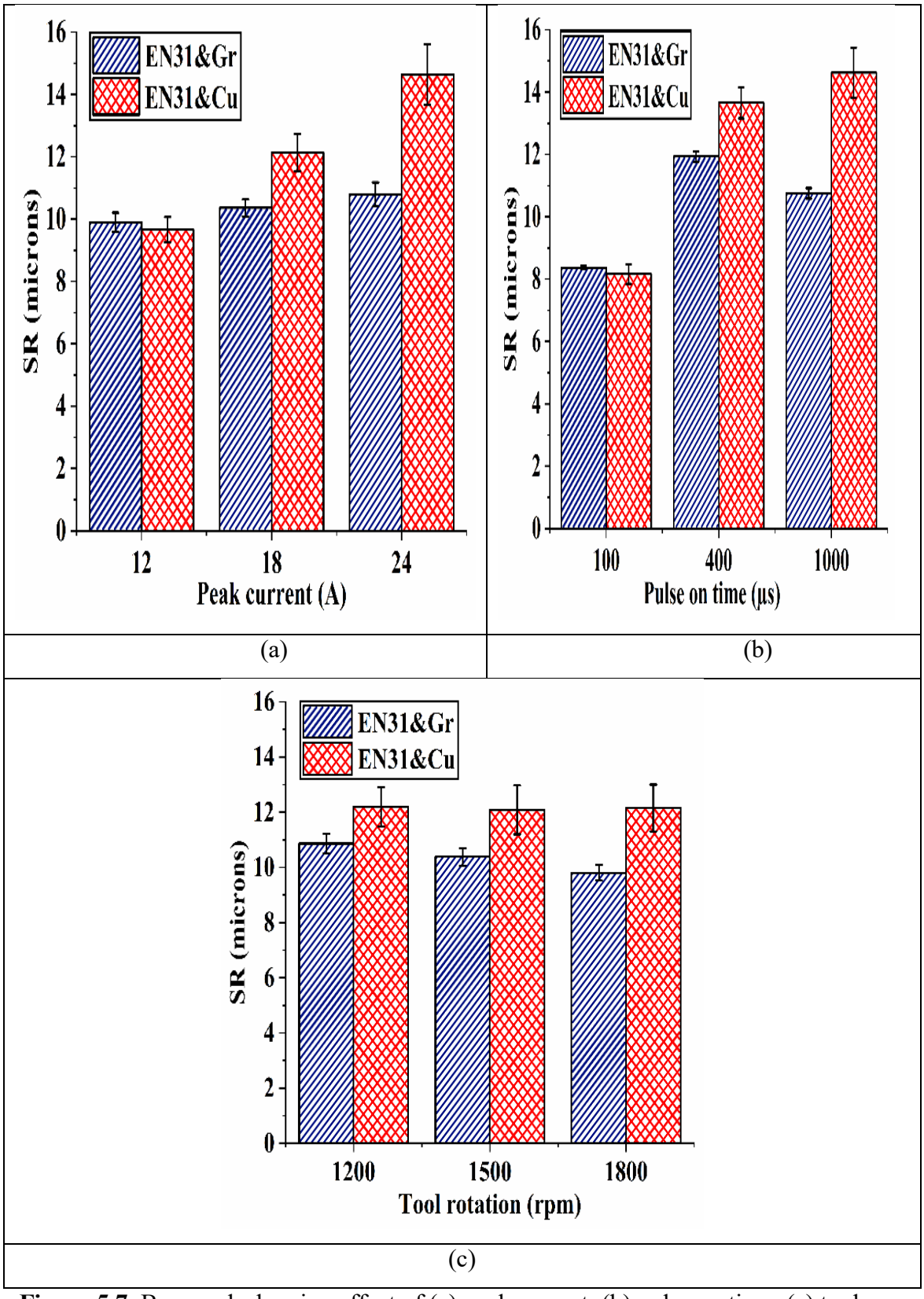

Figure 5.7. Bar graph showing effect of (a) peak current; (b) pulse on time; (c) tool rotation on SR of EN31 steel machined with graphite and copper electrode.

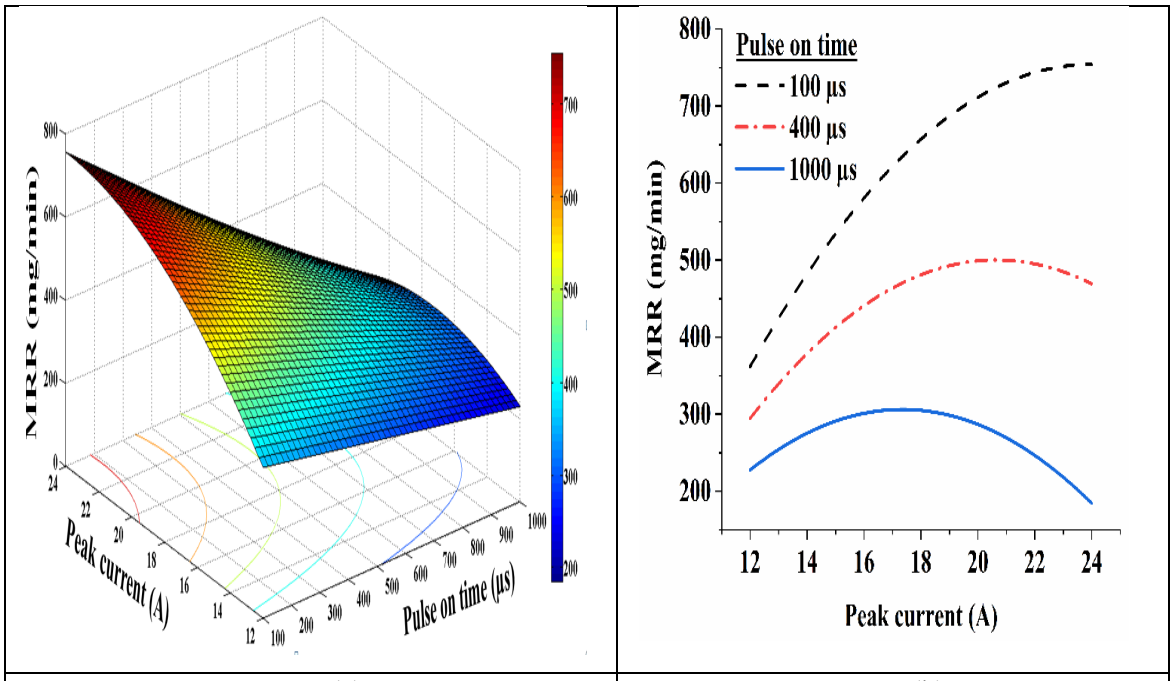

(a) (b)

Figure 5.8. Variation of Pc and Ton on MRR in EN31&Gr: (a) response surface plot; (b) interaction plot.

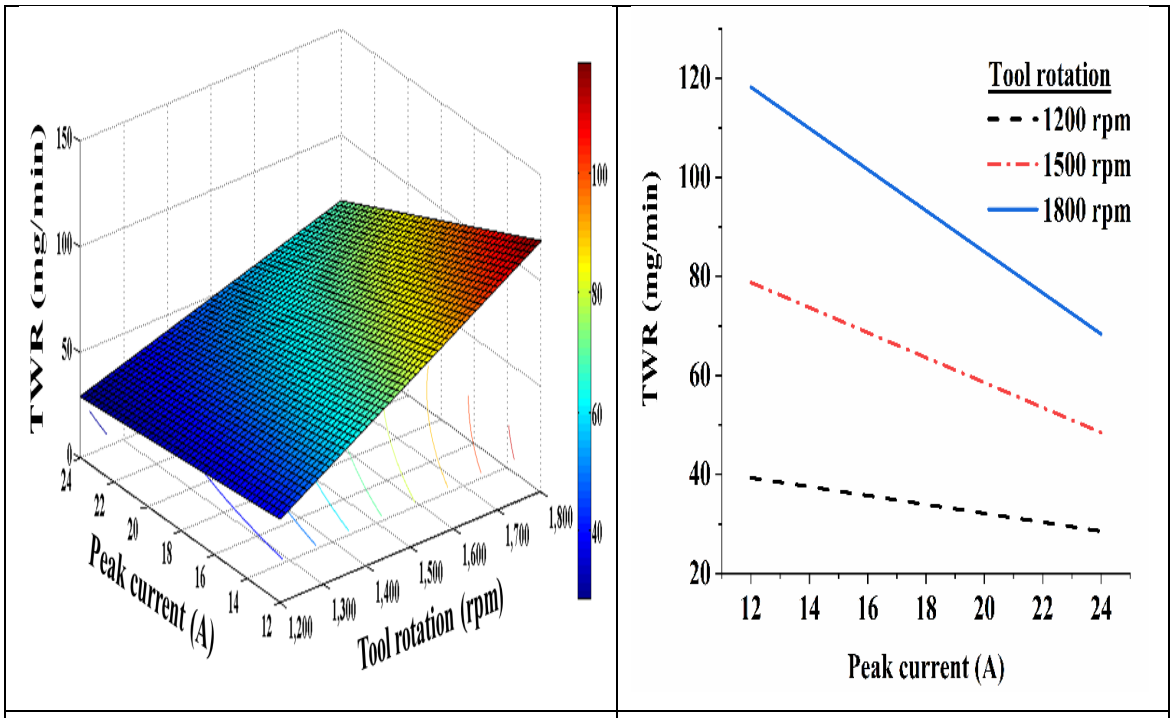

(a) (b)

Figure 5.9. Variation of Pc and Trpm on TWR in EN31&Gr: (a) response surface plot; (b) interaction plot.

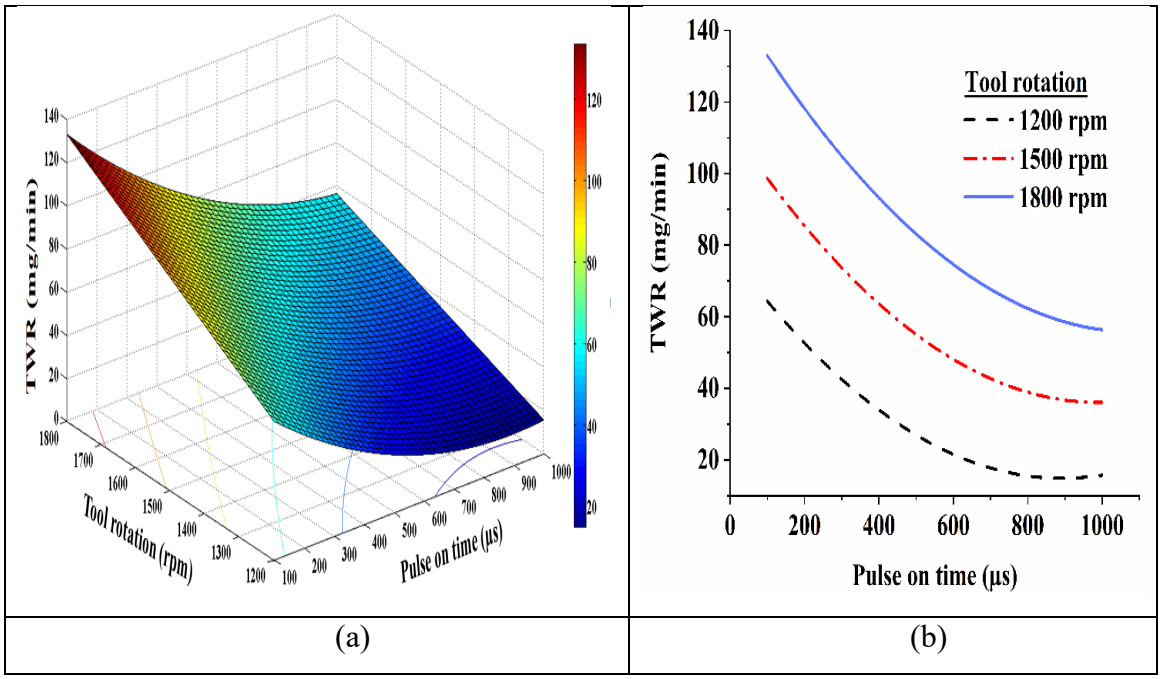

Figure 5.10. Variation of Ton and Trpm on TWR in EN31&Gr: (a) response surface plot; (b) interaction plot.

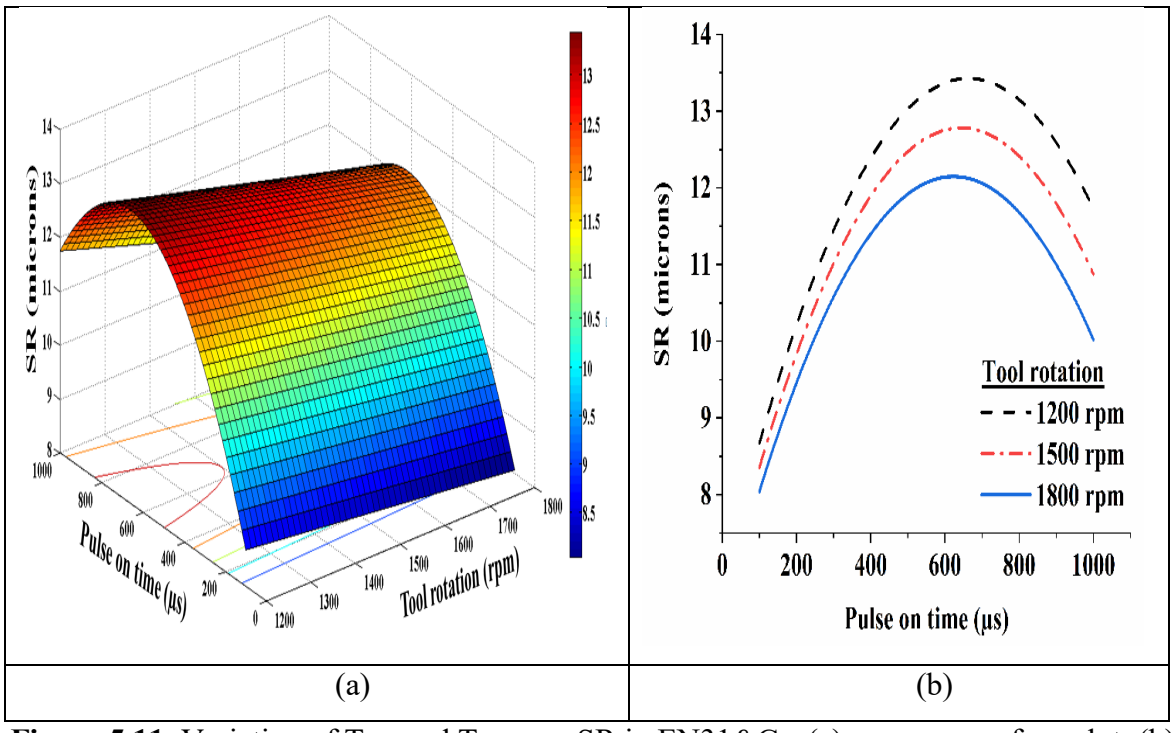

Figure 5.11. Variation of Ton and Trpm on SR in EN31&Gr: (a) response surface plot; (b) interaction plot.

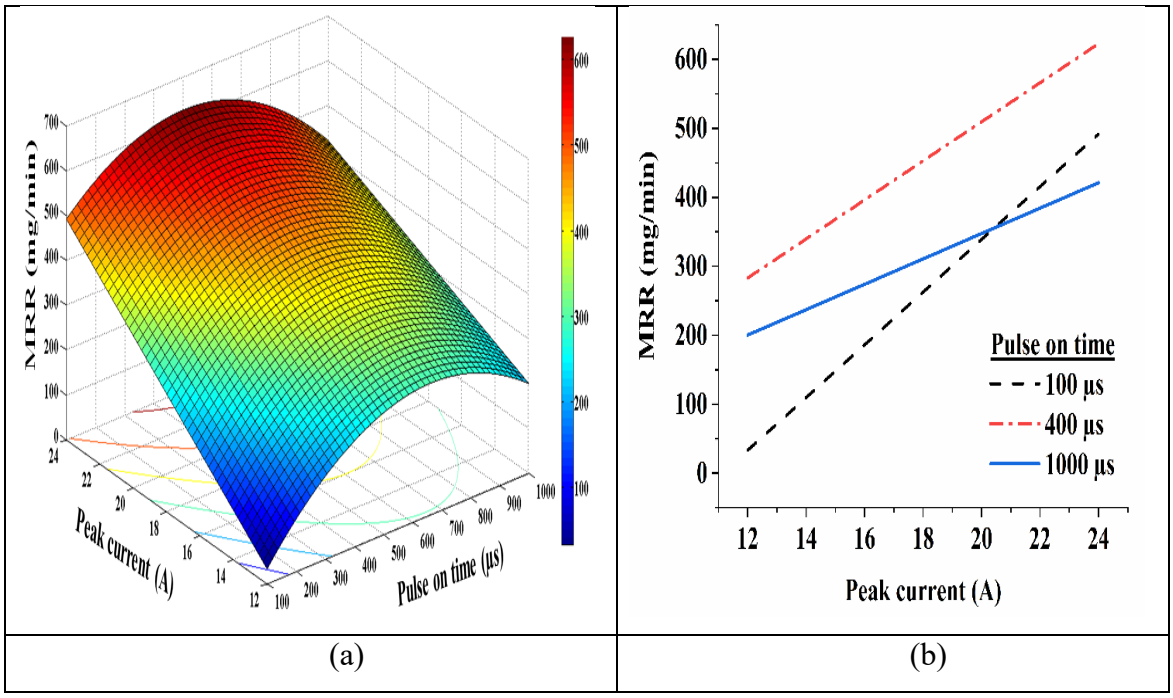

(a) (b)

Figure 5.12. Variation of Pc and Ton on MRR in EN31&Cu: (a) response surface plot; (b) interaction plot.

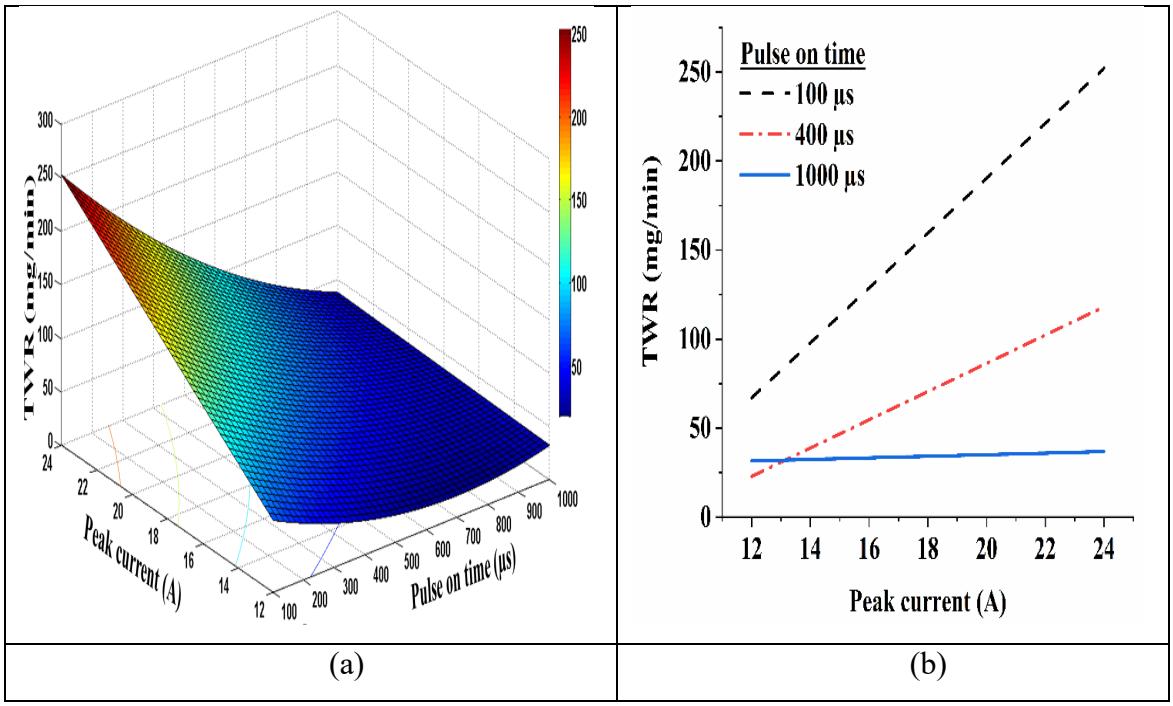

(a) (b)

Figure 5.13. Variation of Pc and Ton on TWR in EN31&Cu: (a) response surface plot; (b) interaction plot.

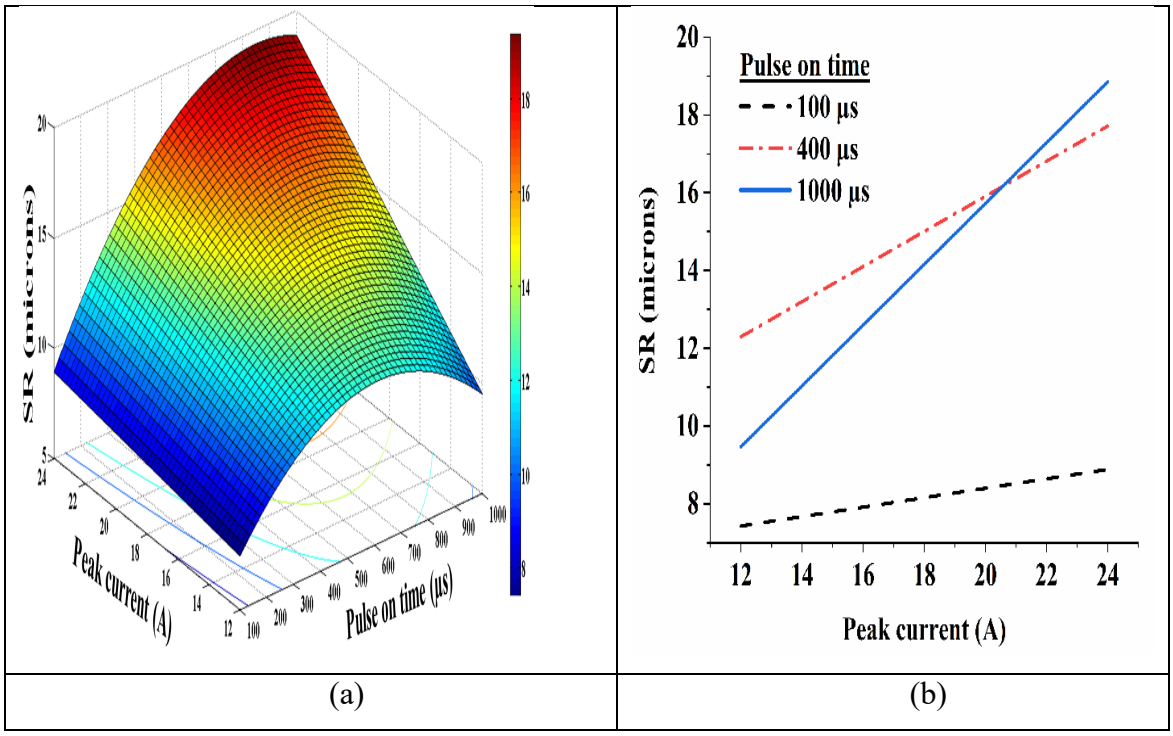

Figure 5.14. Variation of Pc and Ton on SR in EN31&Cu: (a) response surface plot; (b) interaction plot.

5.6.2 Interaction effect on TWR

The TWR was also found to be affected by interaction of Pc and Ton, shown in figure 5.13. The slope of line decreased from first to third level of Ton which almost approximated to zero slope at third level. The lowest TWR was recorded at high level of Pc and high level of Ton. The reason for lowest TWR at this combination is attributed to decrease in tool tip temperature as a result of plasma expansion leading to less temperature and hence less electrode wear.

5.6.3 Interaction effect on SR

The peak current and on-time pulse interaction effect remained consistently prominent for surface roughness as it was for MRR and TWR, shown in figure 5.14. The surface roughness was found in direct proportion to Pc for all Ton levels. The SR was found lowest at low level of Pc and low level of Ton. The reason for lowest surface roughness at this combination is low energy density of spark which results in shallow craters.

5.7 Voltage and current waveform analysis

The voltage and current waveforms were recorded with the help of Keysight Infinii Vision DSO-X 2022A, Digital Storage Oscilloscope. The voltage and current probes were employed to capture the current and voltage waveforms. The recorded waveforms under different parametric settings are presented in figures 5.15, 5.16 and 5.17, respectively. The study of waveforms clearly show smooth spark cycles with graphite electrode while, with copper, ignition delay was noticed. From figure 5.12, it can be observed that with increase in current, occurrence of ignition delay increased with copper electrode. The delay in sparking will affect the machining rate. The same may be verified from the results in table 4.2, 4.3 as well as figures 5.2 (a, b, c). At centre value of parameters, MRR recorded with graphite tool (547.9 mg/min) was higher than that of copper electrode (410.7 mg/min) (refer tables 4.2 and 4.3). Further, figure 5.10 shows the variation with on-time pulse. Here also, it is evident that graphite performs better yielding resulting into more MRR. Lastly, figure 5.17 shows the waveforms showing the effect of tool rotation. Lot of discharge interruption was noticed particularly, with copper electrode.

5.8 Morphology results

Figure 5.18 shows the surface morphology of the samples machined by conventional EDM and abrasive mixed rotary EDM (AREDM). The morphology of the samples machined by conventional EDM was specifically included to compare the results with abrasive mixed rotary EDM (AREDM). The surface images were captured through field emission scanning electron microscope (FESEM) with a working distance of 10 mm. The surface morphology results clearly showed improvements in surface with abrasive mixed rotary EDM with graphite electrode compared to conventional EDM. The conventional EDM surface shows segregated solidified spherical debris, clustered deposited debris, surface cracks and pockmarks as evident from figures 5.18(a, c). In figure 5.18(b), re-deposited material i.e. debris were effectively flushed away due to tool and stirrer rotation resulting in smooth surface.

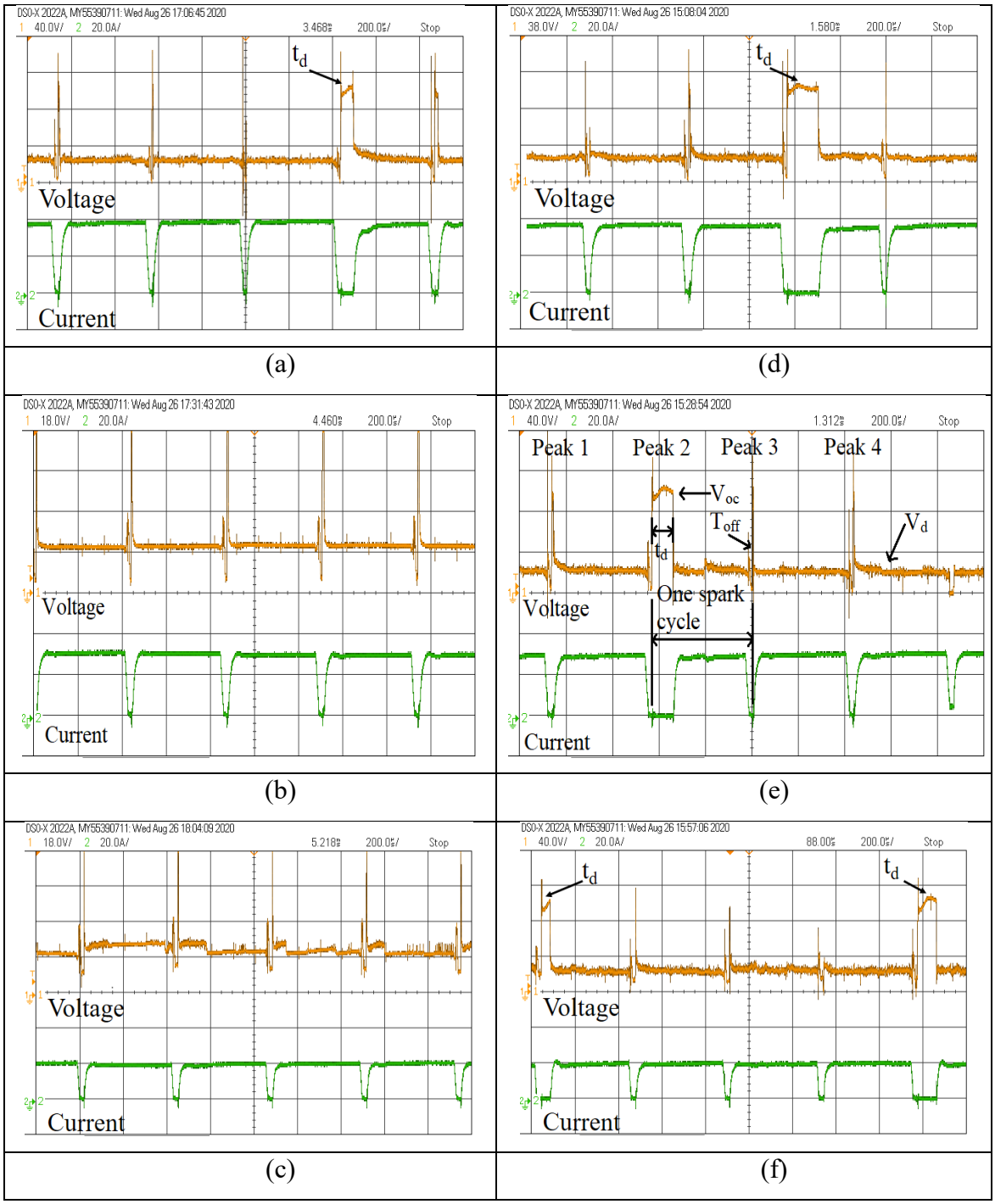

Figure 5.15. Voltage and current waveforms during (a, b, c) EN31 & Gr; (d, e, f) EN31 & Cu. (V_{oc}-open circuit voltage, V_d- discharge voltage, t_d- ignition delay time, T_{off}-pulse off time) (a: Pc=12 A, Ton=400 µs, Trpm=1500 rpm, b: Pc=18 A, Ton=400 µs, Trpm=1500 rpm, c: Pc=24 A, Ton=400 µs, Trpm=1500 rpm, d: Pc=12 A, Ton=400 µs, Trpm=1500 rpm, e: Pc=18 A, Ton=400 µs, Trpm=1500 rpm, f: Pc=24 A, Ton=400 µs, Trpm=1500 rpm).

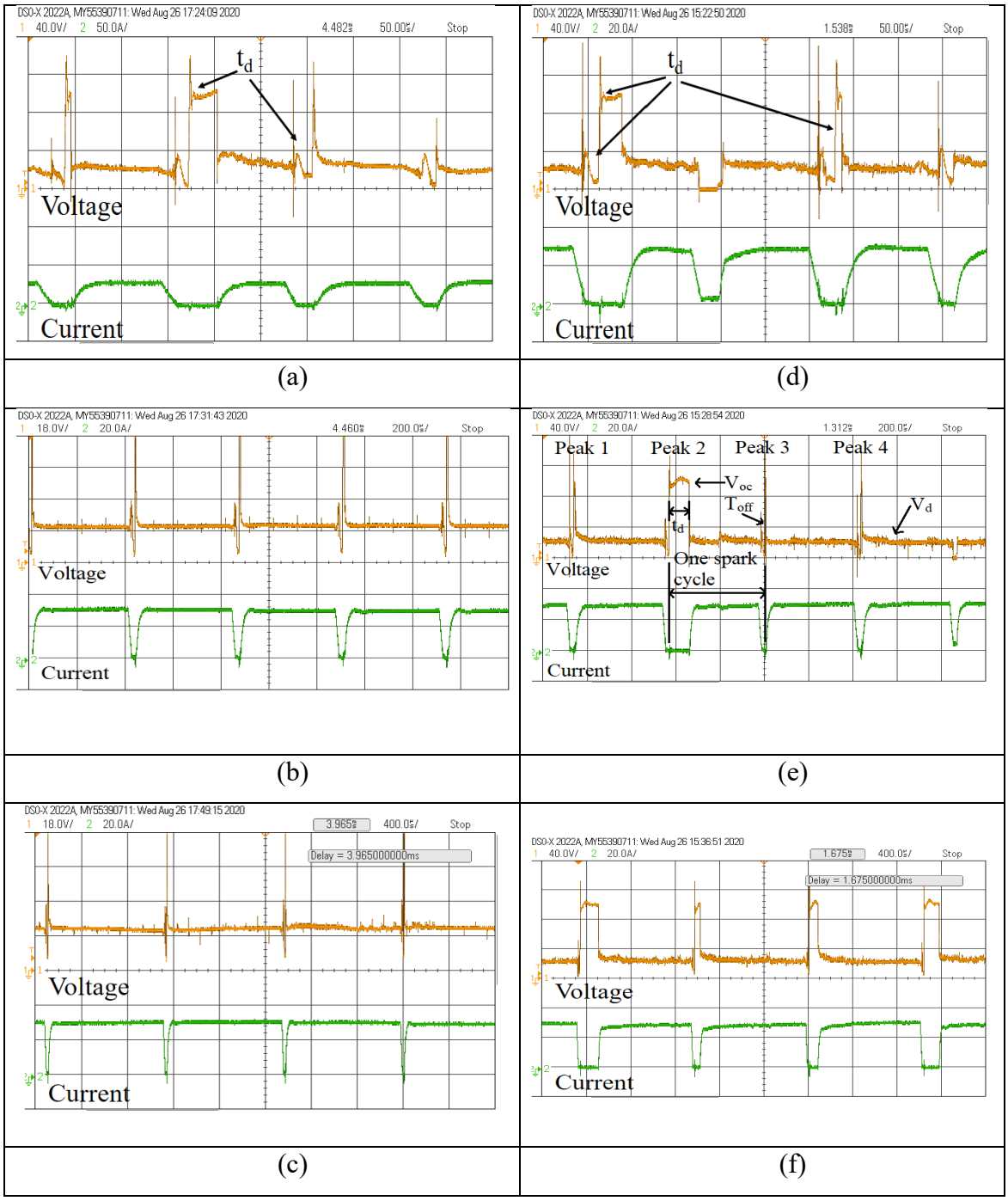

Figure 5.16. Voltage and current waveforms during (a, b, c) EN31 & Gr; (d, e, f) EN31 & Cu. (V_{oc}-open circuit voltage, V_d- discharge voltage, t_d- ignition delay time, T_{off}-pulse off time) (a: Pc=18 A, Ton=100 µs, Trpm=1500 rpm, b: Pc=18 A, Ton=400 µs, Trpm=1500 rpm, c: Pc=18 A, Ton=1000 µs, Trpm=1500 rpm, d: Pc=18 A, Ton=100 µs, Trpm=1500 rpm, e: Pc=18 A, Ton=400 µs, Trpm=1500 rpm, f: Pc=18 A, Ton=1000 µs, Trpm=1500 rpm).

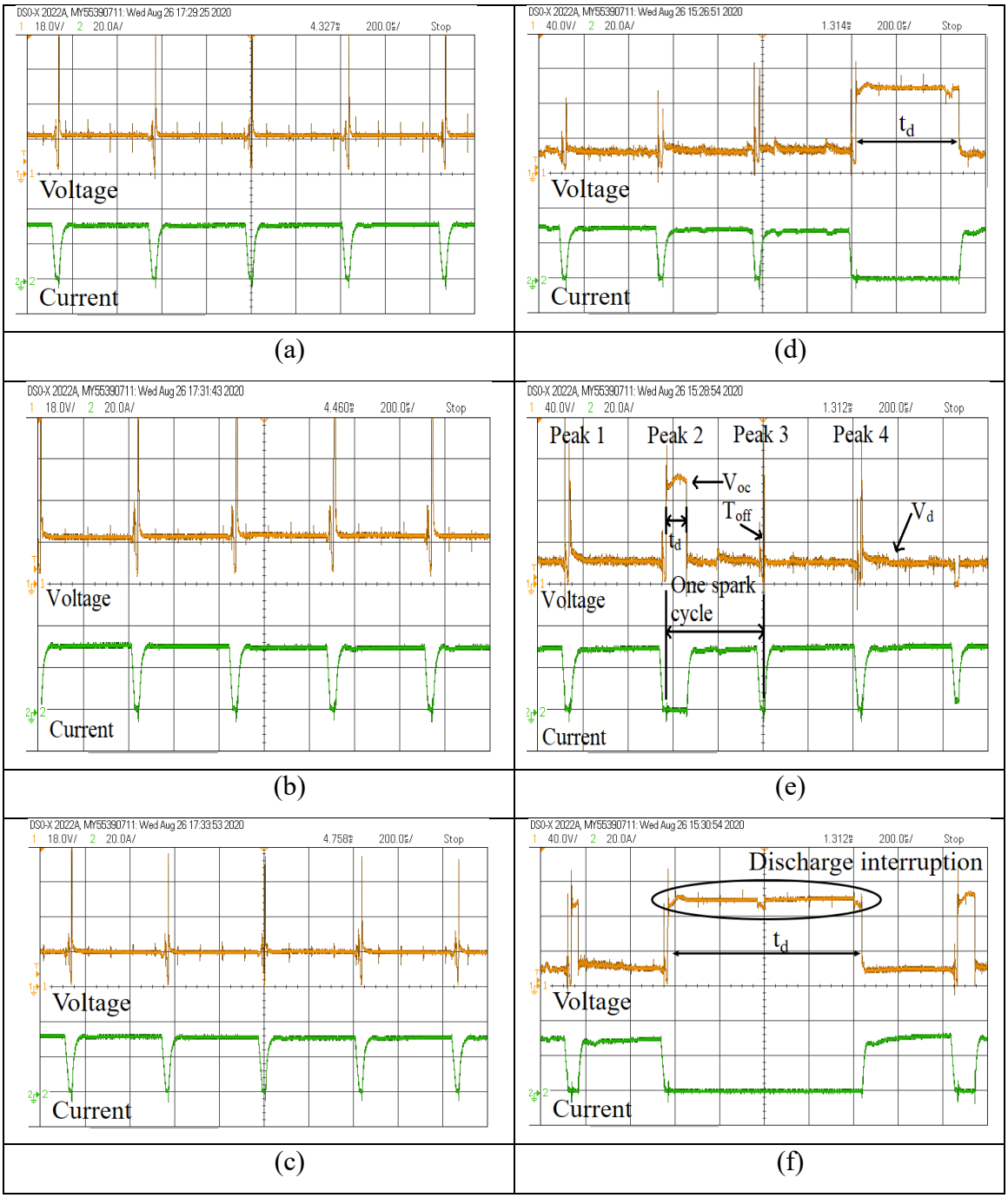

Figure 5.17. Voltage and current waveforms during (a, b, c) EN31 & Gr; (d, e, f) EN31 & Cu. (V_{oc}-open circuit voltage, V_d- discharge voltage, t_d- ignition delay time, T_{off}-pulse off time) (a: Pc=18 A, Ton=400 µs, Trpm=1200 rpm, b: Pc=18 A, Ton=400 µs, Trpm=1500 rpm, c: Pc=18 A, Ton=400 µs, Trpm=1800 rpm, d: Pc=18 A, Ton=400 µs, Trpm=1200 rpm, e: Pc=18 A, Ton=400 µs, Trpm=1500 rpm, f: Pc=18 A, Ton=400 µs, Trpm=1800 rpm).

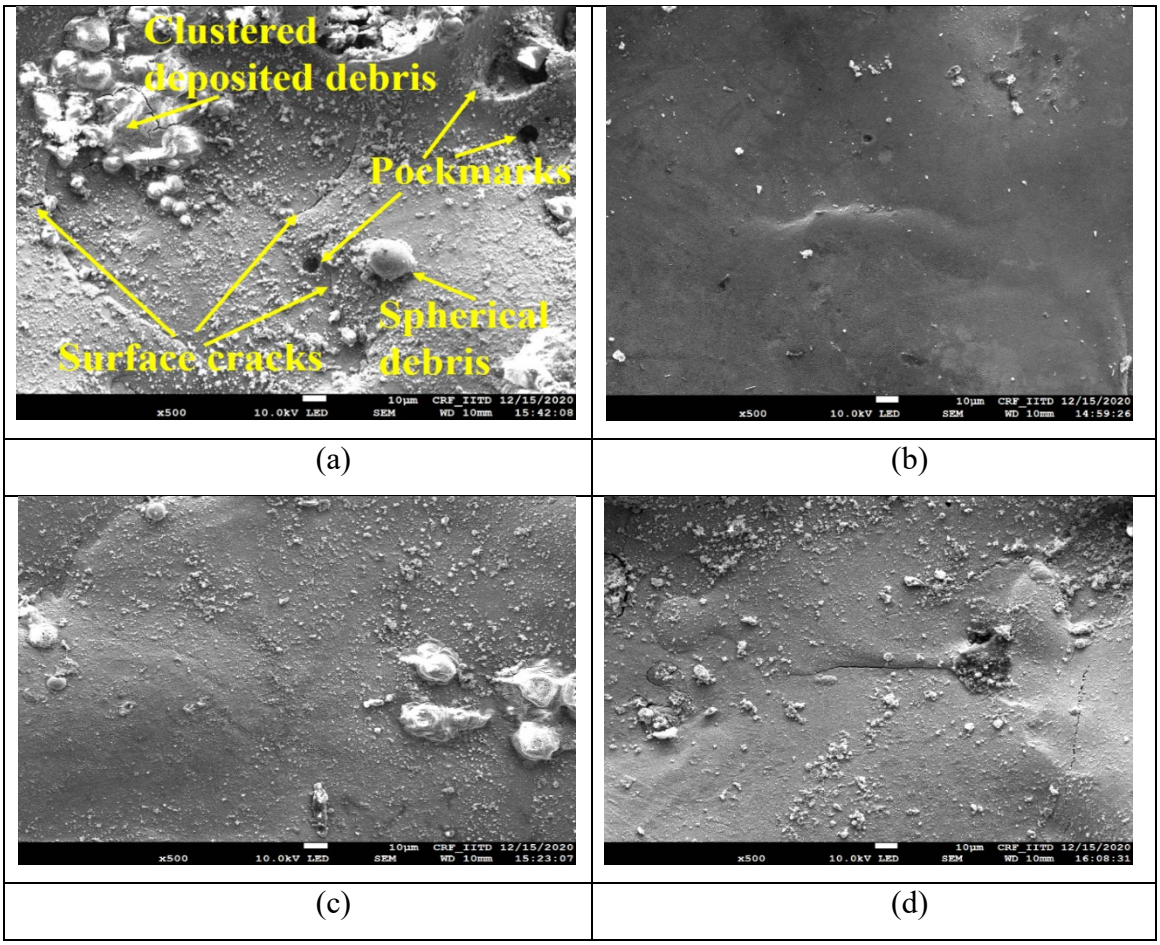

Figure 5.18. Morphology of surface by (a) conventional EDM (EN31&Gr); (b) AREDM (EN31&Gr); (c) conventional EDM (EN31&Cu); (d) AREDM (EN31&Cu). (Pc-18A, Ton-400 µs, Trpm- 1500 rpm).

Furthermore, it is also evident from figure 5.11(a) that energy density of the spark decreased as a consequence of enlargement of plasma at high on-time pulse resulting in smooth surface. The same has also been verified from figure 5.15(b) that the spark cycle remained uniform with graphite electrode again contributing into smooth surface. On the contrary, tool and stirrer rotation effects on copper electrode has not contributed appreciably as the surface cracks along with segregated solidified debris are quite clear from figure 5.18(d). The justification for this may be assigned to increased energy density of the spark at high pulse on time leading to rough surface (refer figure 5.14(b)) and existence of ignition delay and dissimilar spark cycles (refer figure 5.15(e)).

5.8.1 Analysis of recast layer thickness

Recast layer occurs due to redeposited material or debris on the surface of workpiece. Figures 5.19(a-f) and 5.20(a-f) demonstrates the characteristics of recast layer while machining EN31 steel with graphite and copper electrode, respectively. A comparison with conventional EDM is also presented. It has been noticed that the graphite electrode resulted into a better surface with thin recast layer compared to copper electrode in AREDM and conventional EDM with both electrode. It recorded recast layer thickness of 6.12 µm compared to 32.29 µm and 62.25 µm in AREDM and conventional EDM machined with copper electrode, respectively (refer figures 5.19(e) & 5.20(a, d)). Micro-cracks on the surface of recast layer were seen with graphite electrode whereas, no micro-cracks were observed with copper electrode. These cracks develop due to rapid cooling cycle after melting due to flushing action of dielectric fluid. The intensity of micro-cracks were also found to be less with AREDM process refer figure 5.19(c, f). From figure 5.20(b, e), it is apparent that the debris adhered to surface in conventional EDM are very large compared to debris in AREDM process. The formation of thin recast layer and finer surface in terms of smaller redeposited debris makes AREDM process better than the conventional one. The same can also be verified from figure 5.18. No such deposition of debris was noticed with graphite electrode which is the reason why it results in better surface finish. Same may also be verified from surface roughness results portrayed in figure 5.4 (Lamba and Vipin 2022).

5.8.2 Analysis of sub-surface micro-hardness

Struers Duramin 40-M1 Vickers hardness tester of hardness scale HV0.5 was exercised to gauge the sub-surface micro-hardness across the machining surface. As a preparatory requirement, workpieces were first prepared by fixing them in a die. The indenter was subjected to a 500 g load for 10 seconds of dwell time. Readings were taken on the surface in two perpendicular directions, namely along the edge of the surface and transverse to the surface with 8 indentations on each side. As a final outcome, the average values of these indentations were taken. The collected findings are portrayed in table 5.9. It is apparent that the AREDM enhances the surface's micro-hardness. The reason may be assigned to the migration of the powder material which increases the hardness. In this study, SiC powder is responsible for increase of micro-hardness (Lamba and Vipin 2022).

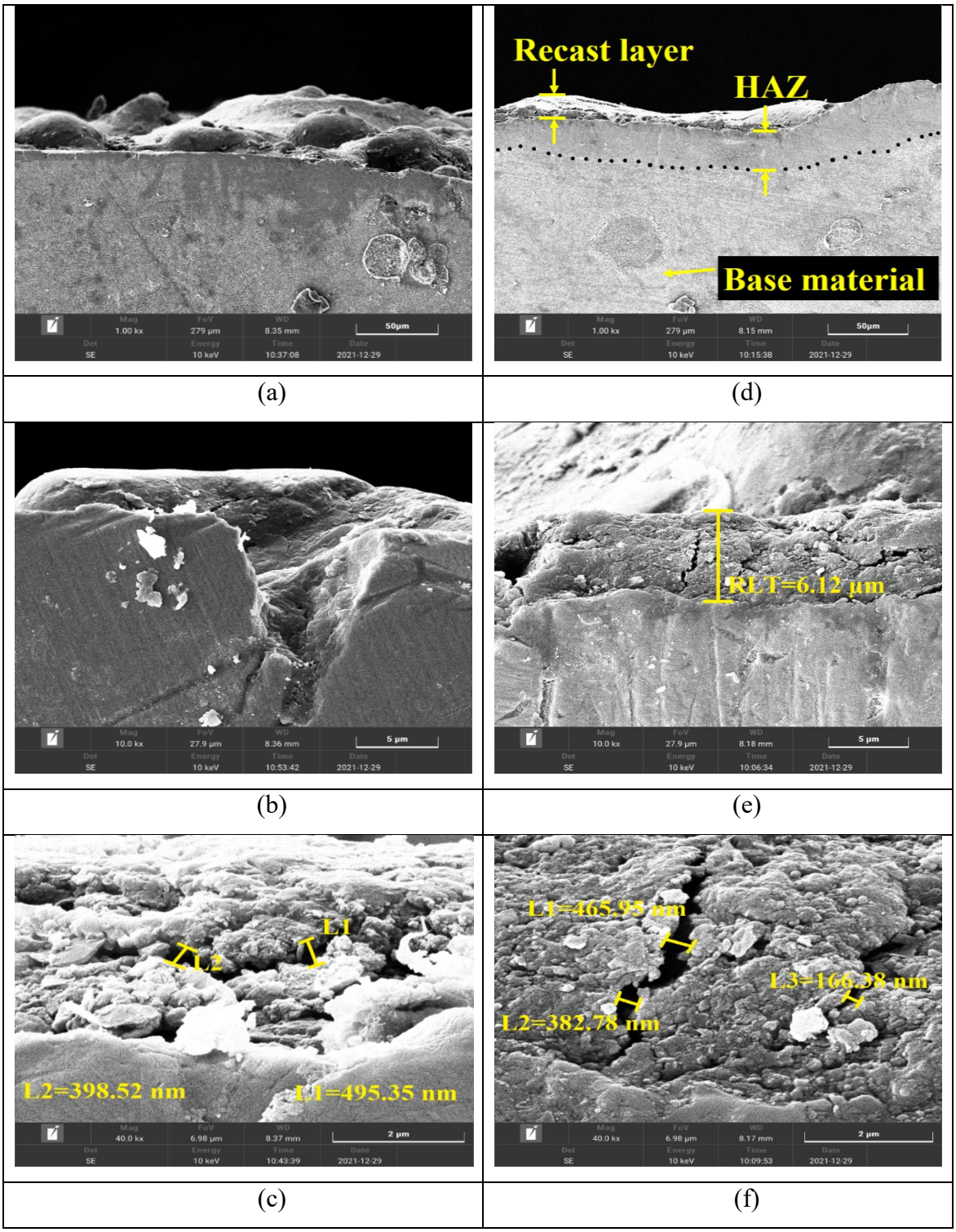

Figure 5.19. FESEM images of recast layer generated in (a, b, c) conventional EDM (EN31&Gr); (d, e, f) AREDM (EN31&Gr). (peak current 18A, pulse on time 400 µs, tool rotation 1500 rpm).

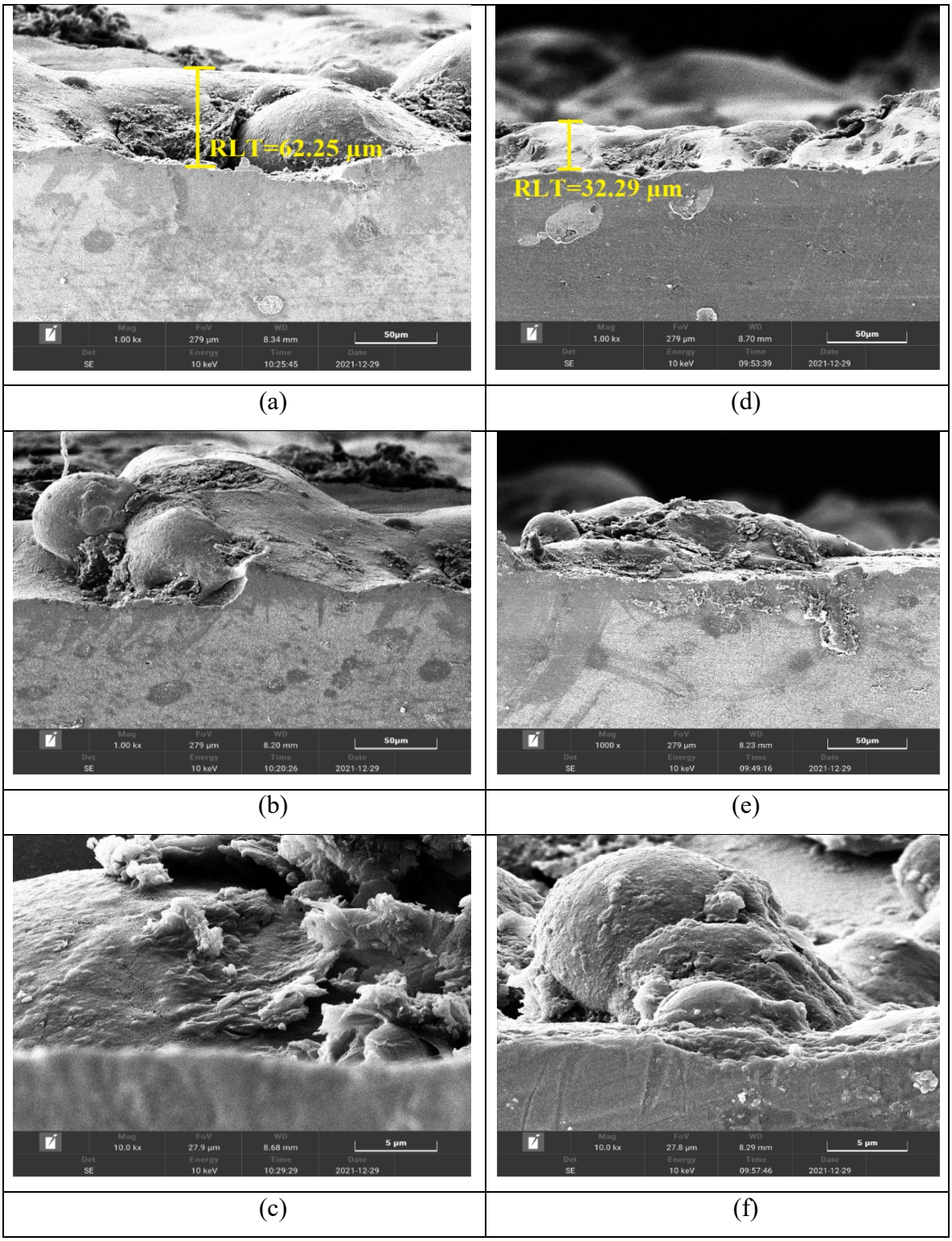

Figure 5.20. FESEM images of recast layer generated in (a, b, c) conventional EDM (EN31&Cu); (d, e, f) AREDM (EN31&Cu). (peak current 18A, pulse on time 400 µs, tool rotation 1500 rpm).

Table 5.9. Results of sub-surface micro-hardness.

Vickers hardness	Process (workpiece & tool)			
	Conventional EDM (EN31&Gr)	AREDM (EN31&Gr)	Conventional EDM (EN31&Cu)	AREDM (EN31&Cu)
Along edge	502.81	529.17	465.07	521.87
Transverse to edge	514.59	533.23	503.33	523.54

5.9 Multi-objective optimization

This work involves a multi-objective optimization like in most EDM applications. In this study, maximization of MRR along with minimization of TWR and SR, were aimed. For this purpose, genetic algorithm was selected to identify the best possible set of parameters. The MATLAB (R2018a) optimization toolbox was used for executing genetic algorithm. The statistical model for MRR, TWR and SR for EN31&Gr, represented by equations (1), (2) & (3) and for EN31&Cu by equations (4), (5) & (6) were used in the optimization. The problem formulation with constraints is as follows

$$\text{Maximize } f_1 = \text{MRR}(\phi)$$

$$\text{Minimize } f_2 = \text{TWR}(\phi)$$

$$\text{Minimize } f_3 = \text{SR}(\phi)$$

where; $\phi = \{\text{Pc, Ton, Trpm}\}$ subjected to

$$12 \leq \text{Pc} \leq 24;\ 100 \leq \text{Ton} \leq 1000;\ 1200 \leq \text{Trpm} \leq 1800$$

The optimum set of process parameters as revealed by genetic algorithm multi-objective optimization technique are shown in table 5.10. Further, the experiments were performed on conventional EDM without abrasive and tool rotation at the optimum values depicted in table 5.10. The comparative results are presented in table 5.11. The obtained results

completely outperforms conventional EDM and are stated to be the best results under the considered experimental conditions.

Table 5.10. Best set of machining variables.

W/p & tool	Optimum parameters			MRR (mg/min)	TWR (mg/min)	SR (microns)
	Pc (A)	Ton (µs)	Trpm (rpm)	Experiment	Experiment	Experiment
EN31&Gr	24	100	1200	783.8	64.4	8.371
EN31&Cu	12	100	1800	130.7	56.2	5.944

Table 5.11. Comparative results of EN31 steel.

W/p & tool	Optimum parameters			MRR (mg/min)	TWR (mg/min)	SR (microns)
	Pc (A)	Ton (µs)	Trpm (rpm)	Conventional, AREDM, % increase	Conventional, AREDM, % decrease	Conventional, AREDM, % decrease
EN31&Gr	24	100	1200	706.1, 783.8, 11	70.9, 64.4, 9.16	10.76, 8.371, 22.2
EN31&Cu	12	100	1800	120.4, 130.7, 8.55	59.4, 56.2, 5.38	6.43, 5.944, 7.55

CHAPTER-6

AREDM OF D3 STEEL WITH GRAPHITE AND COPPER ELECTRODES

6.1 Introduction

This section displays the analysis of variance, regression equations, interactions curve, surface plots, morphology results on D3 steel machined with graphite and copper electrode. The parametric settings and their levels are once again re-iterated here in Table 6.1 for better understanding and reference. In this research work, three process parameters, namely, peak current, pulse on time and tool rotation were selected to record MRR, TWR and SR of D3 steel with graphite and copper electrode.

Table 6.1. Process parameters and their levels.

Process parameters	Symbol	Unit	Selected levels		
			I	II	III
Peak current	P_c	A	12	18	24
Pulse on time	T_{on}	µs	100	400	1000
Tool rotation	T_{rpm}	rpm	1200	1500	1800

6.2 Regression equations and ANOVA results

ANOVA was done to quantify the variance due to process parameters and uncontrollable factors along with the percentage share of different parameters on machining responses. A confidence interval of 95% was used. The statistical models were generated for MRR, TWR and SR in machining of EN31 steel with graphite and copper electrode through regression equations with the help of Minitab 17 software. The uncontrollable factors during experimentation led to the difference between the model output and experimented data.

6.2.1 AREDM of D3 using Graphite Electrode

ANOVA results for SR, TWR and MRR in machining of D3 steel with graphite electrode are shown in Tables 6.2, 6.3 and 6.4, respectively. These tables consist of data after removing insignificant interactions and square terms. Equations (7), (8) and (9) are regression equations for MRR, TWR and SR, respectively. The $R^2_{adjusted}$ for SR, TWR and MRR are and 92.92%, 95.31% and 97.34% respectively which showed good fit for model.

Table 6.2. ANOVA table for SR (D3&Gr) (after removing insignificant interactions and square terms).

Origin	DOF	Seq. SS	Adj. SS	Adj. MS	F	P
Regression	4	135.534	135.534	33.8835	86.26	0.000
Pc	1	57.874	57.874	57.8745	147.33	0.000
Ton	1	11.727	43.119	43.1187	109.77	0.000
Trpm	1	11.803	11.803	11.8033	30.05	0.000
Ton × Ton	1	54.129	54.129	54.1292	137.80	0.000
Error	22	8.642	8.642	0.3928		
Total	26	144.176				

F: Fisher's value. Adj. MS: adjusted mean square; Adj. SS: adjusted sum of squares; DOF: degree of freedom; P: Probability of acceptance based on confidence level.

Table 6.3. ANOVA table for TWR (D3&Gr) (after removing insignificant interactions and square terms).

Origin	DOF	Seq. SS	Adj. SS	Adj. MS	F	P
Regression	6	38111.2	38111.2	6351.86	89.05	0.000
Pc	1	1993.9	881.1	881.14	12.35	0.002
Ton	1	20723.5	607.6	607.61	8.52	0.008
Trpm	1	11514.0	4813.6	4813.57	67.48	0.000
Ton × Ton	1	1782.4	1782.4	1782.35	24.99	0.000
Pc × Trpm	1	1396.4	1396.4	1396.44	19.58	0.000
Ton × Trpm	1	701.0	701.0	701.00	9.83	0.005
Error	20	1426.6	1426.6	71.33		
Total	26	39537.8				

F: Fisher's value. Adj. MS: adjusted mean square; Adj. SS: adjusted sum of squares; DOF: degree of freedom; P: Probability of acceptance based on confidence level.

Table 6.4. ANOVA table for MRR (D3&Gr) (after removing insignificant interaction and square terms).

Origin	DOF	Seq. SS	Adj. SS	Adj. MS	F	P
Regression	5	1202955	1202955	240591	191.33	0.000
Pc	1	264914	93730	93730	74.54	0.000
Ton	1	773685	8978	8978	7.14	0.014
Trpm	1	3235	3235	3235	2.57	0.124
Pc × Pc	1	47149	47149	47149	37.50	0.000
Pc × Ton	1	113971	113971	113971	90.64	0.000
Error	21	26407	26407	1257		
Total	26	1229362				

F: Fisher's value. Adj. MS: adjusted mean square; Adj. SS: adjusted sum of squares; DOF: degree of freedom; P: Probability of acceptance based on confidence level.

$$\begin{aligned} MRR = &-858.0 + (126.6 \times P_c) + (0.1856 \times T_{on}) \\ &+ (0.0447 \times T_{rpm}) - (2.462 \times P_c^2) \\ &- (0.03544 \times P_c \times T_{on}) \end{aligned} \quad (7)$$

$$\begin{aligned} TWR = &-177.6 + (7.24 \times P_c) - (0.1021 \times T_{on}) + (0.2200 \times T_{rpm}) \\ &+ (0.000098 \times T_{on}^2) - (0.00599 \times P_c \times T_{rpm}) \\ &- (0.000056 \times T_{on} \times T_{rpm}) \end{aligned} \quad (8)$$

$$\begin{aligned} SR = &\ 5.909 + (0.2989 \times P_c) + (0.01766 \times T_{on}) \\ &- (0.002699 \times T_{rpm}) - (0.000017 \times T_{on}^2) \end{aligned} \quad (9)$$

6.2.2 AREDM of D3 using Copper Electrode

ANOVA results for SR, TWR and MRR in machining of D3 steel with copper electrode are shown in tables 6.5, 6.6 and 6.7, respectively. The regression equations for MRR, TWR and SR are shown in equations (10), (11) and (12), respectively. The $R^2_{adjusted}$ for MRR, TWR and SR are 95.70%, 94.11% and 94.83%, respectively which showed good fit for model.

$$MRR = 256.5 + (27.41 \times P_c) + (0.711 \times T_{on}) - (0.2517 \times T_{rpm}) - (0.000770 \times T_{on}^2) \quad (10)$$

$$TWR = -76.4 + (12.002 \times P_c) - (0.0973 \times T_{on}) + (0.0118 \times T_{rpm}) + (0.000173 \times T_{on}^2) - (0.01164 \times P_c \times T_{on}) \quad (11)$$

$$SR = 12.976 + (0.2112 \times P_c) + (0.00489 \times T_{on}) - (0.006702 \times T_{rpm}) - (0.000011 \times T_{on}^2) + (0.000004 \times T_{on} \times T_{rpm}) \quad (12)$$

Table 6.5. ANOVA table for SR (D3&Cu) (after removing insignificant interactions and square terms).

Origin	DOF	Seq. SS	Adj. SS	Adj. MS	F	P
Regression	5	95.578	95.578	19.1157	96.29	0.000
Pc	1	28.905	28.905	28.9053	145.61	0.000
Ton	1	6.072	1.397	1.3966	7.04	0.015
Trpm	1	32.67	26.119	26.1187	131.57	0.000
Ton × Ton	1	23.496	23.496	23.4956	118.36	0.000
Ton × Trpm	1	4.435	4.435	4.4348	22.34	0.000
Error	21	4.169	4.169	0.1985		
Total	26	99.747				

F: Fisher's value. Adj. MS: adjusted mean square; Adj. SS: adjusted sum of squares; DOF: degree of freedom; P: Probability of acceptance based on confidence level.

6.3 Validation of Statistical Model

Validation of statistical model is a crucial step before processing to detailed analysis of results. A regression model validation is presented in table 6.8. The regression equations (7), (8), (9) and (10), (11), (12) were used to predict the results for D3&Gr and D3&Cu, respectively. The percentage error between experiment and predicted values were within

10% which showed good approximation. In addition, Figure 6.1 depicts the validation graphs between response predictor equation obtained through regression and experimental results for SR, TWR and MRR in machining D3 steel with graphite and copper electrode. The graphs reveals a closer match with experimented values proving its efficacy.

Table 6.6. ANOVA table for TWR (D3&Cu) (after removing insignificant interactions and square terms).

Origin	DOF	Seq. SS	Adj. SS	Adj. MS	F	P
Regression	5	87920.8	87920.8	17584.2	84.08	0.000
Pc	1	24754.6	33507.4	33507.4	160.22	0.000
Ton	1	45031.9	876.8	876.8	4.19	0.053
Trpm	1	225.6	225.6	225.6	1.08	0.311
Ton × Ton	1	5612.0	5612.0	5612.0	26.83	0.000
Pc × Ton	1	12296.7	12296.7	12296.7	58.80	0.000
Error	21	4391.8	4391.8	209.1		
Total	26	92312.6				

F: Fisher's value. Adj. MS: adjusted mean square; Adj. SS: adjusted sum of squares; DOF: degree of freedom; P: Probability of acceptance based on confidence level.

Table 6.7. ANOVA table for MRR (D3&Cu) (after removing insignificant interactions and square terms).

Origin	DOF	Seq. SS	Adj. SS	Adj. MS	F	P
Regression	4	809304	809304	202326	145.67	0.000
Pc	1	486673	486673	486673	350.39	0.000
Ton	1	108768	69847	69847	50.29	0.000
Trpm	1	102627	102627	102627	73.89	0.000
Ton × Ton	1	111235	111235	111235	80.09	0.000
Error	22	30557	30557	1389		
Total	26	839861				

F: Fisher's value. Adj. MS: adjusted mean square; Adj. SS: adjusted sum of squares; DOF: degree of freedom; P: Probability of acceptance based on confidence level.

Table 6.8. Model validation.

W/p & tool	Run order	Machining parameters			MRR (mg/min)		TWR (mg/min)		SR (microns)	
		Pc (A)	Ton (µs)	Trpm (rpm)	Experiment	Predicted, Residual, % Error	Experiment	Predicted, Residual, % Error	Experiment	Predicted, Residual, % Error
D3& Gr	3	12	400	1500	276.5	277.20, -0.7, -0.25	78.34	72.74, 5.6, 7.15	8.94	9.79, -0.85, -9.51
	16	18	400	1500	481.15	508.42, -27.27, -5.67	63.65	62.22, 1.43, 2.25	11.86	11.58, 0.27, 2.31
	4	24	400	1200	523.54	548.95, -25.41, -4.85	38.5	35.52, 2.98, 7.74	15.01	14.19, 0.82, 5.48
D3& Cu	4	12	100	1500	279.9	271.20, 8.7, 3.11	62.30	63.33, -1.03, -1.65	7.09	6.50, 0.59, 8.35
	2	18	100	1200	516.6	511.14, 5.46, 1.06	118.55	124.82, -6.27, -5.28	9.75	9.64, 0.11, 1.09
	21	24	400	1500	686.75	697.74, -10.99, -1.60	106.25	106.31, -0.06, -0.06	11.12	10.81, 0.31, 2.77

6.4 Effect of machining variables on output

The following segment explains the result of different machining variables and their interactions on response. Figures 6.2, 6.3 and 6.4 show the actual plot and percentage share by each variables on material removal rate, electrode wear rate and SR in D3&Gr and D3&Cu, respectively.

6.4.1 Findings on MRR

Figure 6.2(a, b, c) demonstrates the effect of Pc, Ton and Trpm on MRR in machining of D3 steel with graphite and copper tool, respectively. It was witnessed that copper electrode removed more material compared to graphite electrode at all mid values of process parameters. The reason may be attributed to the large electrical conductivity of copper (5.96×10^7 S/m at 20 ℃) which is higher than that of graphite (2 to 3×10^5 S/m at 20 ℃). Because of large electrical conductivity, copper electrode effectively conducts the electric charge leading to high MRR. Furthermore, temperature being higher at larger Pc values, it decreases the electrical conductivity owing to more vibration and movement between molecules which obstructs in the route of current flow. The effect can be observed through an increased slope looked beyond 18 A till 24 A for both electrodes. Due to this, material removal recorded had a lower value with Gr at 24 A.

Figure 6.2(e) shows that current intensity was the highly influencing factor in MRR with a percentage of 57.95% and with copper electrode.

6.4.2 Findings on TWR

Figure 6.3(a, b, c) depicts the effect of Pc, Ton and Trpm on TWR in machining of D3 steel with Gr and Cu electrode, respectively. It was watched that TWR with Cu was more than that of Gr. In the process of machining, tool also undergoes wear. As copper yielded more MRR, its wear was also found more. Also, at higher peak current of 24 A, heat generated is also high which is effectively sustained by graphite, and not by copper. The reason for the same being higher melting temperature of graphite. At high pulse on time value, both electrodes resulted in less wear because of lesser tool tip temperature as a result of bulge in plasma (Beravala and Pandey 2018).

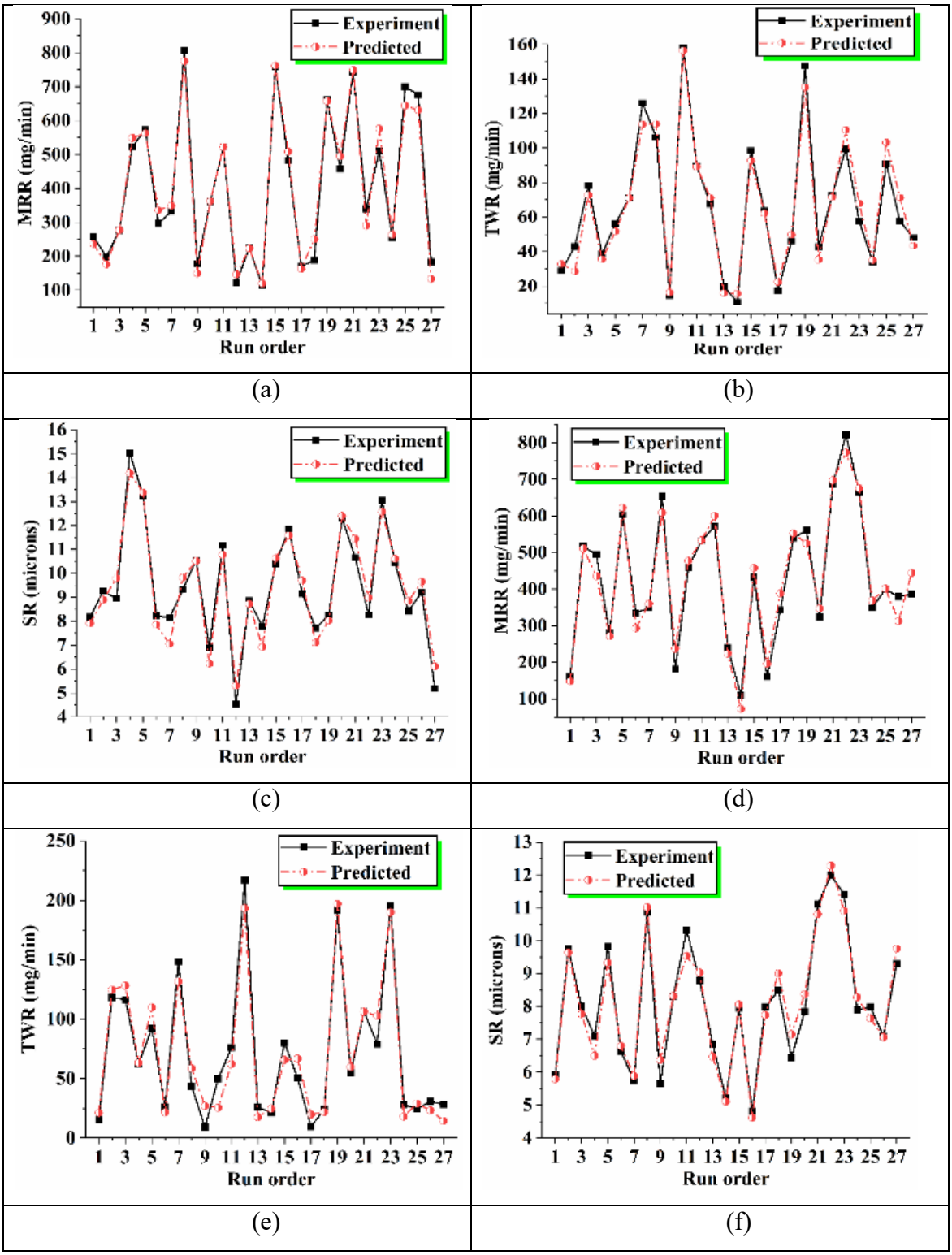

Figure 6.1. Regression model validation for MRR, TWR and SR in D3&Gr (a, b, c); and in D3&Cu (d, e, f).

Figures 6.3(d, e) shows the percentage share by each parameter on TWR in D3&Gr and D3&Cu, respectively. The on-time pulse and electrode rotation were investigated to be highly influencing variables with 52.41% and 29.12%, respectively for graphite electrode. In case of copper electrode, on-time pulse and peak current were investigated to be highly influencing factors with 48.78% and 26.82%, respectively.

6.4.3 Findings on SR

Figures 6.4(a, b, c) illustrates the consequences of machining variables on SR of D3 steel. The SR increased with increase in current for both the electrode. The reason is high heat intensity due to higher value of current resulting into deeper crater dimensions. The deeper craters make the surface rough, and hence higher surface roughness values are obtained. Furthermore, SR was found to be less in case of Cu electrode compared with Gr at all three levels of Pc, Ton and Trpm. It can be clearly elucidated from figure 6.4(c) that higher rotational speed of tool results in lesser SR. Here, it may be noted that lowest surface roughness was recorded with Cu electrode. The most influencing factor for Gr and Cu electrode was Pc and Trpm with percentage of 40.14% and 32.75%, respectively (refer figures 6.4(d, e)).

6.5 Interaction effect in D3&Gr

The interaction effects of Pc and Ton on MRR, Pc and Trpm on TWR, Ton and Trpm on TWR were found to be significant in D3 steel machined with graphite electrode. No interaction found significant on SR.

6.5.1 Interaction effect on MRR

The surface and interaction plot of Pc and Ton on MRR is displayed in figure 6.5. The low level of Ton and high level of Pc resulted in maximum MRR. The reason is attributed to the fact that combination of these two levels makes the arc highly concentrated over the workpiece leading to maximum heat input into the workpiece and, hence, high MRR.

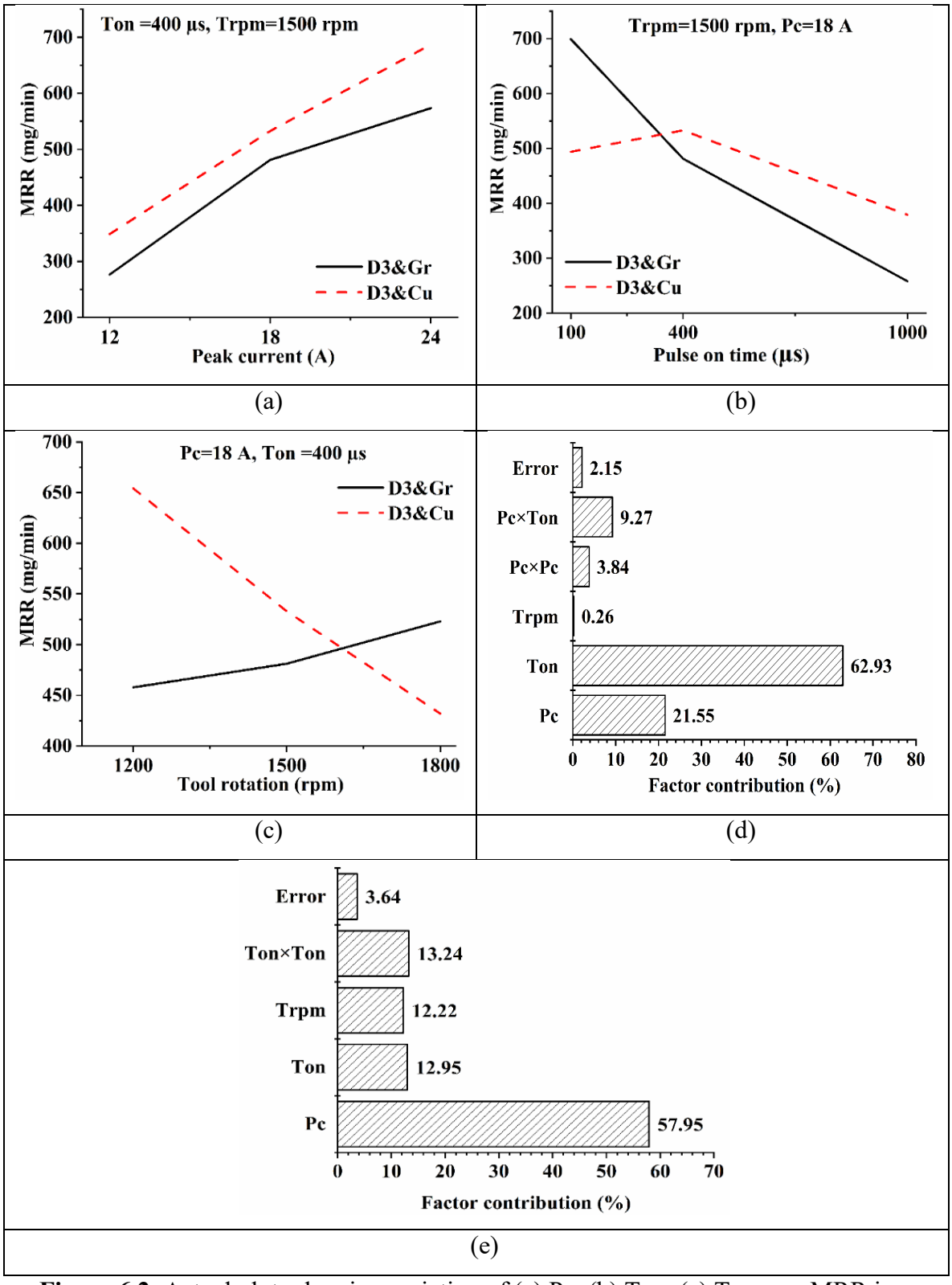

Figure 6.2. Actual plots showing variation of (a) Pc; (b) Ton; (c) Trpm on MRR in D3&Gr and D3&Cu; (d) parameters percentage share on MRR in D3&Gr; (e) parameters percentage share on MRR in D3&Cu.

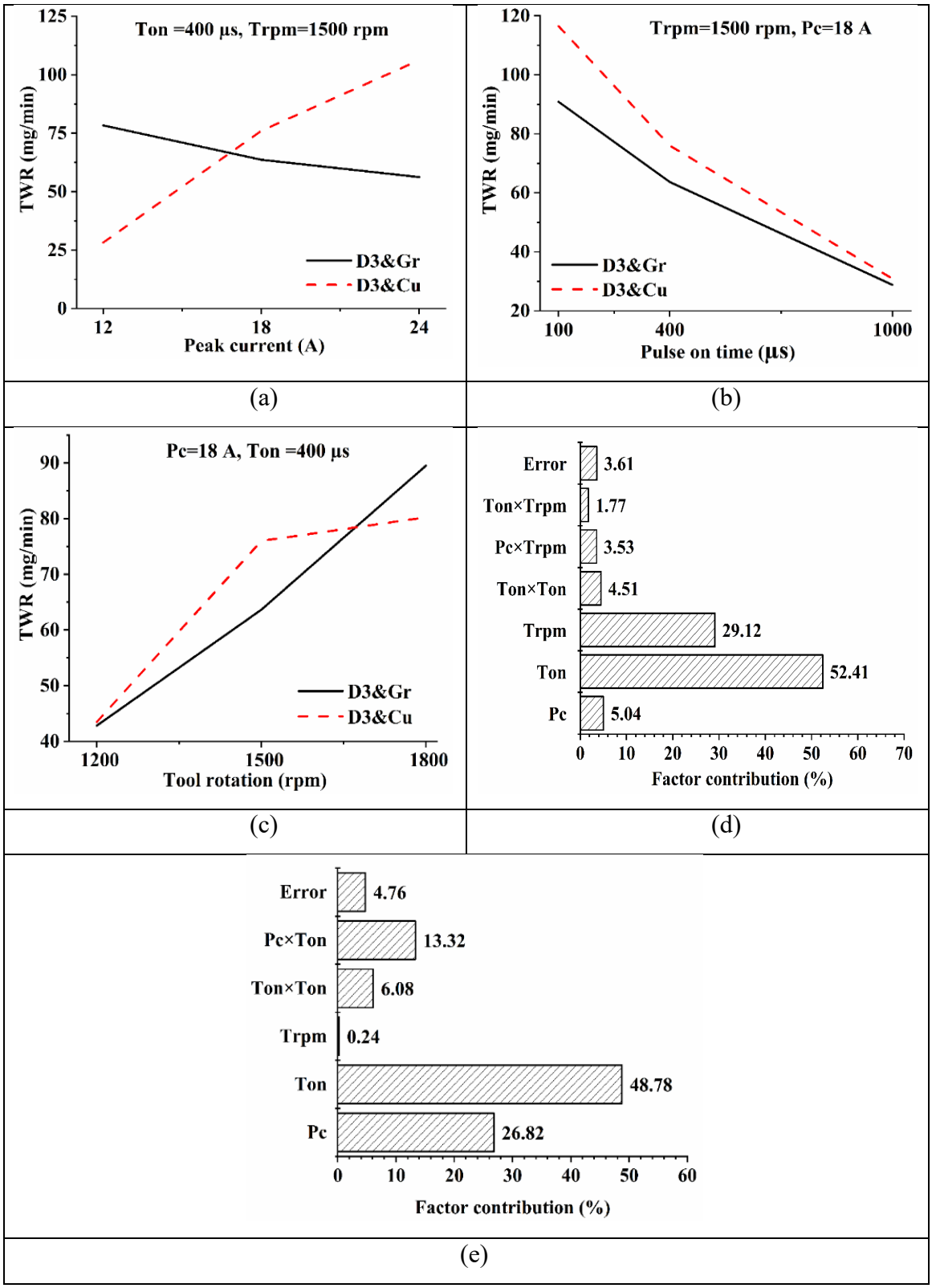

Figure 6.3. Actual plots showing variation of (a) Pc; (b) Ton; (c) Trpm on TWR in D3&Gr and D3&Cu; (d) parameters percentage share on TWR in D3&Gr; (e) parameters percentage share on TWR in D3&Cu.

6.5.2 Interaction effect on TWR

Figure 6.6 illustrates the surface and interaction plot of Pc and Trpm on TWR. The peak current affected TWR in inverse proportion for all tool rotation value except at 1200 rpm where a slight increase was noticed. The effect of increase in peak current resulted in reduction of TWR. With increase in tool rotation, slope of the line was also increased. The lowest TWR occurred at low value of Pc and Trpm.

Figure 6.7 shows the surface and interaction plot of Ton and Trpm on TWR. The on-time pulse also showed the inversely proportional effects on TWR for given tool rotation values. The lowest TWR was observed on high value of Ton and low value of Trpm. The reason for low TWR is reduction in tool tip temperature due to augmentation of plasma channel at high levels of pulse on time.

6.6 Interaction effect in D3&Cu

The interaction effects of Pc and ton on TWR, Ton and Trpm on SR were found significant in processing of D3 steel with cu tool. No interaction found significant on MRR.

6.6.1 Interaction effect on TWR

Figure 6.8 shows the surface and interaction plot of Pc and Ton on TWR. The current intensity effected TWR in direct proportion as TWR increased with rise in Pc for all levels of Ton. The largest slope was recorded on 100 µs, then reduced on 400 µs and lowest on 1000 µs. The lowest TWR was recorded on low level of Pc and intermediate level of Ton. The reason for reduction in slope with rise in Ton is the expansion of plasma in longitudinal direction limiting the energy density of spark.

6.6.2 Interaction effect on SR

The interaction between Ton and Trpm was found significant for SR as depicted in figure 6.9. The surface roughness first increased, then decreased during the selected range of pulse on time. The SR was found lowest at low level of Ton and high level of Trpm. The reason for lowest surface roughness at this combination is low energy sparks imparting shallow craters with effective flushing of debris.

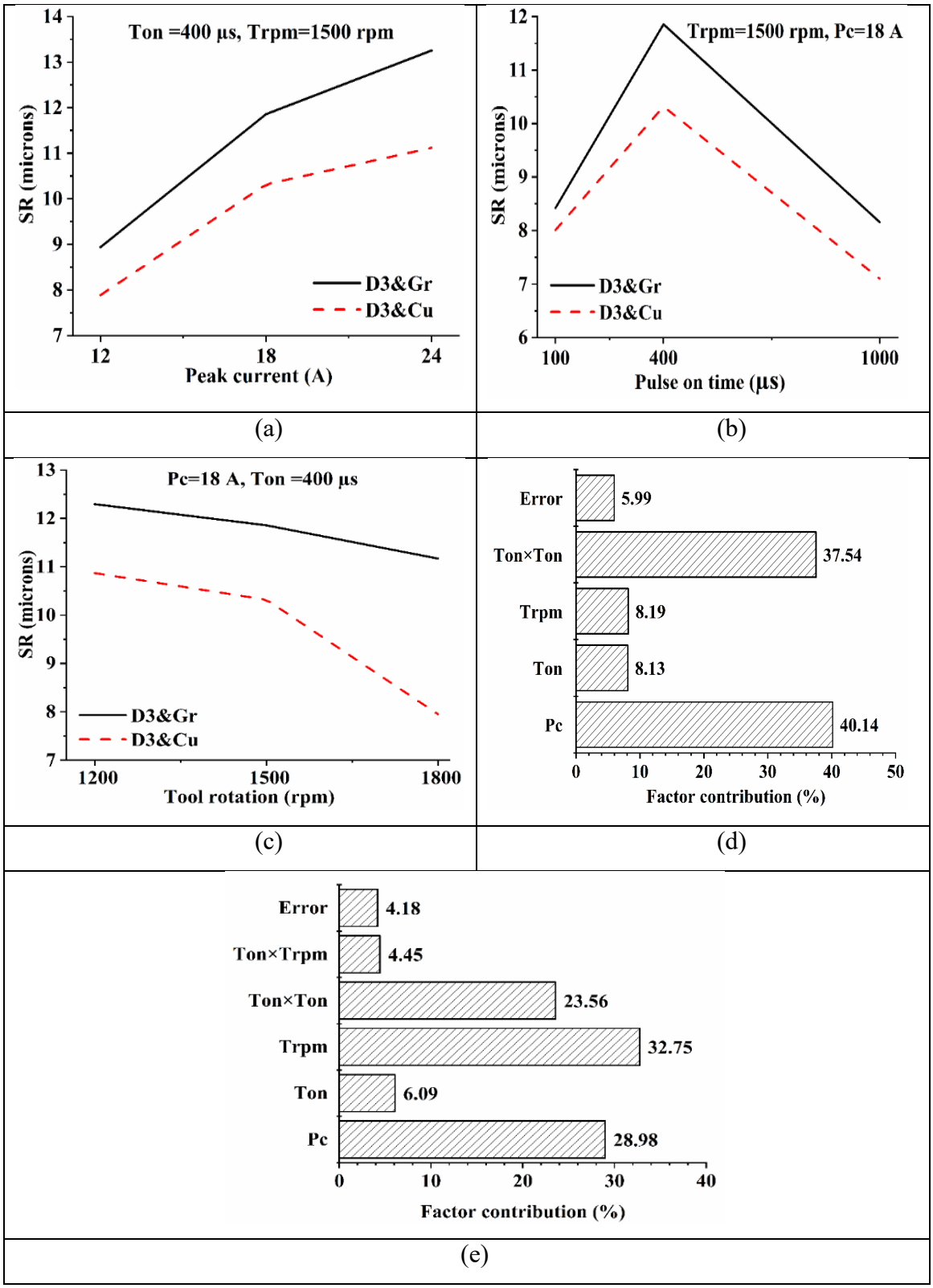

Figure 6.4. Actual plots showing variation of (a) Pc; (b) Ton; (c) Trpm on SR in D3&Gr and D3&Cu; (d) parameters percentage share on SR in D3&Gr; (e) parameters percentage share on SR in D3&Cu.

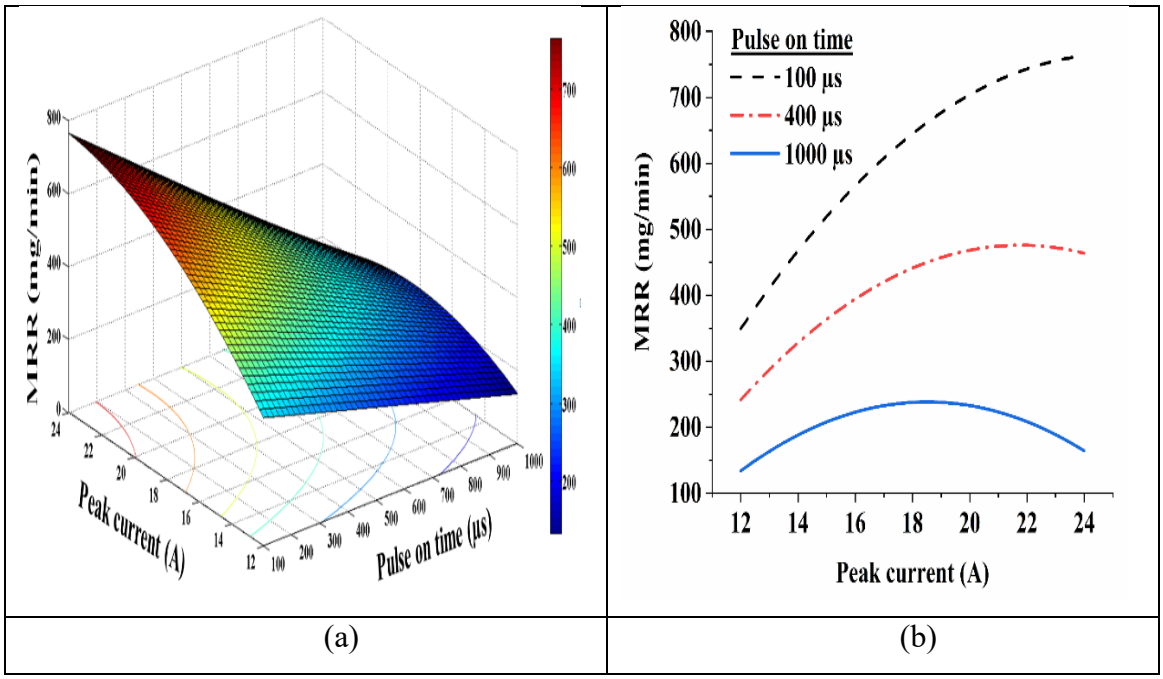

(a) (b)

Figure 6.5. Variation of Pc and Ton on MRR in D3&Gr: (a) response surface plot; (b) interaction plot.

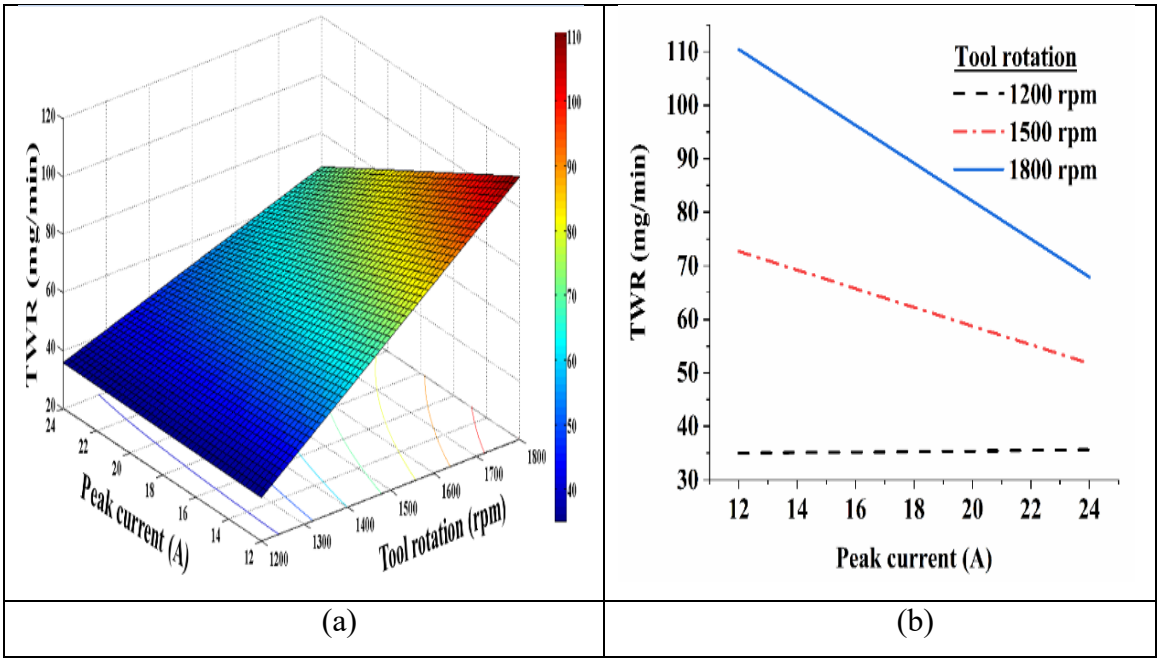

(a) (b)

Figure 6.6. Variation of Pc and Trpm on TWR in D3&Gr: (a) response surface plot; (b) interaction plot.

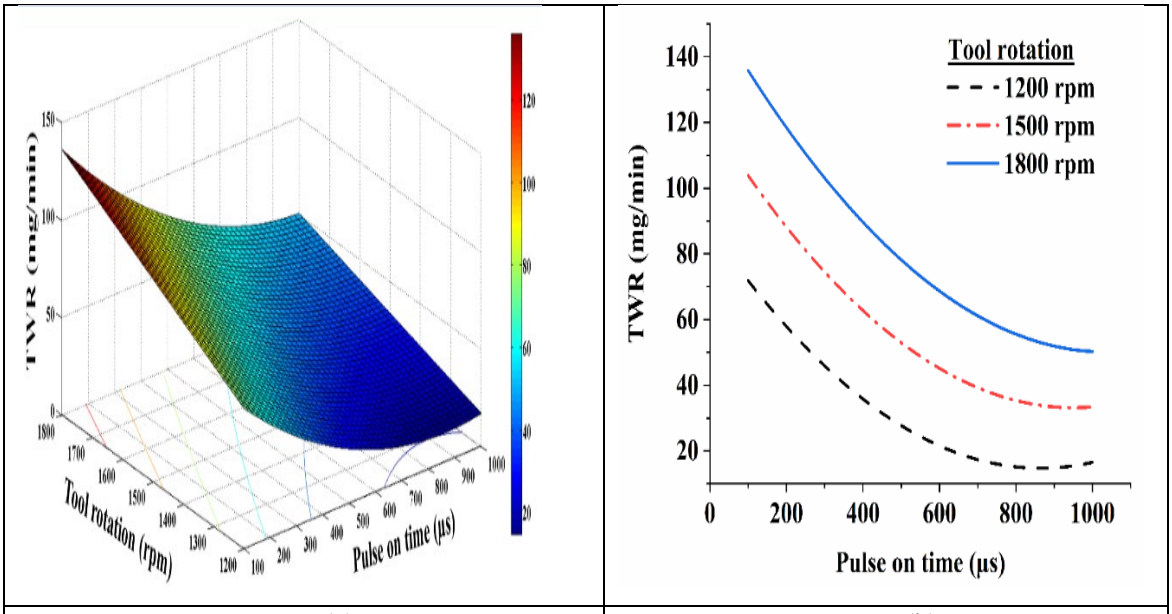

(a) (b)

Figure 6.7. Variation of Ton and Trpm on TWR in D3&Gr: (a) response surface plot; (b) interaction plot.

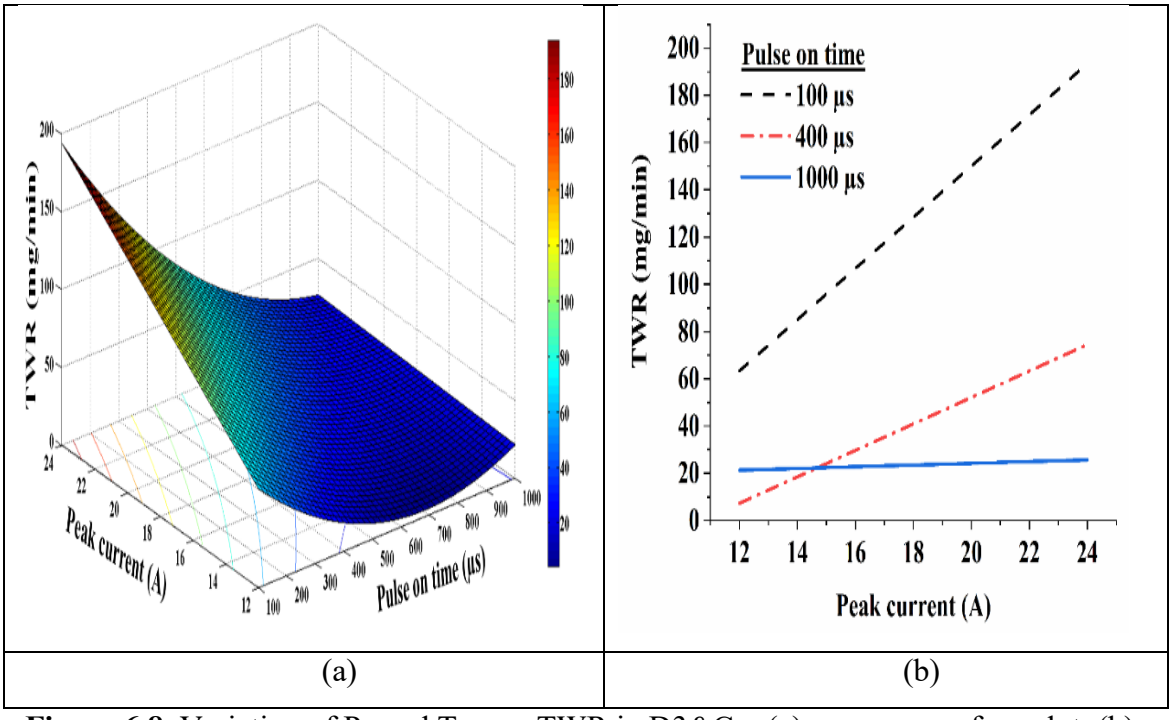

(a) (b)

Figure 6.8. Variation of Pc and Ton on TWR in D3&Cu: (a) response surface plot; (b) interaction plot.

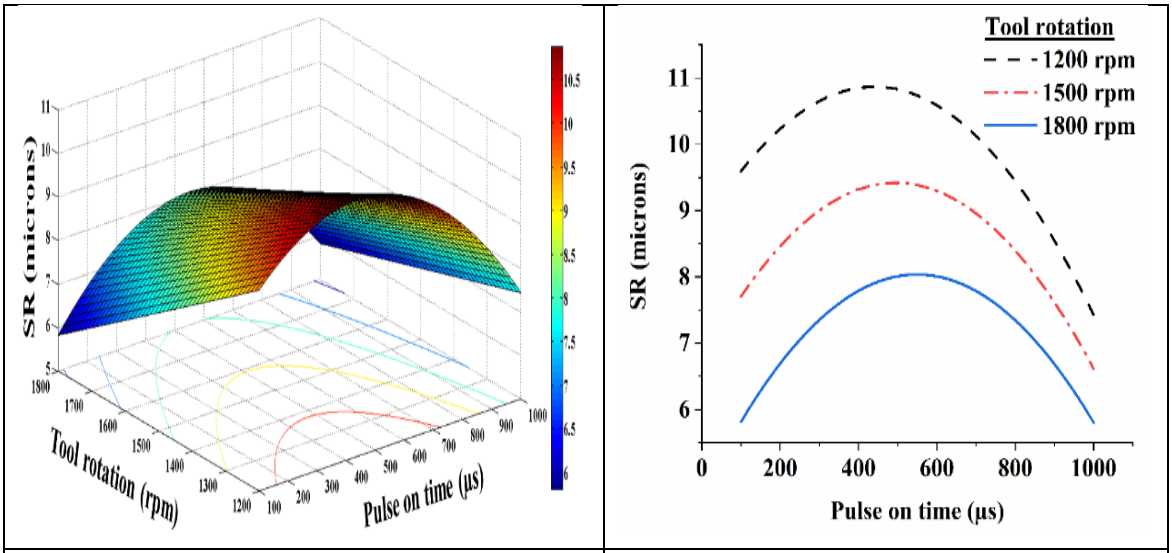

(a) (b)

Figure 6.9. Variation of Ton and Trpm on SR in D3&Cu: (a) response surface plot; (b) interaction plot.

6.7 Voltage and current waveform analysis

The voltage and current waveforms were recorded with the help of Keysight Infinii Vision DSO-X 2022A, Digital Storage Oscilloscope. The voltage and current probes were employed to capture the current and voltage waveforms. The recorded waveforms under different parametric settings are presented in figures 6.10, 6.11 and 6.12, respectively. The study of waveforms clearly show smooth spark cycles with copper electrode while, with graphite, ignition delay was noticed. From figure 6.10, it can be inferred that with rise in current, occurrence of ignition delay increased with graphite electrode. The delay in sparking will affect the machining rate. The same may be verified from the results in table 4.4, 4.5 as well as figures 6.2 (a, b, c). At centre value of parameters, MRR recorded with copper tool (532.95 mg/min) was higher than that of graphite electrode (481.15 mg/min) (refer tables 4.4 and 4.5). Further, figure 6.11 presents the consequences with Ton. Copper tool performed better at mid and high value of Ton, whereas, at smaller value, graphite performs better. Lastly, figure 6.12 shows the waveforms showing the effect of Trpm. Copper performs better at lower and mid value of tool rotation with good consistency in spark cycles. However, at 1800 rpm, graphite results in less disturbance contributing to higher MRR.

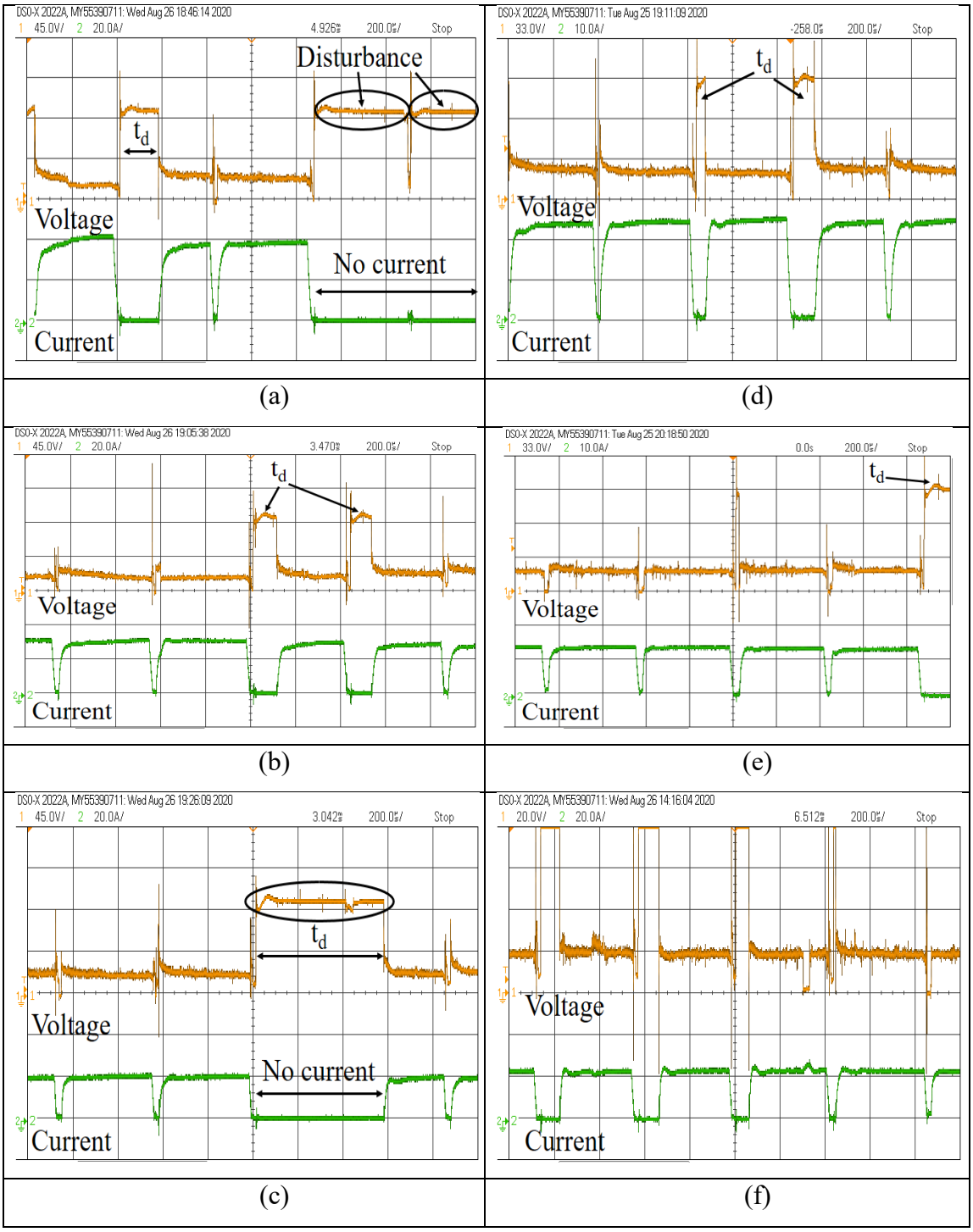

Figure 6.10. Voltage and current waveforms during (a, b, c) D3 & Gr; (d, e, f) D3 & Cu. (V_{oc}-open circuit voltage, V_d- discharge voltage, t_d- ignition delay time, T_{off}-pulse off time) (a: Pc=12 A, Ton=400 µs, Trpm=1500 rpm, b: Pc=18 A, Ton=400 µs, Trpm=1500 rpm, c: Pc=24 A, Ton=400 µs, Trpm=1500 rpm, d: Pc=12 A, Ton=400 µs, Trpm=1500 rpm, e: Pc=18 A, Ton=400 µs, Trpm=1500 rpm, f: Pc=24 A, Ton=400 µs, Trpm=1500 rpm).

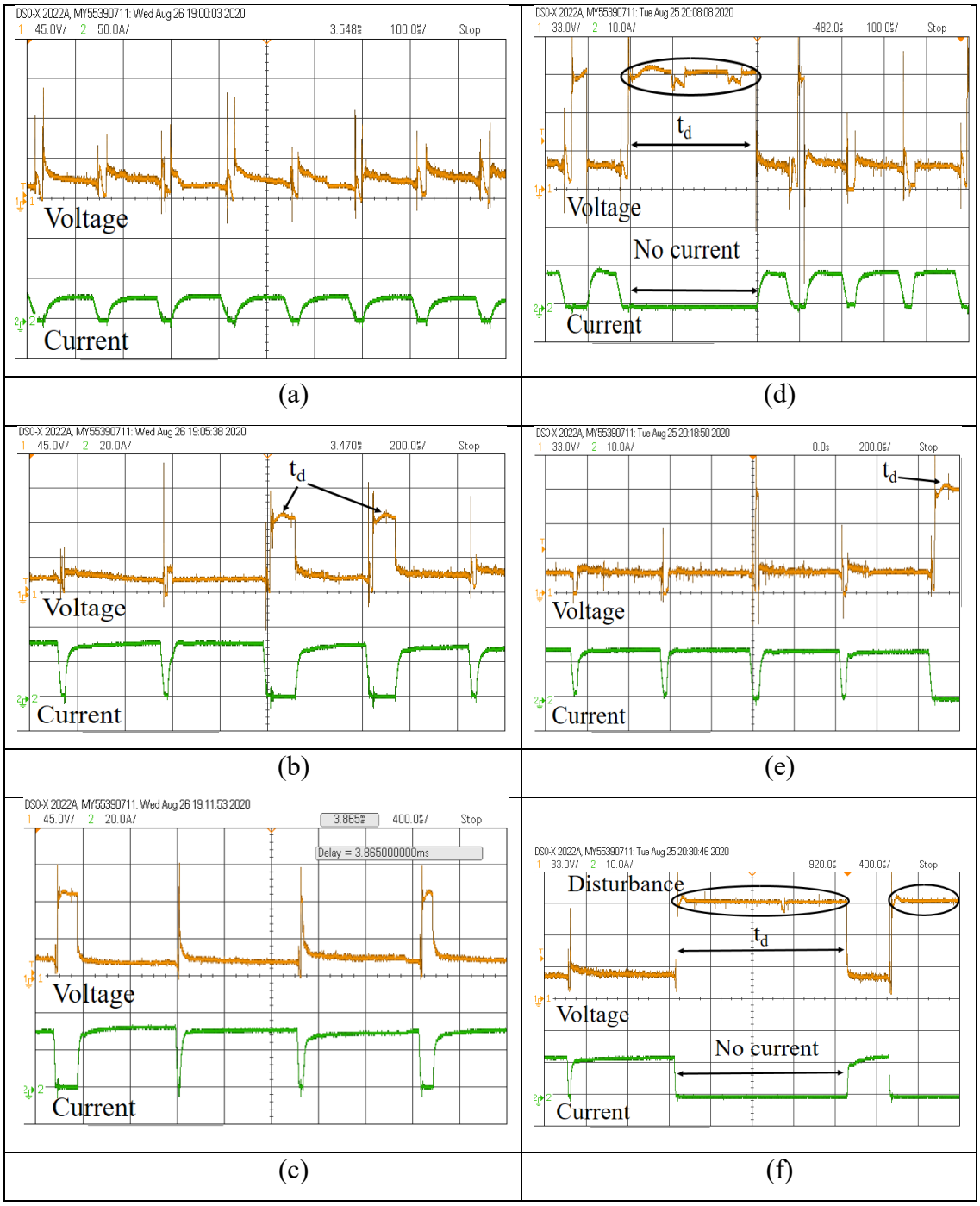

Figure 6.11. Voltage and current waveforms during (a, b, c) D3 & Gr; (d, e, f) D3 & Cu. (V_{oc}-open circuit voltage, V_d- discharge voltage, t_d- ignition delay time, T_{off}-pulse off time) (a: Pc=18 A, Ton=100 µs, Trpm=1500 rpm, b: Pc=18 A, Ton=400 µs, Trpm=1500 rpm, c: Pc=18 A, Ton=1000 µs, Trpm=1500 rpm, d: Pc=18 A, Ton=100 µs, Trpm=1500 rpm, e: Pc=18 A, Ton=400 µs, Trpm=1500 rpm, f: Pc=18 A, Ton=1000 µs, Trpm=1500 rpm).

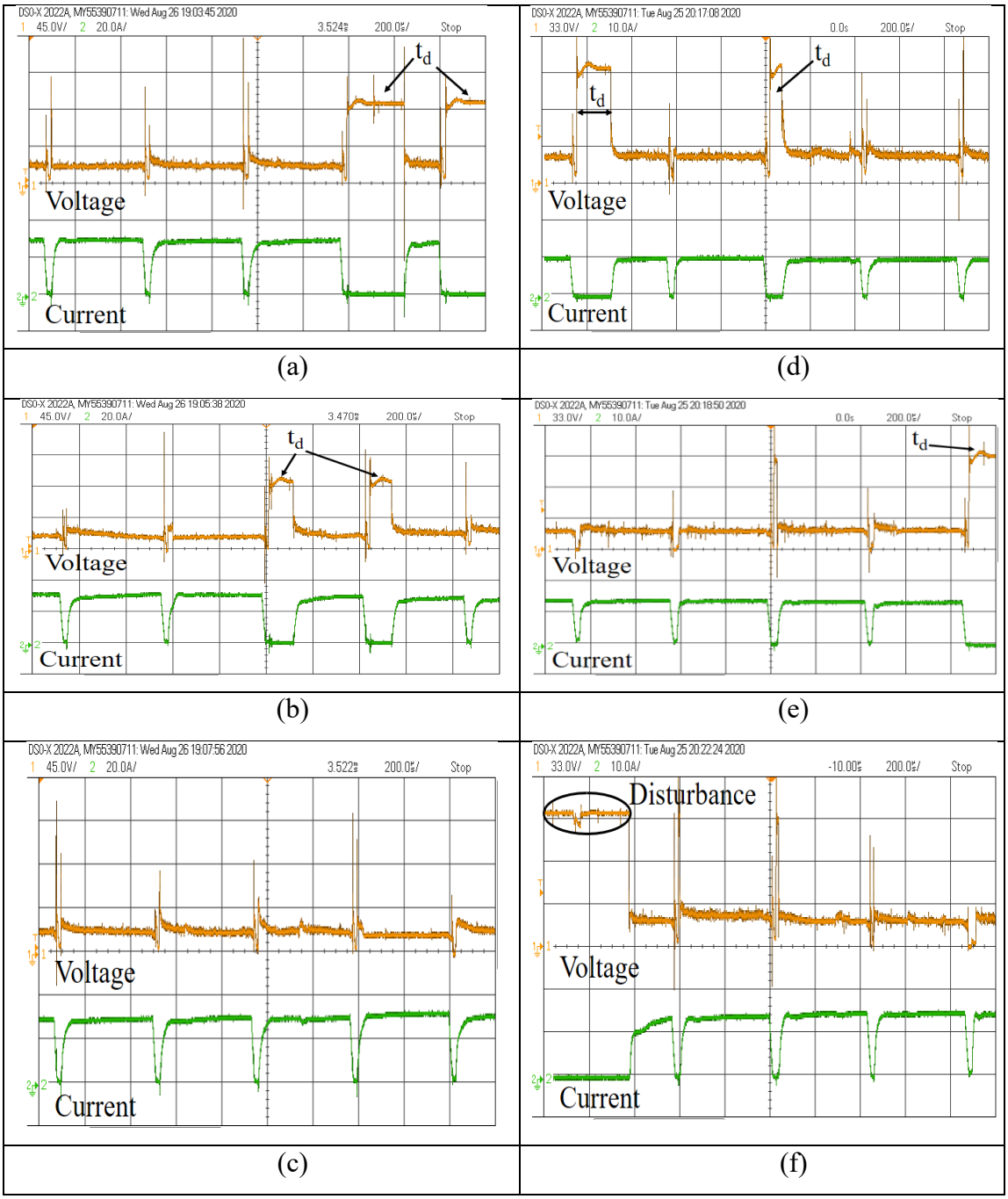

Figure 6.12. Voltage and current waveforms during (a, b, c) D3 & Gr; (d, e, f) D3 & Cu. (V_{oc}-open circuit voltage, V_d- discharge voltage, t_d- ignition delay time, T_{off}-pulse off time) (a: Pc=18 A, Ton=400 µs, Trpm=1200 rpm, b: Pc=18 A, Ton=400 µs, Trpm=1500 rpm, c: Pc=18 A, Ton=400 µs, Trpm=1800 rpm, d: Pc=18 A, Ton=400 µs, Trpm=1200 rpm, e: Pc=18 A, Ton=400 µs, Trpm=1500 rpm, f: Pc=18 A, Ton=400 µs, Trpm=1800 rpm).

6.8 Morphology results

Figure 6.13 elucidates the morphology of the samples processed by conventional EDM and abrasive mixed rotary EDM (AREDM). The surface images were captured through field emission scanning electron microscope (FESEM) with a working distance of 10 mm. The surface morphology results clearly showed improvements in surface with abrasive mixed rotary EDM with graphite electrode compared to conventional EDM. The conventional EDM surface shows segregated solidified spherical debris, clustered deposited debris, surface cracks and pockmarks as evident from figures 6.13(a, c). It is also evident that Cu tool resulted in better surface compared to surface produced by graphite electrode wherein cracks are visible (refer figure 6.13(b, d).

6.9 Multi-objective optimization

This work involves a multi-objective optimization like in most EDM applications. In this study, maximization of MRR along with minimization of TWR and SR, were aimed. For this purpose, grey relational analysis was selected to discover the best possible set of variables. In this technique, firstly, the responses needs to be processed to get the normalized values. The normalized values are estimated based on response characteristics i.e whether the response is “higher-the-better” or “smaller-the-better” type. Here, MRR is “higher-the-better” whereas, TWR and SR are “smaller-the-better” type characteristics. This is essentially done to obtain the values in between 0 and 1 for comparison purpose. The step is known as normalizing. Thereafter, the deviation sequence is estimated which is required for grey relational coefficient, the next step in calculation. The grey relational coefficient is further estimated by considering the deviation sequence, maximum and minimum values of the deviation sequence which are 1 and 0, respectively along with 0.5 as the identification coefficient. Next, grey relational grades and rank are obtained. The optimal values are then selected corresponding to the highest rank i.e. rank 1. Finally, the optimum set of variables for D3 steel as revealed by exercising grey relational analysis approach are listed in table 6.9. Further, the experiments were performed on conventional EDM without abrasive and tool rotation at the optimum values. The comparative results are presented in table 6.10. The obtained results completely outperforms conventional EDM and are stated to be the best results under the considered experimental conditions.

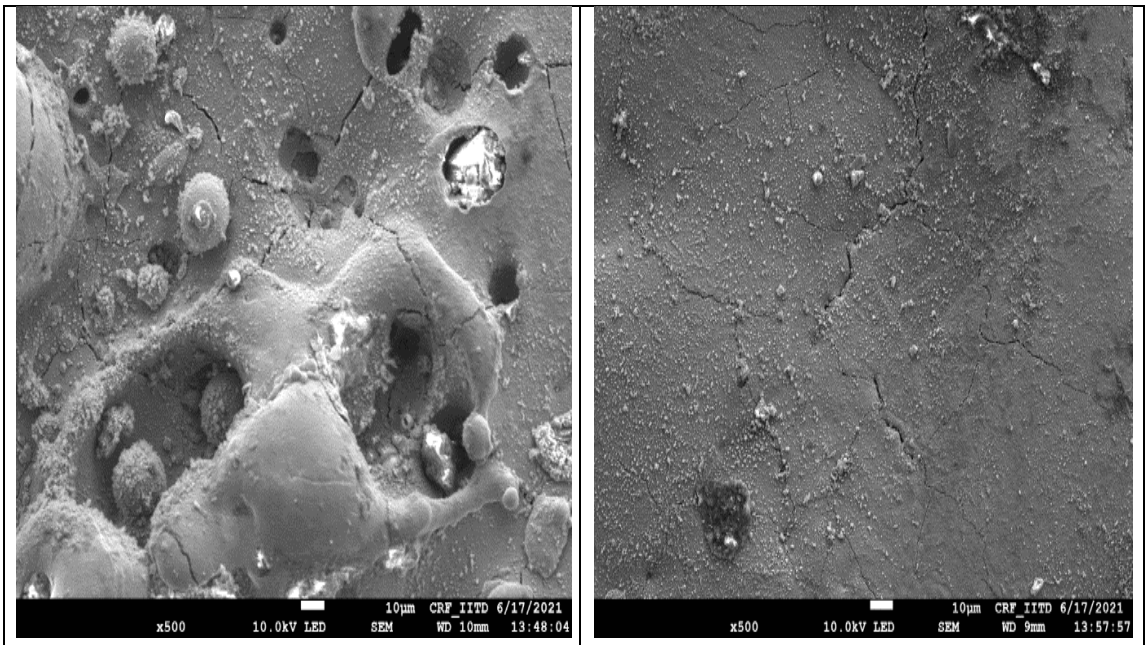

(a) (b)

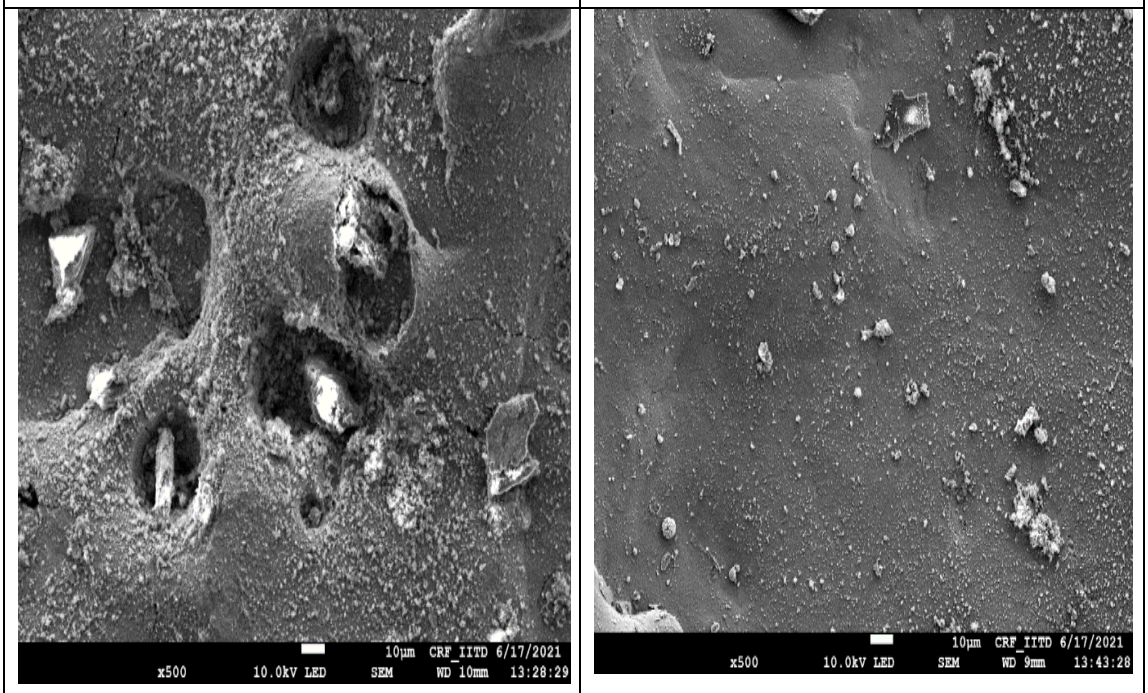

(c) (d)

Figure 6.13. Morphology of surface by (a) conventional EDM (D3&Gr); (b) AREDM (D3&Gr); (c) conventional EDM (D3&Cu); (d) AREDM (D3&Cu). (Pc-18A, Ton- 400 µs, Trpm- 1500 rpm).

Table 6.9. Best set of machining variables.

W/p & tool	Optimum parameters			MRR (mg/min)	TWR (mg/min)	SR (microns)
	Pc (A)	Ton (µs)	Trpm (rpm)	Experiment	Experiment	Experiment
D3&Gr	24	100	1800	806.3	106.3	9.321
D3&Cu	18	1000	1800	181.55	9.2	5.65

Table 6.10. Comparative results of D3 steel.

W/p & tool	Optimum parameters			MRR (mg/min)	TWR (mg/min)	SR (microns)
	Pc (A)	Ton (µs)	Trpm (rpm)	Conventional, AREDM, % increase	Conventional, AREDM, % decrease	Conventional, AREDM, % decrease
D3& Gr	24	100	1800	806.3, 867.24, 7.56	106.3, 97.2, 8.56	9.321, 7.87, 15.56
D3& Cu	18	1000	1800	181.55, 04.99, 12.91	9.2, 8.62, 6.3	5.65, 5.1, 9.73

6.10 Comparison of Results

This section presents a comparative result of the present work done with the prior research on EDM variants in table 6.11. Here, the up and down arrow symbols have been used to show the behaviour of output response measure such as MRR, TWR, and SR in relation to tool rotation. Most of the prior research showed improvement in surface roughness while working on EDM variant namely, REDM as well as PMEDM along with REDM i.e. AREDM referred here in this work. This work achieved higher MRR, lower TWR and SR compared to conventional EDM with maximum improvement of 22.2% in surface roughness while machining EN31 steel with graphite electrode.

Table 6.11. Comparative study with prior research.

EDM variant	W/p	Tool	Powder	Presented comparison with conventional EDM	MRR	TWR	SR	Reference
PMEDM + REDM	AISI D3 tool steel	Copper	-	Yes	-	-	↓	Dwivedi and Choudhury 2016b
PMEDM	Super Co 605	Graphite	Graphite	No	-	-	↓	Singh *et al* 2015
PMEDM	Inconel 825 superalloy	Copper	Alumina	Yes	↑	↓	↓	Kumar *et al* 2019
PMEDM + REDM	45 carbon steel, W18Cr4V high speed steel	Brass, copper	Silicon powder with air and liquid (Three phase mixture)	No	↓	-	-	Bai *et al* 2013
REDM	Al-SiC MMCs	Brass, copper	-	No	↑ $MRR_B > MR$	↓	↓	Mohan *et al* 2002
PMEDM + REDM	Die steel D2	Copper	Aluminium	No	↑	-	-	Gurule and

								Nandurkar 2012
PMEDM + REDM	EN31 steel	Copper	MWCNT	Yes	↑	NA	↓	Bajaj *et al* 2020
PMEDM + REDM	EN31 steel	Graphite	SiC	Yes	NA	↑	↓	Present work
PMEDM + REDM	EN31 steel	Copper	SiC	Yes	↓	↑	↑	Present work
PMEDM + REDM	D3 steel	Graphite	SiC	Yes	↑	↑	↓	Present work
PMEDM + REDM	D3 steel	Copper	SiC	Yes	↓	↑	↓	Present work

HCHCr: high carbon high chromium die steel; MMCs: metal matrix composites; MWCNT: multi-wall carbon nanotube; SiC: silicon carbide; PMEDM: powder mixed EDM; REDM: rotary EDM; NA: response not affected

CHAPTER-7

CONCLUSIONS AND FUTURE SCOPE

7.1 Conclusions

The present work focused on machining of EN31 and D3 steel with graphite and copper in abrasive mixed rotary tool EDM. The final remarks from the current work done are:

1. For EN steel, MRR increased with rise in peak current for both graphite and copper electrode. On comparing, graphite outperformed copper and achieved higher MRR, and lower SR and TWR.

2. While machining EN31 steel with graphite electrode, surface finish improved from 10.8691 μm to 9.8045 μm. On contrary, with copper electrode, it increased from 12.917 μm to 14.58 μm with increase in tool rotation.

3. For EN31 steel, at peak current of 12 A, tool wear recorded with graphite electrode was 67.24% higher compared to copper electrode while at peak current of 24 A, copper electrode wear was 201.64% higher compared to graphite electrode.

4. For EN31 steel, TWR of graphite electrode increased substantially from 39.2444 to 95.5833 mg/min with increase in tool rotation while copper affected minimally. However, minimum TWR value achieved with copper electrode was 87.8233 mg/min at 1500 rpm.

5. For D3 steel, copper outperformed graphite and achieved higher MRR, lower SR. However, copper resulted in more tool wear than graphite.

6. The surface roughness decreased by 5.17% with increase in tool rotation from 1200 rpm to 1800 rpm on machining EN31 steel with graphite. The similar decreasing trend was also recorded with graphite as well as copper electrode while machining D3 steel. In D3 steel, surface roughness decreased by 9.15% and 26.86% with graphite and copper tool, respectively. However, tool wear rate increased for all cases.

7. Statistical modelling of the machining environment encompassing the peak current, pulse on time and tool rotation was successfully studied and verified experimentally.

8. FESEM images clearly showed the improvement on the workpiece surface with AREDM compared to conventional EDM.

9. For EN31 steel, a thin recast layer thickness of 32.29 µm was formed in AREDM compared to 62.25 µm in conventional EDM when machined with copper electrode. Comparing RLT in AREDM with graphite and copper, graphite outperformed copper tool with RLT of 6.12 µm. The graphite tool may be given preference to copper when looking for RLT.

10. AREDM resulted into the enhanced sub-surface microhardness in machining EN31 steel with both graphite and copper electrode compared with conventional EDM. This increase was noticed over the edge as well as on transverse direction.

11. The results of sub-surface microhardness revealed surface modification as one of the important aspect of the abrasive mixed rotary EDM. The sub-surface micro hardness increased from 514.59 HV0.5 to 533.23 HV0.5 in EN31 steel with graphite electrode and from 503.55 HV0.5 to 523.54 HV0.5 with copper electrode. This increase was noticed over the edge as well as on transverse direction.

12. Genetic algorithm and grey relational analysis were successfully used for multi objective optimization.

13. The best set of variables in machining of EN31 steel and graphite (Pc- 24 A, Ton- 100 µs, Trpm- 1200 rpm) was found to score SR, TWR and MRR to be 8.371 µm, 64.4 mg/min and 783.8 mg/min, respectively.

14. The best set of variables in machining of EN31 steel and copper (Pc- 12 A, Ton- 100 µs, Trpm- 1800 rpm) was found to score SR, TWR and MRR to be 5.944 µm, 56.2 mg/min, and 130.7 mg/min, respectively.

15. The best set of variables setting in machining of D3 steel and graphite (Pc- 24 A, Ton- 100 µs, Trpm- 1800 rpm) was found to score SR, TWR and MRR to be 9.321 µm, 106.3 mg/min, and 806.3 mg/min, respectively.

16. The best set of variables in machining of D3 steel and copper (Pc- 18 A, Ton- 1000 µs, Trpm- 1800 rpm) was found to score SR, TWR and MRR to be 5.65 µm, 9.2 mg/min, and 181.55 mg/min, respectively.

7.2 Future scope

The work on EDM may be extended with following considerations:

1. It may be extended with analysis of inter-electrode gap. With exact estimation of gap distance, flushing of debris can be further improved.
2. The spark travel can also be analysed under the influence of electrode rotation as its transverse and inclined travel might affect the discharge crater dimensions.
3. This work may be extended with different combinations of workpiece and tool.
4. The abrasive size can also be varied for checking the results. Further, it can also be seen that how response measures changes with change of different powder.
5. Electrode rotation may also be taken beyond 1800 rpm to further investigate the response measures.

References

Aliakbari E, Baseri H 2012 Optimization of machining parameters in rotary EDM process by using the Taguchi method. Int J Adv Manuf Technol. 62: 1041–1053.

Bahgat MM, Shash AY, Abd-Rabou M, El-Mahallawi IS 2019 Influence of process parameters in electrical discharge machining on H13 die steel, Heliyon 5. e01813.

Bai X, Zhang Q, Zhang J, Kong D, Yang T 2013 Machining efficiency of powder mixed near dry electrical discharge machining based on different material combinations of tool electrode and workpiece electrode. J Manuf Process. 15: 474– 482.

Bajaj R, Dixit AR, Tiwari AK, Chauhan NK 2020 Machining performance enhancement of en-31 diesteel using mwcnt mixed rotary EDM. Indian J Eng Mater Sci. 27: 309–319.

Beravala H, Pandey PM 2018 Experimental investigations to evaluate the effect of magnetic field on the performance of air and argon gas assisted EDM processes. J Manuf Process. 34: 356–373.

Beri N, Maheshwari S, Sharma C, Kumar A 2014 Surface Quality Modification Using Powder Metallurgy Processed CuW Electrode During Electric Discharge Machining of Inconel 718. *Procedia Mater Sci*. 5: 2629–2634.

Bhattacharya A, Batish A, Kumar N 2013 Surface characterization and material migration during surface modification of die steels with silicon, graphite and tungsten powder in EDM process. J Mech Sci Technol. 27: 133–140.

Bhattacharya A, Batish A, Singh G, Singla VK 2012 Optimal parameter settings for rough and finish machining of die steels in powder-mixed EDM. Int J Adv Manuf Technol. 61: 537–548.

Chattopadhyay KD, Verma S, Satsangi PS, Sharma PC 2009 Development of empirical model for different process parameters during rotary electrical discharge machining of copper-steel (EN-8) system. J Mater Process Technol. 209: 1454–1465.

Che Haron CH, Deros BM, Ginting A, Fauziah M 2001 Investigation on the influence of machining parameters when machining tool steel using EDM. *J Mater Process Technol*. 116:

84–87.

Che Haron CH, Ghani JA, Burhanuddin Y, Seong YK, Swee CY 2008 Copper and graphite electrodes performance in electrical-discharge machining of XW42 tool steel. J Mater Process Technol. 201: 570–573.

Choudhary R, Gupta V, Batra Y, Singh A 2015 Performance and Surface Integrity of Nimonic75 Alloy Machined by Electrical Discharge Machining. *Mater Today Proc*. 2: 3481–3490.

Chow HM, Yan BH, Huang FY 1999 Micro slit machining using electro-discharge machining with a modified rotary disk electrode (RDE). J Mater Process Technol. 91: 161–166.

Chow HM, Yang LD, Lin CT, Chen YF 2008 The use of SiC powder in water as dielectric for micro-slit EDM machining. J Mater Process Technol. 195: 160–170.

Çogun C, Akaslan S 2002 The effect of machining parameters on tool electrode edge wear and machining performance in electric discharge machining (EDM). *KSME Int J*. 16: 46–59.

Deepak, Vipin 2020 Investigation of surface roughness for en-31 by redm with graphite electrode. *Indian J Eng Mater Sci*. 27: 872–877.

Dewangan S , Gangopadhyay S , Biswas CK 2015 Multi-response optimization of surface integrity characteristics of EDM process using grey-fuzzy logic-based hybrid approach. *Eng Sci Technol an Int J*. 18: 361–368.

Dhar S, Purohit R, Saini N, Sharma A, Kumar GH 2007 Mathematical modeling of electric discharge machining of cast Al-4Cu-6Si alloy-10 wt.% SiCP composites. J Mater Process Technol. 194: 24–29.

Dwivedi AP, Choudhury SK 2016a Effect of Tool Rotation on MRR, TWR, and Surface Integrity of AISI-D3 Steel using the Rotary EDM Process. *Mater Manuf Process*. 31: 1844–1852.

Dwivedi AP, Choudhury SK 2016b Improvement in the Surface Integrity of AISI D3 Tool Steel Using Rotary Tool Electric Discharge Machining Process. Procedia Technol. 23: 280–287.

Fujun, R, Dechen H, Dianjun W 2004 Analysis of motion laws of machining nonsphere by EDM with rotary electrode, Journal of Materials Processing Technology. 149: 323– 327.

Gopalakannan S, Senthilvelan T, Renganathan S 2013 Statistical optimisation of EDM parameters on machining of aluminium hybrid metal matrix composites by applying taguchi based grey analysis, Journal of Scientific and Industrial Research. 72: 358-365.

Gurule NB , Nandurkar KN 2012 Effect of Tool Rotation on Material Removal Rate during Powder Mixed Electric Discharge Machining of Die Steel. Int J Emerg Technol Adv Eng. 2: 328–332.

Hewidy MS, El-Taweel TA, El-Safty MF 2005 Modelling and machining parameters of wire Electrical Discharge Machining of Inconel 600 using RSM, Journal of Material Processing Technology. 169: 328-336.

Ho KH, Newman ST 2003 State of the art electrical discharge machining (EDM). Int J Mach Tools Manuf. 43: 1287–1300.

Jin W, Fuzhu H, Gang C, Fuling Z 2012 Debris and bubble movements during electrical discharge machining, International Journal of Machine Tools and Manufacture. 58: 11–18.

Kansal HK, Singh S, Kumar P 2005 Parametric optimization of powder mixed electrical discharge machining by response surface methodology. J Mater Process Technol. 169: 427–436.

Kansal HK, Singh S, Kumar P 2007 Effect of silicon powder mixed EDM on machining rate of AISI D2 die steel. J Manuf Process. 9: 13–22.

Karthikeyan R, Narayanan L, Naagarazan RS 1999 Mathematical modeling for electric discharge machining of aluminium-silicon carbide particulate composites, Journal of Materials Processing Technology. 87(1-3): 59-63.

Khan AA 2008 Electrode wear and material removal rate during EDM of aluminum and mild steel using copper and brass electrodes. *Int J Adv Manuf Technol*. 39: 482–487.

Koshy P, Jain VK, Lal GK 1993 Experimental investigations into electrical discharge machining with a rotating disk electrode, Precision Engineering. 15(1): 6–15.

Kumar A, Mandal A, Dixit AR, Das AK, Kumar S, Ranjan R 2019 Comparison in the performance of EDM and NPMEDM using Al 2 O 3 nanopowder as an impurity in DI water dielectric. Int J Adv Manuf Technol. 100: 1327–1339.

Kung K-Y, Horng J-T, Chiang K-T 2009 Material removal rate and electrode wear ratio study on the powder mixed electrical discharge machining of cobalt-bonded tungsten carbide. *Int J Adv Manuf Technol*. 40: 95–104.

Lamba A, Vipin 2022 Experimental Investigation of machining of EN31 Steel in abrasive mixed rotary EDM with graphite and copper electrode. *Sadhana*. 47: 185.

Lin Y-C, Cheng C-H, Su B-L, Hwang L-R 2006 Machining Characteristics and Optimization of Machining Parameters of SKH 57 High-Speed Steel Using Electrical-Discharge Machining Based on Taguchi Method. *Mater Manuf Process*. 21: 922–929.

Mandaloi G, Singh S, Kumar P, Pal K 2016 Effect on crystalline structure of AISI M2 steel using tungsten–thorium electrode through MRR, EWR, and surface finish. 90: 74–84.

Mohan B, Rajadurai A, Satyanarayana KG 2002 Effect of SiC and rotation of electrode on electric discharge machining of Al-SiC composite. J Mater Process Technol. 124: 297–304.

Muthuramalingam T, Mohan B, Saravanakumar D 2015 Evaluation of surface finish of Electrical Discharge Machined AISI 304 Stainless Steel with various pulse generators. Applied Mechanics and Materials. 772: 279–283.

Nizar BS, Farhat G, Kais BA 2006 Numerical study of thermal aspects of electric discharge machining process, International Journal of Machine Tools and Manufacture. 46: 908–911.

Patel KM, Pandey PM, Rao PV 2010 Optimisation of process parameters for multi-performance characteristics in EDM of Al 2O 3 ceramic composite. *Int J Adv Manuf Technol*. 47: 1137–1147.

Patel S, Thesiya D, Rajurkar A 2018 Aluminium powder mixed rotary electric discharge machining (PMEDM) on Inconel 718. *Aust J Mech Eng*. 16: 21–30.

Payal H, Choudhary R, Sidhu S 2008 Analysis of electro discharge machined surfaces of EN-31 tool steel. *J Sci Ind Res (India)*. 67: 1072-1077.

Satsangi PS, Chattopadhyay KD 2010 A study of machining parameters during electrical discharge machining of steel by a rotary copper electrode. Adv Mater Res. 83–86: 756–763.

Schumacher BM , Krampitz R , Kruth JP 2013 Historical phases of EDM development driven by the dual influence of "Market Pull" and "Science Push." *Procedia CIRP*. 6: 5–12.

Shih HR , Shu KM 2008 A study of electrical discharge grinding using a rotary disk electrode. *Int J Adv Manuf Technol*. 38: 59–67.

Simao J, Lee HG, Aspinwall DK, Dewes RC, Aspinwall EM 2003 Workpiece surface modification using electrical discharge machining, International Journal of Machine Tools and Manufacture. 43(2): 121-128.

Singh AK, Kumar S, Singh VP 2015 Effect of the addition of conductive powder in dielectric on the surface properties of superalloy Super Co 605 by EDM process. Int J Adv Manuf Technol. 77: 99–106.

Singh NK, Pandey PM, Singh KK 2017 Experimental investigations into the performance of EDM using argon gas-assisted perforated electrodes. Mater Manuf Process. 32: 940–951.

Singh S, Maheshwari S, Pandey PC 2004 Some investigations into the electric discharge machining of hardened tool steel using different electrode materials. *J Mater Process Technol*. 149: 272–277.

Srivastava V, Pandey PM 2013 Experimental investigation on electrical discharge machining process with ultrasonic-assisted cryogenically cooled electrode. Proc Inst Mech Eng Part B J Eng Manuf. 227: 301–314.

Surani K 2020 Effect on Powder Mixed Electric Discharge Machining (PMEDM) on Various Materials with Different Powders: A Review. Int. J. Res. Appl. Sci. Eng. Technol. 8 (12): 614-630

Tanjilul M, Ahmed A, Kumar AS, Rahman M 2018 A study on EDM debris particle size and flushing mechanism for efficient debris removal in EDM-drilling of Inconel 718, Journal of Materials Processing Technology. 255: 263–274.

Teimouri R, Baseri H 2012 Effects of magnetic field and rotary tool on EDM performance. *J Manuf Process*. 14: 316–322.

Torres A, Puertas I, Luis CJ 2015 Modelling of surface finish, electrode wear and material removal rate in electrical discharge machining of hard-to-machine alloys. Precis Eng. 40: 33–45.

Wang CC, Yan BH 2000 Blind-hole drilling of Al2O3/6061Al composite using rotary electro-discharge machining. J Mater Process Technol. 102: 90–102.

Younis A, Abbas S, Gouda A, Mahmoud H, Abd-Allah A 2015 Effect of electrode material on electrical discharge machining of tool steel surface, Ain Shams Engineering Journal. 6(3): 977-986.